The Emulated Ensemble

Real-Time Simulation of Musical Instruments using Finite-Difference Time-Domain Methods

Ph.D. Dissertation

Silvin Willemsen

Dissertation submitted June 24, 2021

Thesis submitted: June 24, 2021

PhD Supervisor: Prof. Stefania Serafin
Aalborg University

PhD Committee: Prof. X, Y University
Prof. X, Y University
Prof. X, Y University

PhD Series: Technical Faculty of IT and Design, Aalborg University

Department: Department of Architecture, Design and Media Technology

ISSN: xxxx-xxxx
ISBN: xxx-xx-xxxx-xxx-x

Published by:
Aalborg University Press
Skjernvej 4A, 2nd floor
DK – 9220 Aalborg Ø
Phone: +45 99407140
aauf@forlag.aau.dk
forlag.aau.dk

Printed in Denmark by Rosendahls, 2021

Curriculum Vitae

Silvin Willemsen

Here is the CV text.

Acknowledgements

I would like to thank my mom..

Both Stefan Bilbao and his seminal work *Numerical Sound Systhesis* have been invaluable to the result of this project...

List of Publications

Listed below are the publications that I (co)authored during the Ph.D. project. These are grouped by: the main publications, which are also included in Part **??**, papers where I had a supervisory role, and finally, other publications from various collaborative efforts.

Abstract

English abstract

Abstract

Resumé

Danish Abstract

Contents

Todo list

Preface

Starting this Ph.D. project, I did not have a background in mathematics, physics or computer science, which were three equally crucial components in creating the result of this project. After the initial steep learning curve of notation and terminology, I was surprised to find that the methods used for physical modelling are actually quite straightforward!

Of course it should take a bit of time to learn these things, but

Many concepts that seemed impossible at the beginning

I feel that the literature lacks a lot of the intuition needed for readers without a background in any of these topics. Rather, much of the literature I came across assumes that the reader has a degree in at least one of the aforementioned topics. Stefan Bilbao's seminal work *Numerical Sound Synthesis*, which is the most complete work to date describing how to physically model musical instruments using finite-difference time-domain methods says that "A strong background in digital signal processing, physics, and computer programming is essential." Even though some basic calculus knowledge is assumed to understand the concepts used in this work, a degree in any of the aforementioned topics is (hopefully) unnecessary. Furthermore, some experience with MATLAB and C++ is assumed for the code examples

Some working titles: *Physical Modelling for Dummies Physical Modelling for the faint-hearted*

Also, I came across a lot of "it can be shown that's without derivations. This is why I decided to write this work a bit more pedagogical, and perhaps more elaborate than what could be expected.

I believe that anyone with some basic skills in mathematics and programming is able to create a simulation based on physics within a short amount of time, given the right tools, which I hope that this dissertation could be.

The knowledge dissemination of this dissertation is thus not only limited to the research done and publications made over the course of the project, but also its pedagogical nature hopefully allowing future (or past) students to benefit from.

As with a musical instrument itself, a low entry level, a gentle learning curve along with a high virtuosity level is desired. Take a piano, for instance.

Most will be able to learn a simple melody — such as "Frère Jacques" — in minutes, but to become virtuous requires years of practice.

This is the way I wanted to write this dissertation: easy to understand the basic concepts, but many different aspects touched upon to allow for virtuosity. Hopefully by the end, the reader will at least grasp some highly complex concepts in the fields of mathematics, physics and computer science (which will hopefully take less time than it takes to become virtuous at playing the piano).

As Smith states in his work *Physical Audio Signal Processing* [**?**] "All we need is Newton", and indeed, all Newton's laws of motion will make their appearance in this document.

I wanted to show my learning process and (hopefully) explain topics such as *Energy Analysis*, *Stability Analysis*, etc. in a way that others lacking the same knowledge will be able to understand.

Make physical modelling more accessible to the non-physicist.

Interested in physically impossible manipulations of now-virtual instruments.

The dissertation is divided into several parts which in their turn are divided in chapters.

Part ??: Introduction introduces the field of physical modelling for musical instruments in Chapter **??** by giving a brief history of the field and provides and background for the project. At the end, the project objectives and contributions to the field will be detailed. Chapter **??** will provide a thorough introduction to finite-difference time-domain methods using simple sound-generating systems as examples, after which Chapter **??** will introduce several analysis techniques in a tutorial-like fashion.

Part ??: Resonators introduces various physical models in isolation that have been used extensively throughout the project.

Part ??: Exciters shows two different ways that the

Part ??: Interactions shows two different ways that the resonators can interact with each other:

Silvin Willemsen
Aalborg University, June 24, 2021

Part I

Introduction

Chapter 1

Physical Modelling of Musical Instruments

Digital sound synthesis an increased interest in the last few decades. In the 1960s, efficient sinusoidal-based sound synthesis techniques such as additive synthesis [**?**], or FM (frequency modulation) synthesis [**?**] were invented. The latter became widely popular through the Yamaha DX7 synthesiser created in 1983 that synthesised sounds based solely on this technique [**?**]. Through a simple change of variables

As computing power increased, so did the popularity of using physically-based simulations of musical instruments. using digital counterparts of

to more to more computationally demanding techniques in the

The simulation[1] of traditional musical instruments has seen . From

haha.. not sure whether to include

Stefania, I need you here for the proper references :)

The interest in creating virtual or digital musical instruments

Virtualisation or digitisation

A simulation of a musical instrument is defined as an implementation of

where the sound is generated on the spot. Sample-based sound synthesis, where the sound of a real instrument has been recorded and is played back through a digital device is not considered a simulation.

The umbrella term would be digital musical instrument,

Physical modelling is a technique /approach to synthesise sound. It is widely accepted that physical modelling is the best way to realistically and naturally simulate real-world musical instruments [**?**, **?**, **?**]. As this technique simulates the instrument based on its physics rather than using pre-recorded samples, it is more flexible to player-interaction and thus more realistic when

[1]The term *emulated* is only used in the title of this work (because of the alliteration), but is synonymous to *simulated* in this context.

synthesising sound in performance. Although physical models could potentially sound indistinguishable from the instrument that they are simulating, it has been impossible, until recently, to make highly physically accurate physical models 'playable' in real-time [**?**]. With the computational power we currently possess, we can run the simulations in real-time and make them available for musicians in latency-less applications. These applications include digital instrument plug-ins that can be used by music producers, but also resurrect old or rare instruments that can not be played anymore due to damage, or because they are too valuable.

The history of physical modelling of musical instruments..?

1.1 Physical Modelling Techniques

The time-evolution of dynamic systems, including that of musical instruments, can be well described by partial differential equations (PDEs) [**?**, **?**]. Examples of a dynamic systems are a guitar string, a drum-membrane, or air propagation in a concert hall; three very different concepts, but all based on the same types of equations of motion. Many of these equations and other knowledge currently available on the physics of musical instruments have been collected by Fletcher and Rossing in [**?**]. Though these equations are very powerful, only few have a closed-form solution, and in order for them to be implemented, they need to be approximated. In the past decades, much research has been done on implementing these PDEs to model and simulate different musical instruments. Great overviews of implementation techniques are given by, for example, Vesa Välimäki et al. in [**?**] and Julius O. Smith in [**?**, **?**].

Some techniques that are described in this literature can be found below:

Modal Synthesis decomposes a system into a series of uncoupled 'modes of vibration'. First used in a musical context by Morrison and Adrien in [**?**], it is a technique that is still used today due to its computational efficiency, especially when simulating higher dimensional systems such as (two-dimensional) plates or (three-dimensional) rooms. It is especially effective when used to describe a linear system [**?**] with a small number of long-resonating modes [**?**]. When used to describe non-linear systems, however, the modes become 'coupled' and the system will quickly become more computationally expensive. Recent developments using the FAUST programming language allow a 3D-mesh model of any three-dimensional object to directly be decomposed into its modes of vibration [**?**].

Finite-Difference Time Domain methods (FDTD) aim to solve PDEs by approximating them with difference equations, discretising a continuous system into grid-points in space and time. In a musical context, this technique was first

used for the case of string vibration in [**?**, **?**, **?**] and later in [**?**, **?**]. Stefan Bilbao extensively describes this method in [**?**, **?**]. Although computationally expensive, especially when working with higher-dimensional systems, this technique can accurately model any system, whether it is linear or non-linear, time-invariant or time-variant.

Digital Waveguide Modelling (or Digital Waveguides (DWGs)) is a modelling technique that discretises wave propagation and scattering. The technique was first presented in [**?**], and is mostly used for one-dimensional systems, such as strings and acoustic tubes and decomposes their system into travelling wave components. This technique has also been used in higher-dimensional systems, but is superior in efficiency when used in the one-dimensional case [**?**]. Some authors have combined DWGs with FD schemes (such as in [**?**, **?**]) to accurately model non-linear behaviour while maintaining high-speed implementation.

Mass-spring networks can be similar in nature to FDTD methods, but treat each grid point as an individual mass connected to other masses through springs in a network. Pioneered in a musical context by Cadoz in [**?**, **?**, **?**] it is currently being further developed by Leonard and Villeneuve in a real-time, interactive environment [**?**, **?**].

Other techniques include Functional Transformation Method [**?**], state-space modelling [**?**], wave-domain modelling and energy-based port-Hamiltonia should I include this

This work focuses on FDTD methods

The main advantage of FDTD methods is that they are extremely general and flexible in terms of the type and amount of systems they can model. They allow any set of PDEs can be directly numerically simulated without making any assumptions regarding the

modular: PDEs can be connected

Compared to other techniques ....

DWGs could be considered 'physically inspired' FDTD methods

Energy techniques: [**?**] von Neumann analysis: [**?**]

Using FDTD methods can be quite computationally heavy. Moore's law [**?**]

Nearly any musical instrument can be subdivided into a resonator component, an exciter component, and the interaction between them. This modular approach to musical instruments was first introduced by Borin, De Poli and Sarti in [**?**] and is used to structure this work. Examples or resonator-exciter combinations are the violin and the bow, or the trumpet and the lips of the player. Note that Part **??** does not include the interactions between the resonator and exciter, but rather the interactions between different parts of the resonator itself, for example, the interactions between the string and the body of a violin, which both are resonators. interactions in [**?**] are not the same as the interactions "Part" here..

reread

A resonator is a passive system, in this work mostly assumed to be linear,

that does not emit sound unless triggered by an external source. Exciters can be seen as these external sources, and generally have a nonlinear element. Exciters insert energy into a resonator and cause it to vibrate and emit sound.

In the real world, the interaction between the exciter and the resonator is bi-directional, hence called an interaction. In other words, the exciter not only affects the state of the resonator, but the resonator affects the exciter as well. For the most part, this is also what is attempted to model in this work.

1.2 Real-Time Implementation

Although many techniques to digitally simulate musical instruments exist

proving that we have only recently reached the computing power in personal computers to make real-time playability of these models an option. The biggest challenge in real-time audio applications as opposed to those only involving graphics, is that the sample rate is extremely high. As Nyquist's sampling theory tells us, a sampling rate of at least 40 kHz is necessary to produce frequencies up to the human hearing limit of 20 kHz **[Nyquist]**. Visuals

Even though physical modelling has been a popular research field in the past few decades, relatively little research has been done on making the models work in real-time, i.e., 'playable' **[?]**. Several virtual string instruments and different electric pianos have been made real-time by Pfeifle and Bader in **[?, ?, ?]**. They used field programmable gate arrays (FPGAs) for implementing models based on FDTD methods. Furthermore, Roland's V-series use COSM (Composite Object Sound Modelling) technology **[?]** that implement real-time physical models in hardware instruments. In the NESS project **[?, ?]**, Stefan Bilbao and his team focused on implementing systems using FDTD methods in real-time.

Real-time: no noticeable latency

exactly as in [?]

1.3 Why?

So why would we go through all this hassle of modelling musical instruments? Could we not use a recording of the original and play that back at the right moment? Or taking another step back, why not buy a real instrument and learn to play that instead? "I'm a musician. Will I be out of a job if you keep making physical models?"

Physical modelling is not here to replace the original instruments and the musicians playing them. Instead, it can be used as a tool to understand the physics of existing instruments and possibly go beyond. Simulated instruments are not restricted by physics anymore and could provide new ways of expression for the musician.

1.3.1 Samples vs. Physical Modelling

Digital musical instruments based on recordings of an actual instrument, referred to as *samples*, have an advantage of having an optimally realistic sound. As the output of the digitised instrument is exactly that of the original instrument, the digital version should sound indistinguishable from the original. Furthermore, using samples is extremely computationally efficient as it simply requires loading the data and playing this back to the player.

That said, these are the only advantages of using samples over physical models for digitising a musical instrument. Samples are static and unable to adapt to changes in performance; the recording is made by one player, using a specific microphone and location. Moreover, capturing the the entire interaction space of an instrument is nearly impossible. Imagine recording a violin with every single combination of bowing force, velocity, position, duration and other aspects such as vibrato, pizzicato. Even if a complete sample library could be created, this would contain an immense amount of data. Using physical models to simulate the musical instrument, on the other hand, allows the sound to be generated on the spot based on physical parameters that the user can interact with. The

Trade off between storage and speed, or hard-disk and processing power.

1.3.2 Resurrect Old or Rare Instruments

Why not use the real instrument in the first place? In some cases, recording samples of an instrument is not even possible as they are too old, too rare or too vulnerable to be played. The physics of the instrument, including the geometry and material properties, are available, and could potentially be modelled digitally.

Even popular instruments require maintenance and might need to be replaced after years of usage.

Entire orchestras come from plug-ins

FULL DOC SWEEP: plug-ins or plug-ins

1.3.3 Go beyond what is physically possible

check wording

As a virtualinstrument is not restricted to the laws of physics in the real world, this opens up a world of possibilities.

Musical instrument simulations make it possible for parameters like shape, size, material properties, etc. to be dynamically changed, which is physically impossible or very hard to do. Furthermore, different instrument components can be combined to create hybrid instruments. For example, one could bow the air in a trumpet, or lip-excite a string (similar to what Smith states in [**?**]). This could potentially resulting in unique sounds that can only be created using physical models.

1.4 Project Objectives and Main Contributions

Over the past few decades, much work has been done on the accurate modelling of physical phenomena. In the field of sound and musical instruments..

From [**?**] to [**?**]

The main objective of this thesis is to implement existing physical models simulated using FDTD methods in real time. Many of the physical models and methods presented in this thesis are taken from the literature and are thus not novel.

Secondly, to combine the existing physical models to get complete instruments and be able to control them in real time.

As FDTD methods are quite rigid, changing parameters on the fly, i.e., while the instrument simulation is running, is a challenge. Other techniques, such as modal synthesis, are much more suitable for this, but come with the drawbacks mentioned in Section **??**. Therefore, a novel method was devised to smoothly change parameters over time, introducing this to FDTD methods.

exactly as in [**?**]

1.5 Thesis Outline

Introduction to finite-difference methods and analysis techniques

Less focus on continuous equations and mathematical substantiation, but more on the practical and implementation side of things.

Despite the "collection of papers" format that I chose to use for this work, the style of

Models used over the course of the project divided into resonators in part **??**, exciters in part **??** and the interactions between them in **??**.

Focus on real-time implementation and control of the models in part **??**

- Physical models
  - Resonators
  - Exciters
  - Interactions
- Dynamic Grids
- Real-Time Implementation and Control
- Complete instruments
  - Large-scale physical models
  - Tromba Marina
  - Trombone

Notes

- Think about how to define real-time.
- Create an intuition for different parts of the equation
- Talk about input and output locations and how that affects frequency content (modes).

One over number $\rightarrow$ reciprocal of number

Example: When the waveform consists entirely of harmonically related frequencies, it will be periodic, with a period equal to the reciprocal of the fundamental frequency (from An Introduction to the Mathematics of Digital Signal Processing Pt 2 by F. R. Moore)

Chapter 2

Introduction to Finite-Difference Time-Domain Methods

"Since Newton, mankind has come to realize that the laws of physics are always expressed in the language of differential equations."
- Steven Strogatz

This chapter introduces some important concepts needed to understand finite-difference time-domain (FDTD) methods. These techniques are what the implementation of the physical models presented later on in this document are based on. By means of a simple mass-spring system and the 1D wave equation, the notation and terminology used throughout this document will be explained. Unless denoted otherwise, the notation has been taken from [**?**], most of which originates from [**?**].

2.1 Differential Equations

Differential equations are used to describe the motion of dynamic systems, including vibrations in musical instruments. In this work, these equations are used to describe, among others, the movement of a string, an instrument body and the air pressure in an acoustic tube.

A characteristic feature of these equations is that, rather than an absolute value or *state* of a system, the time derivative of its state – its velocity – or the second time derivative – its acceleration – is described. From this, the absolute state of the system can then be computed. This state is usually described by

the variable u which is always a function of time, i.e., $u = u(t)$. If the system is distributed in space, u also becomes a function of space, i.e., $u = u(x, t)$, or with two spatial dimensions, $u = u(x, y, t)$, etc. Though this work only describes systems of up to two spatial dimensions, one can easily extend to three dimensions [**?**] and potentially higher-dimensional systems! See Section **??** for more information on dimensions.

If u is univariate, and only a function of time, the differential equation that describes the motion of this system is called an *ordinary differential equation* (ODE). Various ways to describe the second derivative in time of u, or the acceleration of u are

$$\begin{aligned} \frac{d^2u}{dt^2} &\quad \text{(Leibniz's notation)}, \\ \ddot{u} &\quad \text{(Newton's notation)}, \\ D_t^2 u &\quad \text{(Euler's notation)}. \end{aligned}$$

Leibniz' notation could be considered the most standard notation but is not necessarily compact. Newton's notation on the other hand allows for an ultra compact notation using a dot above the function to denote a time-derivative. In this work, for ODEs in isolation, Newton's notation will be used for this reason. The drawback of this notation is that it only be used for univariate functions. Finally, Euler's notation indicates a derivative using an operator which can be applied to a function.

If u is also a function of at least one spatial dimension, the equation of motion is a called a *partial differential equation* (PDE). The literature uses different types of notation for taking (continuous-time) partial derivatives. Applied to a state variable u these can look like

$$\begin{aligned} \frac{\partial^2 u}{\partial t^2} &\quad \text{(Leibniz's notation)}, \\ u_{tt} &\quad \text{(subscript notation)}, \\ \partial_t^2 u &\quad \text{(Euler's notation)}, \end{aligned}$$

where the subscript notation could be seen as the partial derivative counterpart to Newton's notation due to its compactness. In the remainder of this document, Euler's notation will be used for PDEs, due to their similarity to operators in discrete time (introduced in Section **??**) and as it allows for creation of bigger operators for more compactness when working with multiple (connected) systems (see e.g. Chapter **??**). Also, state-of-the-art literature in the field of FDTD methods sound synthesis use this notation [**?**].

2.1.1 Dimensions and Degrees of Freedom

All objects in the physical world are three-dimensional (3D) as they have a non-zero width, length and depth. Moreover, these objects can move in these

three dimensions and thus have three translational *degrees of freedom (DoF)* (the three rotational DoF are ignored here). To reduce the complexity of the model as well as computational complexity (computational cost), simplifications can be made to reduce both the dimensionality of the spatial distribution of a physical object as well as that of the translational DoF.

Generally, the spatial distribution of an object can be simplified if one (or more) of the dimensions is orders of magnitude smaller than the others without affecting its behaviour much. A guitar string, for instance, has much greater length than its width or depth and can therefore be reduced to a one-dimensional (1D) system. If a 3D description were to be kept, the relative displacement between two locations on one cross-section along the length of the string would be taken into account. One could imagine that this displacement will always be orders of magnitude smaller than the relative displacement of two points along the string length and is thus negligible. Similarly, the thickness of a drum membrane is much smaller than its length and width and can therefore be simplified to a two-dimensional (2D) system.

check whether this needs to be per point along a system

The translational DoF, on the other hand, describe now many "coordinates" a state variable includes. In much of the literature on FDTD methods in the field of musical acoustics, the state variable only has one coordinate. In most string models, for example, only the transverse displacement in one polarisation is considered (see Chapter **??**) and the other polarisation as well as the longitudinal motion of the string (motion along the string length) is ignored. In other words, every point along the string can only move up and down, not side-to-side and not forward and back. Although this greatly simplifies the system at hand and reduces computational complexity, this is not what happens in reality, and non-linear effects such as phantom partials and pitch glides due to tension modulation are not present in the simplified model.

Work has been done on strings with dual (transverse) polarisation by Desvages [**?**] and Desvages and Bilbao [**?**] using FDTD methods. Models including longitudinal string vibration, where the longitudinal and transversal displacements are couples can be found in [**?**, **?**]. In [**?**], Villeneuve and Leonard present a mass-spring network where the state of every individual mass has three translational DoF. Due to these additional DoF, these networks do capture the aforementioned effects, but greatly increase the computational complexity of the models.

Although the dimensionality reduction ignores some of the physical processes, surprisingly realistic sounding models can be made despite these simplifications. Due to computational considerations, all models used in this work thus only have 1 translational DoF.

Notation

When describing the state of a system, the spatial dimensions it is distributed over appears in the argument of the state variable. For example, the state of a 2D system, with 1 translational DoF is written as $u(x, y, t)$.

The translational DoF, on the other hand, determines the amount of coordinates that the state variable describes. A 1D system with 3 translational DoF can thus be written as $\mathbf{u}(x, t)$ where $\mathbf{u}$ is a vector containing the coordinates for all three translational DoF.

2.1.2 Ranges of Definition and Domains

When modelling physical systems, one needs to provide a *range of definition* over which they are defined. For a 1D system $u = u(x, t)$, ranges of definition must be given for x and t. Usually, the temporal range $t \geq 0$, meaning that the system is defined for non-negative time.

In space, the range of definition is usually referred to as a (spatial) *domain*, denoted by the symbol $\mathcal{D}$. Using the example above, x may be defined over $\mathcal{D}$, which is written as $x \in \mathcal{D}$. For analysis purposes, infinite domains ($\mathcal{D} = \mathbb{R} = (-\infty, \infty)$) or semi-infinite domains ($\mathcal{D} = \mathbb{R}^+ = [0, \infty)$) may be used, but for implementation purposes, a finite domain needs to be established. For higher dimensional systems, one needs to define higher dimensional domains. A 2D system $u = u(x, y, t)$, may be defined over 'horizontal domain' $\mathcal{D}_x$ and 'vertical domain' $\mathcal{D}_y$, which are both 1D domains. The system is then defined for $(x, y) \in \mathcal{D}$ where $\mathcal{D} = \mathcal{D}_x \times \mathcal{D}_y$.

2.2 Discretisation using FDTD methods

Differential equations are powerful tools to describe the motion of physical systems. Despite this, only few of these have a closed-form, or analytical, solution. More complex systems require methods that do not perfectly solve, but rather *approximate* the solutions to these equations. FDTD methods are the most straightforward approach to numerically approximate differential equations. These methods are considered of the most general and flexible techniques in terms of the systems they can model, and frankly, relatively simple to understand once some familiarity with them is obtained. The main concern with these methods is the numerical stability of the eventual approximation. Conditions for stability can be mathematically derived and will be introduced in Section **??**.

FDTD methods essentially subdivide a continuous differential equation into discrete points in time and space, a process called *discretisation*. Once an ODE or PDE is discretised using these methods it is now called a *finite-difference (FD) scheme* which approximates the original differential equation. In

the following, for generality and ease of explanation, a 1D system will be used. Unless denoted otherwise, the equations and theory used in this chapter has been taken from [**?**].

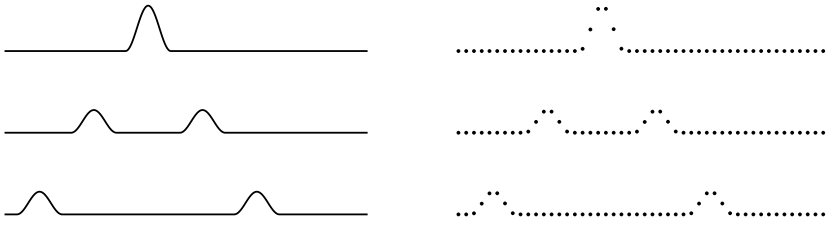

Fig. 2.1: A continuous PDE is discretised...

Figure and caption are not done yet

FULL DOC SWEEP: check capitalisation of headings throughout document

grid figure

2.2.1 Grid Functions

The first step to approximate continuous PDEs, is to define a discrete *grid* over time and space. A system described by state $u = u(x, t)$ defined over time t and one spatial dimension x, can be discretised to a *grid function* u_l^n. Here, integers l and n describe the spatial and temporal indices respectively and arise from the discretisation of the continuous variables x and t according to $x = lh$ and $t = nk$. The spatial step h, also called the *grid spacing* describes the distance (in m) between two neighbouring *grid points*, and is closely related to the stability of the FD scheme. The temporal step k, or *time step* is the time (in s) between two consecutive temporal indices and can be calculated $k = 1/f_\mathrm{s}$ for a sample rate f_s (in Hz). In many audio applications $f_\mathrm{s} = 44100$ Hz which will be used in this work (unless denoted otherwise).

As mentioned in Section **??**, a 1D system needs to be defined over a temporal range of definition and one spatial domain. In discrete time, $t \geq 0$ is discretised to $n \in \mathbb{N}^0$.[1] The spatial domain $\mathcal{D}$ can be subdivided into N equal sections, or intervals, of length h (see Figure **??**). The grid points describing the state of the system are placed between and around these intervals. The spatial range of interest then becomes $l \in \{0, \ldots, N\}$ and the total number of grid points is $N + 1$, which is one more than the number of intervals.

To summarise, for a 1D system

this might be unnecessary, but I thought that it might be nice to have this in an equation for clarity

$$u(x, t) \approxeq u_l^n \quad \text{with} \quad x = lh \quad \text{and} \quad t = nk,$$

$$l \in \{0, \ldots, N\} \quad \text{and} \quad n \in \mathbb{N}^0.$$

[1] In this work, $\mathbb{N}^0$ is used to denote the set of non-negative integers ($\mathbb{N}^0 = 0, 1, 2, \ldots$).

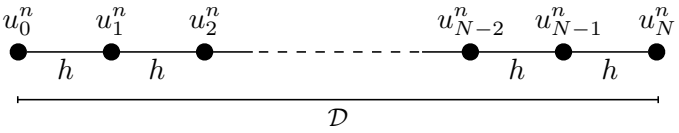

Fig. 2.2: When a 1D system $u(x,t)$ with $x \in \mathcal{D}$ is discretised to a grid function u_l^n, the spatial domain $\mathcal{D}$ is divided into N intervals of length h and spatial range of interest $l = \{0, \ldots, N\}$.

2.2.2 Finite-Difference Operators

Now that the state variable has a discrete counterpart, this leaves the derivatives to be discretised, or approximated. We start by introducing shift operators that can be applied to a grid function and 'shifts' its indexing, either temporally or spatially. Forward and backward shifts in time, together with the identity operation are

$$e_{t+}u_l^n = u_l^{n+1}, \quad e_{t-}u_l^n = u_l^{n-1}, \quad \text{and} \quad 1u_l^n = u_l^n. \tag{2.1}$$

Similarly, forward and backward shifts in space are

$$e_{x+}u_l^n = u_{l+1}^n, \quad \text{and} \quad e_{x-}u_l^n = u_{l-1}^n. \tag{2.2}$$

many figures for shift and FD operators

These shift operators are rarely used in isolation, though they do appear in energy analysis techniques detailed in Section **??**. The operators do, however, form the basis of commonly used *finite-difference (FD) operators*. The first-order derivative in time can be discretised three different ways. The forward, backward and centred difference operators are

FULL DOC SWEEP: check centred instead of centered

these spacings are different in overleaf...

$$\partial_t \approx \begin{cases} \delta_{t+} \triangleq \frac{1}{k}\left(e_{t+} - 1\right), & \text{(2.3a)} \\ \delta_{t-} \triangleq \frac{1}{k}\left(1 - e_{t-}\right), & \text{(2.3b)} \\ \delta_{t\cdot} \triangleq \frac{1}{2k}\left(e_{t+} - e_{t-}\right), & \text{(2.3c)} \end{cases}$$

where "$\triangleq$" means "equal to by definition". These operators can then be applied to grid function u_l^n to get

$$\partial_t u \approx \begin{cases} \delta_{t+}u_l^n = \frac{1}{k}\left(u_l^{n+1} - u_l^n\right), & \text{(2.4a)} \\ \delta_{t-}u_l^n = \frac{1}{k}\left(u_l^n - u_l^{n-1}\right), & \text{(2.4b)} \\ \delta_{t\cdot}u_l^n = \frac{1}{2k}\left(u_l^{n+1} - u_l^{n-1}\right), & \text{(2.4c)} \end{cases}$$

and all approximate the first-order time derivative of u. Note that the centred difference has a division by $2k$ as the time difference between $n+1$ and $n-1$ is, indeed, twice the time step.

figure here visualising operators (with reference to grid figure)

Similar operators exist for a first-order derivative in space, where the for-

ward, backward and centred difference are

$$\partial_x \approxeq \begin{cases} \delta_{x+} \triangleq \frac{1}{h}\left(e_{x+} - 1\right), & \text{(2.5a)} \\ \delta_{x-} \triangleq \frac{1}{h}\left(1 - e_{x-}\right), & \text{(2.5b)} \\ \delta_{x\cdot} \triangleq \frac{1}{2h}\left(e_{x+} - e_{x-}\right), & \text{(2.5c)} \end{cases}$$

and when applied to u_l^n are

$$\partial_x u \approxeq \begin{cases} \delta_{x+} u_l^n = \frac{1}{h}\left(u_{l+1}^n - u_l^n\right), & \text{(2.6a)} \\ \delta_{x-} u_l^n = \frac{1}{h}\left(u_l^n - u_{l-1}^n\right), & \text{(2.6b)} \\ \delta_{x\cdot} u_l^n = \frac{1}{2h}\left(u_{l+1}^n - u_{l-1}^n\right). & \text{(2.6c)} \end{cases}$$

Higher order differences can be approximated through a composition of first-order difference operators where their definitions are multiplied. The second-order difference in time may be approximated using

$$\partial_t^2 \approxeq \delta_{t+}\delta_{t-} = \delta_{tt} \triangleq \frac{1}{k^2}\left(e_{t+} - 2 + e_{t-}\right), \tag{2.7}$$

where "2" is the identity operator applied twice. This can similarly be done for the second-order difference in space

$$\partial_x^2 \approxeq \delta_{x+}\delta_{x-} = \delta_{xx} \triangleq \frac{1}{h^2}\left(e_{x+} - 2 + e_{x-}\right), \tag{2.8}$$

both of which can be applied to a grid function u_l^n in a similar fashion. Figure **??** shows the *stencils* of the operators introduced above. A stencil shows the grid points needed to perform the operation of a FD operator.

in energy analysis, interleaved grids, etc.

Also useful are averaging operators, all of which approximate the identity operation. The temporal forward, backward and centred averaging operators are

$$1 \approxeq \begin{cases} \mu_{t+} \triangleq \frac{1}{2}\left(e_{t+} + 1\right), & \text{(2.9a)} \\ \mu_{t-} \triangleq \frac{1}{2}\left(1 + e_{t-}\right), & \text{(2.9b)} \\ \mu_{t\cdot} \triangleq \frac{1}{2}\left(e_{t+} + e_{t-}\right). & \text{(2.9c)} \end{cases}$$

Notice how these definitions are different than the difference operators in (**??**): the terms in the parentheses are added rather than subtracted, and rather than a division by the time step k there is a division by 2. Finally, the centred averaging operator does not have an extra division by 2 as in (**??**). Applied to u_l^n, Eqs. (**??**) become

$$u_l^n \approxeq \begin{cases} \mu_{t+} u_l^n = \frac{1}{2}\left(u_l^{n+1} + u_l^n\right), & \text{(2.10a)} \\ \mu_{t-} u_l^n = \frac{1}{2}\left(u_l^n + u_l^{n-1}\right), & \text{(2.10b)} \\ \mu_{t\cdot} u_l^n = \frac{1}{2}\left(u_l^{n+1} + u_l^{n-1}\right). & \text{(2.10c)} \end{cases}$$

Similarly, spatial averaging operators are

$$1 \approx \begin{cases} \mu_{x+} \triangleq \frac{1}{2}\left(e_{x+} + 1\right), & \text{(2.11a)} \\ \mu_{x-} \triangleq \frac{1}{2}\left(1 + e_{x-}\right), & \text{(2.11b)} \\ \mu_{x\cdot} \triangleq \frac{1}{2}\left(e_{x+} + e_{x-}\right), & \text{(2.11c)} \end{cases}$$

and when applied to u_l^n

$$u_l^n \approx \begin{cases} \mu_{x+} u_l^n = \frac{1}{2}\left(u_{l+1}^n + u_l^n\right), & \text{(2.12a)} \\ \mu_{x-} u_l^n = \frac{1}{2}\left(u_l^n + u_{l-1}^n\right), & \text{(2.12b)} \\ \mu_{x\cdot} u_l^n = \frac{1}{2}\left(u_{l+1}^n + u_{l-1}^n\right). & \text{(2.12c)} \end{cases}$$

Finally, using forward and backward averaging operators, second-order temporal and spatial averaging operators can be created according to

$$1 \approx \mu_{tt} = \mu_{t+}\mu_{t-} \triangleq \frac{1}{4}\left(e_{t+} + 2 + e_{t-}\right), \tag{2.13}$$

and

$$1 \approx \mu_{xx} = \mu_{x+}\mu_{x-} \triangleq \frac{1}{4}\left(e_{x+} + 2 + e_{x-}\right). \tag{2.14}$$

Operators and derivatives in 2D will be discussed in Chapter **??**.

Accuracy

As FDTD methods approximate continuous systems, the resulting solution is rarely 100% accurate. To determine the accuracy of the FD operators above,

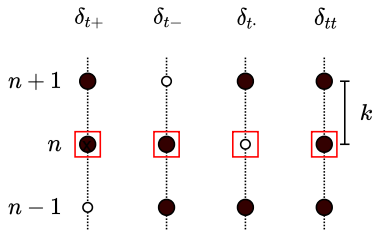

(a) Temporal operators.

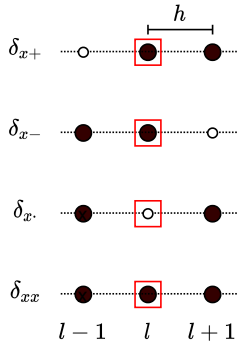

(b) Spatial operators.

Fig. 2.3: The stencils of various FD operators applied to the grid point highlighted with a red square. Black grid points are used in the calculation, and white grid points are not. The averaging operators follow the same pattern.

one can perform a *Taylor series analysis*. The Taylor series is an infinite sum and its expansion of a function f about a point a is defined as

$$f(x) = \sum_{n=0}^{\infty} \frac{(x-a)^n}{n!} f^{(n)}(a) \tag{2.15}$$

where superscript (n) denotes the n^{th} derivative of f with respect to x. The analysis will be performed on the temporal operators in this section, but also apply to the spatial operators presented.

Using continuous function $u = u(t)$ and following Bilbao's "slight abuse of notation" in [**?**], one may apply FD operators to continuous functions according to

$$\delta_{t+} u(t) = \frac{u(t+k) - u(t)}{k} \,. \tag{2.16}$$

Assuming that u is infinitely differentiable, $u(t+k)$, i.e., u at the next time step (in continuous time), can be approximated using a Taylor series expansion of u about t according to

$$u(t+k) = u(t) + k\dot{u} + \frac{k^2}{2}\ddot{u} + \frac{k^3}{6}\dddot{u} + \mathcal{O}(k^4). \tag{2.17}$$

Here, (following Newton's notation introduced in Section **??**) the dot describes a single temporal derivative and $\mathcal{O}$ includes additional terms in the expansion. The power of k in the argument of $\mathcal{O}$ describes the order of accuracy, the higher the power of k the more accurate the approximation. Equation (**??**) can be rewritten to

$$\frac{u(t+k) - u(t)}{k} = \dot{u} + \frac{k}{2}\ddot{u} + \frac{k^2}{6}\dddot{u} + \mathcal{O}(k^3),$$

and using Eq. (**??**) can be written to

$$\delta_{t+} u(t) = \dot{u} + \mathcal{O}(k). \tag{2.18}$$

This says that the forward difference operator approximates the continuous first order derivative with an additional error term that depends on k. As the power of k in $\mathcal{O}$'s argument is 1, the forward operator is first-order accurate. One can also observe that, as expected, the error gets smaller as the time step k gets smaller and indicates that higher sample rates result in more accurate simulations (through $k = 1/f_s$). confirming our intuition

One can arrive at a similar result for the backward operator. Applying Eq. (**??**) to $u(t)$ yields

$$\delta_{t-} u(t) = \frac{u(t) - u(t-k)}{k}. \tag{2.19}$$

One can then approximate $u(t-k)$ by performing a Taylor series expansion of u about t according to

$$u(t-k) = u(t) + (-k)\dot{u} + \frac{(-k)^2}{2}\ddot{u} + \frac{(-k)^3}{6}\dddot{u} + \mathcal{O}(k^4), \tag{2.20}$$

$$\frac{u(t-k)-u(t)}{k} = -\dot{u} + \frac{k}{2}\ddot{u} - \frac{k^2}{6}\dddot{u} + \mathcal{O}(k^3),$$

$$\delta_{t-}u(t) = \dot{u} + \mathcal{O}(k). \tag{2.21}$$

Notice that the sign of $\mathcal{O}$ does not matter.

Applying the centred operator in Eq. (**??**) to $u(t)$ yields

$$\delta_{t\cdot}u(t) = \frac{u(t+k)-u(t-k)}{2k}, \tag{2.22}$$

indicating that to find the order of accuracy for this operator, both Eqs. (**??**) and (**??**) are needed. Subtracting these and substituting their definitions yields

$$u(t+k) - u(t-k) = 2k\dot{u} - \frac{2k^3}{6}\dddot{u} + 2\mathcal{O}(k^5),$$

$$\frac{u(t+k)-u(t-k)}{2k} = \dot{u} + \mathcal{O}(k^2),$$

$$\delta_{t\cdot}u(t) = \dot{u} + \mathcal{O}(k^2), \tag{2.23}$$

and shows that the centred difference operator is second-order accurate.

As a first-order derivative indicates the *slope* of a function, the differences in accuracy between the above operators can be visualised as in Figure **??**. It can be observed that the derivative approximation – the slope – of the centred operator much more closely matches the the true derivative of u at t.

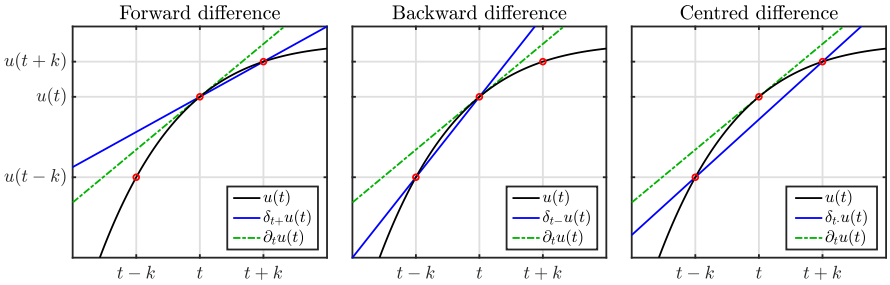

Fig. 2.4: The accuracy of the forward, backward and centred difference operators in (**??**) visualised. One can observe that the centred difference operator much more closely approximates the derivative, or the slope, of u at t than the forward and backward difference operators.

Higher-order differences, such as the second-order difference in time operator in Eq. (**??**) can also be applied to $u(t)$ to get

$$\delta_{tt}u(t) = \frac{u(t+k) - 2u(t) + u(t-k)}{k^2}, \tag{2.24}$$

and can be proven to be second-order accurate by adding Eqs. (**??**) and (**??**):

$$\begin{aligned} u(t+k) + u(t-k) &= 2u(t) + k^2\ddot{u} + \mathcal{O}(k^4), \\ \frac{u(t+k) - 2u(t) + u(t-k)}{k^2} &= \ddot{u} + \mathcal{O}(k^2), \\ \delta_{tt}u(t) &= \ddot{u} + \mathcal{O}(k^2). \end{aligned} \tag{2.25}$$

The accuracy of averaging operators can be found in the same way and follow a similar pattern.

$$\begin{aligned} \mu_{t+}u(t) &= u(t) + \mathcal{O}(k), \quad \mu_{t-}u(t) = u(t) + \mathcal{O}(k), \\ \mu_{t\cdot}u(t) &= u(t) + \mathcal{O}(k), \quad \mu_{tt}u(t) = u(t) + \mathcal{O}(k^2). \end{aligned} \tag{2.26}$$

2.2.3 Identities

For working with FD schemes, either for implementation or analysis, it can be extremely useful to rewrite the operators presented above to equivalent versions of themselves. These are called *identities* and for future reference, some useful ones are listed below:

$$\delta_{tt} = \frac{2}{k}\left(\delta_{t\cdot} - \delta_{t-}\right), \tag{2.27a}$$

$$\delta_{t\cdot} = \delta_{t+}\mu_{t-} = \delta_{t-}\mu_{t+}, \tag{2.27b}$$

$$\mu_{t+} = \frac{k}{2}\delta_{t+} + 1. \tag{2.27c}$$

That these equalities hold can easily be proven by expanding the operators defined in Section **??**. Naturally, these identities also hold for spatial operators by simply substituting the 't' subscripts for 'x'.

see whether the negative version of identity (**??**) is also used later on

2.3 The Mass-Spring System

Though a complete physical modelling field on their own (see Chapter **??**), mass-spring systems are also sound-generating systems and lend themselves well to illustrating and explaining FDTD methods in practice. Starting with the continuous-time ODE, this section continues to discretise it to an FD scheme using the operators described in Section **??**. Finally, the scheme is rewritten to an update equation that can be implemented and the output of the system is shown.

2.3.1 Continuous-time

Using dots to indicate a temporal derivative, the ODE of a simple mass-spring system is defined as

$$M\ddot{u} = -Ku, \tag{2.28}$$

where $u = u(t)$ is the distance from the equilibrium position (in m), $M > 0$ is the mass of the mass (in kg) and $K \geq 0$ is the spring constant (in N/m). Equation (**??**) can be written as

$$\ddot{u} = -\omega_0^2 u, \tag{2.29}$$

with angular frequency (in rad/s)

$$\omega_0 = \sqrt{K/M}. \tag{2.30}$$

This way of writing the mass-spring ODE is more compact and can more directly be related to the fundamental frequency $f_0 = \omega_0/2\pi$ (in Hz) of the system.

Apart from the choices of K and M, the behaviour of the mass-spring system is determined by its *initial conditions*, being $u(0)$ and $\partial_t u(0)$, i.e., the displacement and velocity of the mass at $t = 0$. If the initial conditions are non-zero, the path that the displacement of the mass follows over time is sinusoidal (see Figure **??**), which is also why the mass-spring system is often referred to as the *simple harmonic oscillator*. The amplitude of the sinusoid is determined by the initial conditions, whereas the frequency is determined by M and K.

Intuition

The behaviour of the mass-spring system in Eq. (**??**) arises from two basic laws of physics: *Newton's second law* and *Hooke's law*.

Starting with Newton's second law – *force equals mass times acceleration* – and relating this to the variables used in Eq. (**??**) yields an expression for force

$$F = M\ddot{u}. \tag{2.31}$$

This equation in isolation can be used to, for example, calculate the force necessary to accelerate a mass of M kg to $\ddot{u}$ m/s^2. Next, the force generated

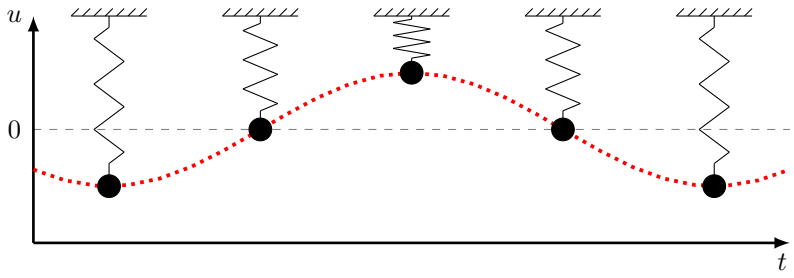

Fig. 2.5: Mass spring system over time. The system follows a harmonic (sinusoidal) motion.

by the spring follows Hooke's law:

$$F = -Ku, \tag{2.32}$$

which simply states that the force generated by a spring with stiffness K is negatively proportional to the value of u. In other words, the further the spring is extended (from the equilibrium $u = 0$), the more force will be generated in the opposite direction. Finally, as the sole force acting on the mass is the one generated by the spring, the two expressions for the force F can be set equal to each other and yields the equation for the mass-spring system in (**??**).

The sinusoidal behaviour of the mass-spring system, or a least the fact that the mass "gets pulled back" to the equilibrium, is apparent from the minus-sign in Eq. (**??**). The frequency of the sinusoid, depends on the value of K as the "pull" happens to a higher degree for a higher spring stiffness. That the frequency of the system is also dependent on the mass M can be explained by the fact that a lighter object is more easily moved and vice versa, which is apparent from Eq. (**??**). In other words, the pull of the spring has a greater effect on the acceleration of a lighter object than a heavier one.

Finally, if $u = 0$ there is no spring force present and the acceleration remains unchanged. This is exactly what Newton's first law states: if the net force acting on an object is zero, its velocity will be constant. If the mass is not in motion, this means that it remains stationary. If it is, the velocity is unchanged and it will continue moving with the same speed.

2.3.2 Discrete-time

Following the discretisation process introduced in Section **??**, one can approximate the PDE in Eq. (**??**). The displacement of the mass is approximated using

$$u(t) \approx u^n, \tag{2.33}$$

with time $t = nk$, time step $k = 1/f_\mathrm{s}$, sample rate f_s and temporal index and $n \in \mathbb{N}^0$. Note that the "grid function" does not have a subscript l as u is not distributed in space and is now simply called a *time series*.

Using the operators found in Section **??**, Eq. (**??**) can be discretised as follows:

$$M\delta_{tt}u^n = -Ku^n, \tag{2.34}$$

which is the first appearance of a FD scheme in this work. Expanding the δ_{tt} operator yields

$$\frac{M}{k^2}\left(u^{n+1} - 2u^n + u^{n-1}\right) = -Ku^n,$$

and solving for u^{n+1} results in the following recursion or *update equation*:

$$u^{n+1} = \left(2 - \frac{Kk^2}{M}\right)u^n - u^{n-1}, \tag{2.35}$$

which can be implemented in a programming language such as MATLAB.

2.3.3 Implementation and Output

A simple MATLAB script implementing the mass-spring system described in this section is shown in Appendix **??**. The most important part of the algorithm happens in a for-loop recursion, where update equation (**??**) is implemented. At the end of each loop, the system states are updated and prepared for the next iteration.

To be able to calculate the scheme at $n = 0$ (the first time index of the simulation), values must be provided for u^0 and u^{-1}. These are determined by the initial conditions mentioned in Section **??**. A simple way to obtain a sinusoidal motion with an amplitude of 1, is to set the initial conditions as follows (using the backwards time difference operator for discretising the first-order time derivative):

$$u^0 = 1 \quad \text{and} \quad \delta_{t-} u^n = 0. \tag{2.36}$$

figure out if this is valid as it falls outside of the defined temporal region of operation

The latter equality can be solved for u^{-1} to obtain its definition:

$$\begin{aligned} & \frac{1}{k}\left(u^0 - u^{-1}\right) = 0, \\ \overset{u^0=1}{\Longleftrightarrow} \quad & 1 - u^{-1} = 0, \\ & u^{-1} = 1. \end{aligned}$$

maybe a bit short...

In short, setting $u^0 = u^{-1} \neq 0$ yields an oscillatory behaviour.

The values for K and M are restricted by a stability condition

$$k < 2\sqrt{\frac{M}{K}}, \tag{2.37}$$

which will be elaborated on in Section **??**. If this condition is not satisfied, the system will exhibit (exponential) growth and is *unstable*.

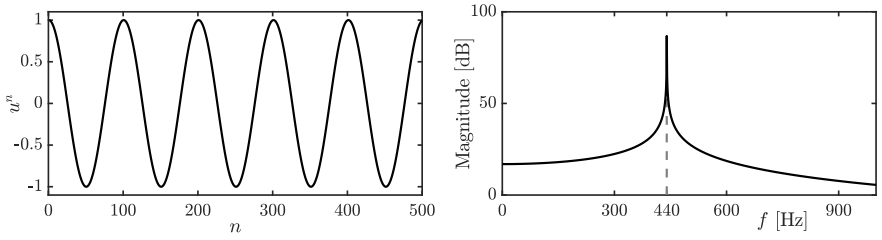

Fig. 2.6: The time-domain and frequency-domain output of a mass-spring system with $f_0 = 440$ Hz.

The output of the system can be obtained by 'recording' the displacement of the mass and listening to this at the given sample rate f_s. An example of this can be found in Figure **??** where the frequency of oscillation $f_0 = 440$ Hz.

2.4 The 1D Wave Equation

Arguably the most important PDE in the field of physical modelling for sound synthesis is the 1D wave equation. It can be used to describe transverse vibration in an ideal string, longitudinal vibration in an ideal bar or the pressure in an acoustic tube (see Chapter **??**). Although the behaviour of this equation alone does not appear in the real world as such – as no physical system is ideal – it is extremely useful as a test case and a basis for more complicated models.

2.4.1 Continuous time

FULL DOC SWEEP: check hyphen in titles

unit?

The 1D wave equation is a PDE that describes the motion of a system distributed in one dimension of space. Consider the state of a 1D system $u = u(x, t)$ of length L (in m) defined for time $t \geq 0$ and $x \in \mathcal{D}$ with $\mathcal{D} = [0, L]$. The PDE describing its motion is

$$\partial_t^2 u = c^2 \partial_x^2 u, \tag{2.38}$$

where c is the wave speed of the system (in m/s).

Intuition

As with the mass-spring system in Section **??** the working of the PDE in (**??**) arises from Newton's second law, even though this connection might be less apparent.

The 1D wave equation in (**??**) states that the acceleration of $u(x, t)$ at location x is determined by the second-order spatial derivative of u at that same location (scaled by a constant c^2). In the case that u describes the transverse displacement of an ideal string, this second-order derivative denotes the *curvature* of this string. As c^2 is always positive, the sign (or direction) of the acceleration is fully determined by the sign of the curvature. In other words, a 'positive' curvature at location x along the ideal string yields a 'positive' or upwards acceleration at that same location.

What a 'positive' or 'negative' curvature implies is more easily seen when we take a simple function describing a parabola, $y(x) = x^2$, and take its second derivative to get $y''(x) = 2$. The answer is a positive number which means that y has a positive curvature.

So, what does this mean for the 1D wave equation? As a positive curvature implies a positive or upwards acceleration as per Eq. (**??**), u with a positive

curvature at a location x will start to move upwards and vice versa. Of course, the state of a physical system such as u will rarely have a perfect parabolic shape, but the argument still applies. See Figure **??** for a visualisation of the forces acting on u due to curvature.

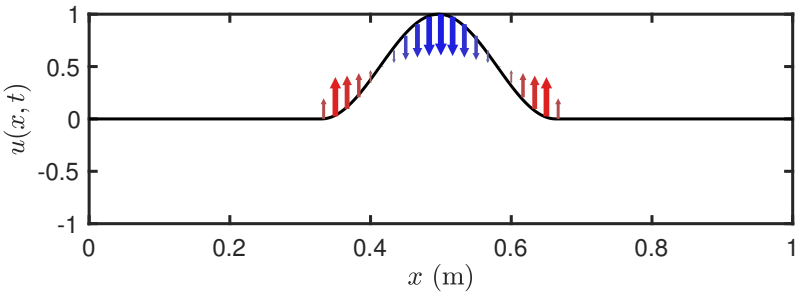

Fig. 2.7: The forces acting on the 1D wave equation described by $u(x,t)$ due to curvature. The arrows indicate the direction and magnitude of the force, and simultaneously the acceleration as these are connected through Eq. (**??**).

different wording in caption

Boundary Conditions

When a system is distributed in space, *boundary conditions* must be determined. Recalling that x is defined over domain $\mathcal{D} = [0, L]$, the boundaries, or end points of the system are located at $x = 0$ and $x = L$. Two often-used alternatives for the boundary conditions are

$$u(0,t) = u(L,t) = 0 \quad \text{(Dirichlet, fixed)}, \tag{2.39a}$$
$$\partial_x u(0,t) = \partial_x u(L,t) = 0 \quad \text{(Neumann, free)}. \tag{2.39b}$$

The Dirichlet boundary condition says that at the end points of the system, the state is 0 at all times. The Neumann condition on the other hand, says that rather the slope of these points needs to be 0, but that the end points are free to move transversely. In the former case, incoming waves to invert after reaching the boundary whereas in the latter incoming waves are reflected un-inverted. See Figure **??**.

add why this is relevant?

If both boundaries of the 1D wave equation share the same condition, the fundamental frequency of the simulation can be calculated using

$$f_0 = \frac{c}{2L} \,. \tag{2.40}$$

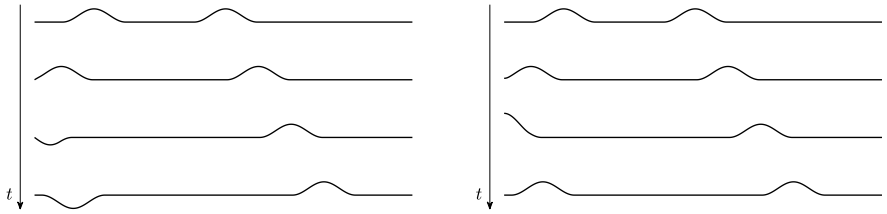

(a) The Dirichlet boundary condition in Eq. (**??**) fixes the boundary, which causes the incoming waves to invert.

(b) The Neumann or free boundary condition in Eq. (**??**) fixes the slope at the boundary, causing the incoming waves to not invert.

Fig. 2.8: The behaviour of the 1D wave equation with (a) Dirichlet or (b) Neumann boundary conditions.

Scaling

As this work follows much of Bilbao's *Numerical Sound Synthesis* [**?**], it might be good to talk about a major discrepancy between the PDEs and FD schemes that appear there and those used here. Non-dimensionalisation, or *scaling*, is extensively used in [**?**] and much of the literature published around that time (fx. [**?**, **?**]) and can be useful to reduce the amount of parameters used to describe a system.

Scaling techniques normalise the domain $x \in [0, L]$ to $x' \in [0, 1]$ with $x' = x/L$. The 1D wave equation in (**??**) can then be rewritten to

$$\partial_t^2 u = \gamma^2 \partial_{x'x'} u, \tag{2.41}$$

where scaled wave speed $\gamma = c/L$ has units of frequency. The scaling has removed the necessity for both c and L and simply specifying the scaled wave speed γ is enough to parameterise the behaviour of the system. The parameter reduction gets more apparent for more complex systems and could greatly simplify of the models used, at least in notation and parameter control.

Although this parameter reduction might be useful for resonators in isolation, when multiple resonators interact with each other (see Part **??**), it is better to keep the systems dimensional. As a big part of this work includes interaction between multiple resonators, only dimensional systems will appear here.

check whether still correct

2.4.2 Discrete time

Coming back to the PDE presented in Eq. (**??**), we continue by finding a discrete-time approximation for it. The most straightforward discretisation of

FULL DOC SWEEP: check straightforward or straight-forward

Eq. (**??**) is the following FD scheme

$$\delta_{tt} u_l^n = c^2 \delta_{xx} u_l^n, \tag{2.42}$$

with $l \in \{0, \ldots, N\}$ and number of grid points $N+1$. Other schemes exist (see fx. [**?**]), but are excluded as they have not been used in this work. Expanding the operators using the definitions given in Section **??** yields

$$\frac{1}{k^2}\left(u_l^{n+1} - 2u_l^n + u_l^{n-1}\right) = \frac{c^2}{h^2}\left(u_{l+1}^n - 2u_l^n + u_{l-1}^n\right). \tag{2.43}$$

and solving for u_l^{n+1} yields

$$u_l^{n+1} = \left(2 - 2\lambda^2\right) u_l^n + \lambda^2 \left(u_{l+1}^n + u_{l-1}^n\right) - u_l^{n-1}. \tag{2.44}$$

Here,

$$\lambda = \frac{ck}{h} \tag{2.45}$$

is called the *Courant number* and plays a big role in stability and quality of the FD scheme. More specifically, λ needs to abide the (famous) Courant-Friedrichs-Lewy or *CFL condition* for short [**?**]

$$\lambda \leq 1, \tag{2.46}$$

which acts as a stability condition for scheme (**??**). More details on this are given in Section **??**.

As c, k and h are interdependent due to the CFL condition, it is useful to rewrite Eq. (**??**) in terms of known variables. As the time step k is based on the sample rate and thus (usually) fixed, and c is a user-defined wave speed, the CFL condition can be rewritten in terms of the grid spacing h:

$$h \geq ck, \tag{2.47}$$

which, in implementation, is used as a stability condition for the scheme. See Section **??** for more information on how to derive a stability condition from a FD scheme.

Stencil

As was done for several FD operators in Figure **??**, it can be useful to visualise the *stencil*, or region of operation, of a FD scheme. A stencil of a scheme visualises what grid values are necessary to calculate the state at the next time step u_l^{n+1}. Figure **??** shows the stencil for scheme (**??**) and – in essence – visualises the various shifts of the grid function in (**??**).

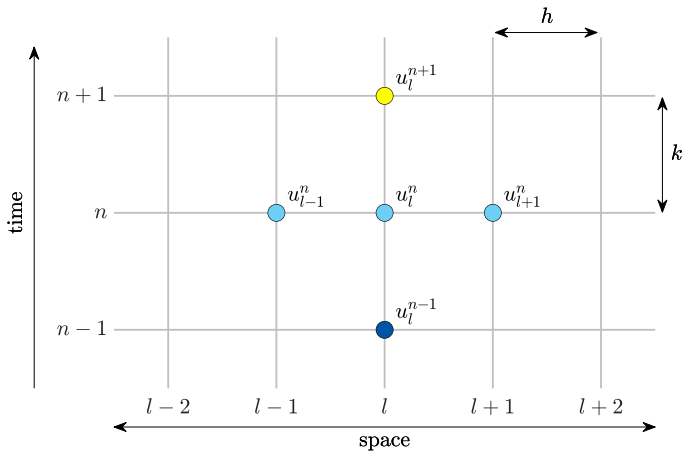

Fig. 2.9: The stencil, or region of operation, for the FD scheme in (**??**).

Boundary Conditions and Virtual Grid Points

The end points of the discrete domain are located at $l = 0$ and $l = N$. Substituting these locations into Eq. (**??**) seemingly shows that grid points outside of the defined domain are needed, namely u_{-1}^n and u_{N+1}^n. These can be referred to as *virtual grid points* and can be accounted for by discretising the boundary conditions in Eq. (**??**). Discretising these (using the most accurate centred spatial difference operator for the Neumann condition) yields

$$u_0^n = u_N^n = 0, \quad \text{(Dirichlet)} \tag{2.48a}$$

$$\delta_{x.} u_0^n = \delta_{x.} u_N^n = 0. \quad \text{(Neumann)} \tag{2.48b}$$

If Dirichlet boundary conditions are used, the states of the boundary points will always be zero and can therefore can be excluded from the calculations. The range of calculation then simply becomes $l \in \{1, \ldots, N-1\}$ and no virtual grid points are needed when performing the update.

If, on the other hand, Neumann conditions are used, the range of calculation remains $l \in \{0, \ldots, N\}$ and definitions for the virtual grid points need to be found. Expanding the operators in Eq. (**??**) and solving for u_{-1}^n and u_{N+1}^n provides the definitions for these virtual grid points based on values inside the defined domain:

$$\begin{aligned} &\frac{1}{2h}\left(u_1^n - u_{-1}^n\right) = 0, \\ &u_1^n - u_{-1}^n = 0, \\ &u_{-1}^n = u_1^n. \end{aligned} \qquad \begin{aligned} &\frac{1}{2h}\left(u_{N+1}^n - u_{N-1}^n\right) = 0, \\ &u_{N+1}^n - u_{N-1}^n = 0, \\ &u_{N+1}^n = u_{N-1}^n. \end{aligned}$$

At the boundaries, the update equation in (**??**) will then have the the above definitions for the virtual grid points substituted and will become

$$u_0^{n+1} = \left(2 - 2\lambda^2\right) u_0^n + 2\lambda^2 u_1^n - u_0^{n-1}, \tag{2.49}$$

and

$$u_N^{n+1} = \left(2 - 2\lambda^2\right) u_N^n + 2\lambda^2 u_{N-1}^n - u_N^{n-1}, \tag{2.50}$$

at the left and right boundary respectively.

2.4.3 Implementation: Excitation and Output

See Appendix **??** for a `MATLAB` implementation of the 1D wave equation.

A simple way to excite the system is to initialise the state using a raised cosine, or Hann window. More information on excitations will be given in Part **??**, but for completeness, the formula for a discrete raised cosine will be given here.

The discrete raised cosine can be parameterised by its center location l_c and width w from which the start index l_s and end index l_e can be calculated, according to

$$l_\mathrm{s} = l_\mathrm{c} - \lfloor w/2 \rfloor \quad \text{and} \quad l_\mathrm{e} = l_\mathrm{c} + \lfloor w/2 \rfloor, \tag{2.51}$$

where $\lfloor \cdot \rfloor$ denotes the flooring operation and needs to be used as all the above variables are integers. Furthermore, both l_s and l_e must fall into the defined spatial range of calculation. Then, a raised cosine with an amplitude of 1 can be calculated and used as an initial condition for the system according to

$$u_l^0 = u_l^{-1} = \begin{cases} 0.5 - 0.5\cos\left(\frac{2\pi(l - l_\mathrm{s})}{w-1}\right), & l_\mathrm{s} \leq l < l_\mathrm{e}, \\ 0, & \text{otherwise.} \end{cases} \tag{2.52}$$

As done for the implementation of the mass-spring system in Section **??**, both u_l^0 and u_l^{n-1} are initialised with the same state, as to only have an initial displacement, and not an initial velocity.

In `MATLAB`, an easier way to obtain a raised cosine is to use the `hann(w)` function which returns a raised cosine (or Hann window) of width `w`.

Output and Modes

After the system is excited, one can retrieve the output of the system by selecting a grid point l_out and listening to that at at the given sample rate f_s. An example using the parameters in Table **??** and Dirichlet boundary conditions is shown in Figure **??**.

As can be seen from Figure **??**, the output of the 1D wave equation contains many peaks in the frequency spectrum on top of the fundamental frequency. These are called *harmonic partials* or *harmonics* for short and arise from the

Name	Symbol (unit)	Value
User-defined parameters		
Length	L (m)	1
Wave speed	c (m/s)	1470
Sample rate	f_s (Hz)	44100
Derived parameters		
Fundamental frequency	f_0 (Hz)	735
No. of intervals	N (-)	30
Time step	k (s)	$\approx 2.27 \cdot 10^{-5}$
Grid spacing	h (m)	≈ 0.033
Courant number	λ (-)	1
Excitation and output		
Center location	l_c (-)	$0.2N$
Width	w (-)	4
Output location	l_out	3

Table 2.1: Parameters used for 1D wave equation example used in this section. The user-defined parameters have been chosen such that $\lambda = 1$.

various modes of vibration present in the system (see Figure **??**). Although the PDE has not been discretised using modal synthesis (another physical modelling technique discussed in Chapter **??**), the system can still be decomposed into different modes of vibration, each corresponding to a harmonic frequency. These modes are assumed to vibrate independently, and their weighted sum yields the eventual behaviour of the system.

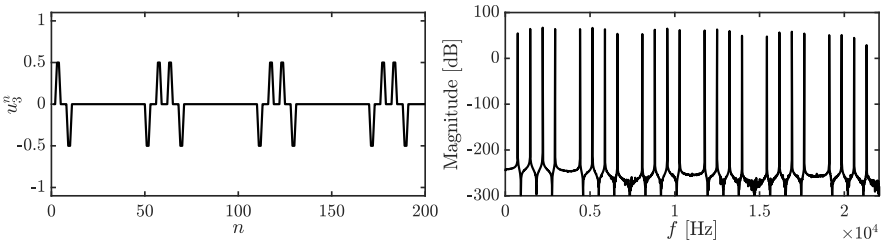

Fig. 2.10: The time-domain and frequency-domain output of the 1D wave equation with $f_0 = 735$ Hz and $f_\mathrm{s} = 44100$ Hz ($N = 30$ and $\lambda = 1$) and Dirichlet boundary conditions. The system is initialised with a raised cosine described in Eq. (**??**) with $l_\mathrm{c} = 0.2N$) and $w = 4$ and the output is retrieved at $l_\mathrm{out} = 3$.

The amount of modes present in the continuous PDE of the 1D wave equation is theoretically infinite. The amount present in the discrete FD scheme, however, is determined by the number of moving points in the system. If Dirichlet boundary conditions are used, this means that there are $N-1$ modes,

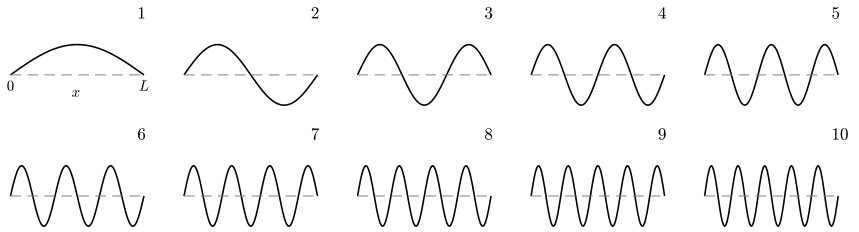

Fig. 2.11: The first 10 modal shapes of the 1D wave equation with Dirichlet boundary conditions defined for $x \in [0, L]$ (only shown for mode 1). All modes are The modes are normalised to have the same amplitude. The number of the shape can be determined by the amount of antinodes present in the shape.

and $N + 1$ modes for Neumann boundary conditions. If the CFL condition is satisfied with equality, the frequencies of these modes are integer multiples of the fundamental: $f_m = mf_0$ for mode number $m \in \{1, \ldots, N-1\}$ for Dirichlet and $m \in \{0, \ldots, N\}$ for Neumann boundary conditions. The frequency of the harmonics – and even the modal shapes – can be analytically derived using modal analysis as will be explained in Section **??**.

The amplitude of the different modes depends on the excitation location (and type) and the output location. Figure **??**, for example, seemingly shows that the system only exhibits 24 modes, rather than the 29 ($N - 1$) predicted. As the system is excited at $0.2N$, or in other words, $1/5^{\text{th}}$ of the length of the system, this means that that every 5^{th} mode will be attenuated. To understand how and/or why this happens, one can refer to Figure **??** and see that every 5^{th} modal shape has a node at $1/5^{\text{th}}$ its length. If the system is excited exactly there, this modal shape will not obtain any energy and will thus not resonate. Similarly, if the system is excited exactly in the middle, every 2^{nd} modal frequency will be attenuated as there is a node present in the corresponding modal shape. The output would then only contain odd-numbered modes.

2.4.4 Stability and Simulation Quality

As shown in Eq. (**??**), the Courant number needs to abide the CFL condition in order for the scheme to be stable. A system is regarded *unstable* if it exhibits (exponential) unbounded growth. If Neumann boundary conditions (free) are used, it is possible that the system drifts off over time. This does not mean that the system is unstable, and is actually entirely physically possible![2]

Besides stability, the value of λ is closely related to the quality of the simulation. If $\lambda = 1$, Eq. (**??**) is actually an exact solution to Eq. (**??**), which is quite

[2]Imagine a 'free' guitar string where the ends are not connected to the nut and bridge of a guitar. The string can be taken far away from the guitar without it breaking or exploding.

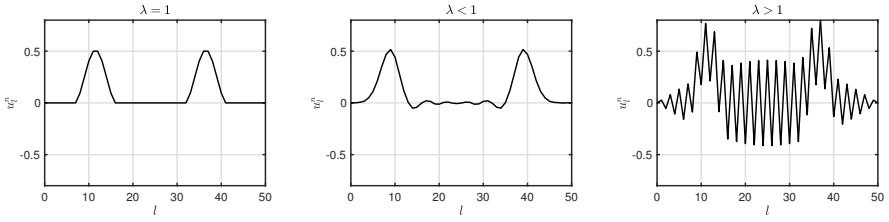

(a) $\lambda = 1$ **(b)** $\lambda = 0.9$ **(c)** $\lambda = 1.001$

Fig. 2.12: Grid function u_l^n visualised ~ 100 samples after excitation. (a) If $\lambda = 1$, the solution is exact. (b) If $\lambda < 1$ dispersive behaviour shows. (c) If $\lambda > 1$ the CFL condition in Eq. (**??**) is not satisfied and the system is unstable.

uncommon in the realm of differential equations! See Figure **??**. Identically, if Eq. (**??**) is satisfied with equality, the FD scheme is an exact solution to the PDE, and if h deviates from this condition, the quality of the simulation decreases.

If $\lambda < 1$, the quality of the simulation quality decreases in an effect called *numerical dispersion*. Dispersion is a phenomenon where some frequencies travel faster through a medium than others, which is desired in some models (see fx. Chapter **??**). Numerical dispersion, however, which is due to numerical inaccuracy, is usually not. Figure **??** shows an example when $\lambda = 0.9$, and one can observe that the wave propagation does not match the ideal case as Figure **??** shows. Moreover, bandlimiting effects occur, meaning that the highest frequency that the system can generate decreases. See Figure **??**. Higher modes get 'squished' together and are not exact multiples of the fundamental anymore. Section **??** elaborates on how to calculate the exact modal frequencies of a FD implementation of the 1D wave equation.

Finally, if $\lambda > 1$ the system becomes unstable. An example is shown in Figure **??**. Unstable behaviour usually comes in the form of high frequencies (around the Nyquist frequency of $f_\mathrm{s}/2$) growing without bounds.

So in what situation would the stability condition not be satisfied with equality? As mentioned in Section **??**, a continuous domain $\mathcal{D} = [0, L]$ for a system of length L needs to be divided into N equal sections of length h in the discretisation process. A logical step to calculate N would be to divide L by h calculated using Eq. (**??**) satisfied with equality to get the highest possible simulation quality. However, this calculation might not result in an integer value, which N should be! To stay as close to the stability condition as possible, the following calculations are performed in order:

$$h := ck, \quad N := \left\lfloor \frac{L}{h} \right\rfloor, \quad h := \frac{L}{N}, \quad \lambda := \frac{ck}{h}. \tag{2.53}$$

In other words, Eq. (**??**) is satisfied with equality and used to calculate integer

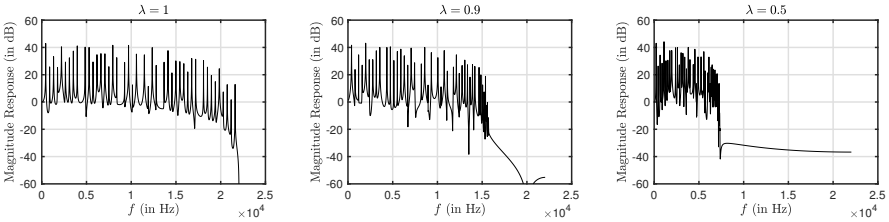

(a) $\lambda = 1$ **(b)** $\lambda = 0.9$ **(c)** $\lambda = 1.001$

Fig. 2.13: Frequency spectra of the simulation output. The Courant number is set to (a) $\lambda = 1$, (b) $\lambda = 0.9$ and (c) $\lambda = 0.5$. One can observe that for lower values of λ the bandwidth of the output decreases drastically.

N. After this, h is recalculated based on N and used to calculate the Courant number using Eq. (**??**). This process assures that N is an integer and that the CFL condition is satisfied, though not necessarily with equality.

To understand why h needs to be recalculated, consider the following example. Consider the 1D wave equation defined over domain $\mathcal{D} = [0, L]$ where $L = 1$. Furthermore, we say that the system should produce a fundamental frequency of $f_0 = 750$ Hz which requires a wave speed of $c = 1500$ m/s according to Eq. (**??**). If we use the commonly-used sample rate of $f_\mathrm{s} = 44100$ Hz, and recalling that $k = 1/f_\mathrm{s}$, these values can be filled into (**??**) satisfied with equality and yields $h \approx 0.034$. If we divide the length by the grid spacing, we get $L/h = 29.4$, meaning that exactly 29.4 intervals of size h fit in the domain $\mathcal{D}$. However, the number of intervals needs to be an integer and – using Eq. (**??**) – we get $N = 29$. If h is not recalculated according to (**??**), the total length will be 29 times the grid spacing h. This results in $L \approx 0.986$ and is slightly less than the original length of 1. Although the CFL condition will be satisfied with equality, the fundamental frequency will be slightly higher than desired: $f_0 \approx 760.34$ Hz. If h is recalculated based on N, then L and f_0 will be unchanged, and the system will have the correct fundamental frequency. The Courant number $\lambda \approx 0.986$ is still very close to satisfying condition (**??**), and the decrease in quality will be perceptually irrelevant – or at the very least, less perceptually relevant than the change in f_0 if h is not recalculated.

more intuition on stability and gridspacing here

Chapter 3

Analysis Techniques

This chapter provides some useful techniques to analyse FD schemes. Techniques to analyse PDEs also exist, but the focus here is of a practical nature and will especially revolve around the discrete schemes. This chapter can be seen as a 'tutorial' on how to use these techniques. Starting off with some necessary theory on matrices and other mathematical tools, this chapter continues to introduce

- *Frequency domain analysis*, which can be used to determine stability conditions of (linear and time-invariant) FD schemes,
- *Energy analysis*, which can both used to debug implementations of FD schemes, as well as determine stability conditions in a more general fashion, and
- *Modal analysis* which can be used to determine the modal frequencies (and damping per mode) that a FD scheme exhibits.

perhaps also dispersion analysis?

3.1 Matrices

For several purposes, such as implementation in `MATLAB` and several analysis techniques described shortly, is useful to write a FD scheme in *matrix form*. A matrix is a rectangular array with numerical elements and its dimensions are denoted using "$row \times column$". A 3×5 matrix, for example, thus has 3 rows and 5 columns (see Figure **??**). Along those lines, a *row vector* is a matrix with 1 row and more than 1 column and a *column vector* is a matrix with 1 column and more than 1 row. If a matrix has only 1 row and 1 column, it can be used as a *scalar*.

In this document, matrices and vectors are written using bold symbols. A matrix is denoted by a capital letter – such as $\mathbf{A}$ – whereas vectors are decapitalised – such as $\mathbf{u}$. An element in a matrix is denoted with a non-bold, decapitalised variable, where the subscripts indicate the indices of the row and column. For example, the element in the 2nd row and the 4th column of a matrix $\mathbf{A}$ is denoted as a_{24}. An element in a vector only has one subscript, regardless of whether it is a row or a column vector.

3.1.1 Operations

Adding, subtracting, multiplying and dividing a matrix by a scalar (a single number) is valid and happens on an element-by-element basis. For a 2×2 matrix $\mathbf{A}$ and scalar p the following operations hold

$$p + \mathbf{A} = \mathbf{A} + p = \begin{bmatrix} p + a_{11} & p + a_{12} \\ p + a_{21} & p + a_{22} \end{bmatrix}, \quad p - \mathbf{A} = \mathbf{A} - p = \begin{bmatrix} p - a_{11} & p - a_{12} \\ p - a_{21} & p - a_{22} \end{bmatrix}$$

$$p\mathbf{A} = \mathbf{A}p = \begin{bmatrix} p \cdot a_{11} & p \cdot a_{12} \\ p \cdot a_{21} & p \cdot a_{22} \end{bmatrix}, \quad \text{and} \quad \mathbf{A}/p = \begin{bmatrix} a_{11}/p & a_{12}/p \\ a_{21}/p & a_{22}/p \end{bmatrix}.$$

Notice that although a matrix can be divided by a scalar, a scalar can not necessarily be divided by a matrix. See Section **??** for more information.

Matrix transpose

A matrix or vector can be *transposed*, and is indicated with the T operator. Transposing a matrix $\mathbf{A}$ is denoted by $\mathbf{A}^T$. means that the elements in the i^{th} row and the j^{th} column of the original matrix become the elements in the j^{th} row and the i^{th} column of the transposed matrix. Essentially the row and column indices of the elements inside the matrix get switched according to

$$a_{ij} = a_{ji}. \tag{3.1}$$

Also see Figure **??**. For a row vector, the transpose operation simply changes it to a column vector and vice versa. Another way of seeing a transpose is that all the elements get flipped over the *main diagonal* of the matrix. The main diagonal comprises the elements a_{ij} where $i = j$ and a transpose does not affect the location of these elements.

Matrix Multiplication

Matrix multiplication (this includes matrix-vector multiplication) is different from regular multiplication in that it needs to abide several extra rules. In order for matrix multiplication to be valid, the number of columns of the first matrix needs to be equal to the number of rows in the second matrix. The

$$\mathbf{A} = \begin{bmatrix} a_{11} & a_{12} & a_{13} & a_{14} & a_{15} \\ a_{21} & a_{22} & a_{23} & a_{24} & a_{25} \\ a_{31} & a_{32} & a_{33} & a_{34} & a_{35} \end{bmatrix} \qquad \mathbf{A}^T = \begin{bmatrix} a_{11} & a_{21} & a_{31} \\ a_{12} & a_{22} & a_{32} \\ a_{13} & a_{23} & a_{33} \\ a_{14} & a_{24} & a_{34} \\ a_{15} & a_{25} & a_{35} \end{bmatrix}$$

(a) A 3×5 matrix $\mathbf{A}$. **(b)** A transposed matrix $\mathbf{A}^T$ of size 5×3.

Fig. 3.1: A matrix $\mathbf{A}$ and its transpose $\mathbf{A}^T$. The elements get flipped along the main diagonal of the matrix according to Eq. (**??**).

result will then be a matrix with a number of rows equal to that of the first matrix and a number of columns equal to that of the second matrix. See Figure **??** for reference.

As an example, consider the $L \times M$ matrix $\mathbf{A}$ and a $M \times N$ matrix $\mathbf{B}$ with $L \neq N$. The multiplication $\mathbf{AB}$ is defined as the number of columns of matrix $\mathbf{A}$ (M) is equal to the number of rows of matrix $\mathbf{B}$ (also M). The result, $\mathbf{C}$, is a $L \times N$ matrix. The multiplication $\mathbf{BA}$ is undefined as the number of columns of the first matrix does not match the number of rows in the second matrix. A valid multiplication of two matrices written in their dimensions is

$$\overbrace{(L \times M)}^{\mathbf{A}} \cdot \overbrace{(M \times N)}^{\mathbf{B}} = \overbrace{(L \times N)}^{\mathbf{C}}. \tag{3.2}$$

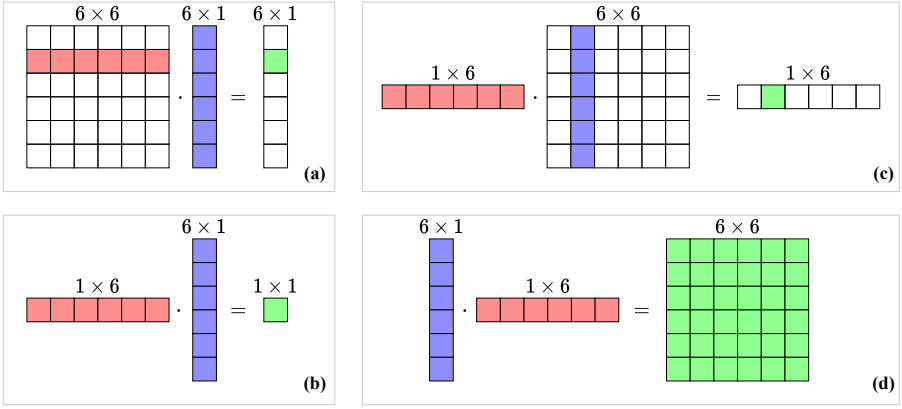

Fig. 3.2: Visualisation of valid matrix multiplications. The "inner" dimensions (columns of the left matrix and rows of the right) must match and result in a matrix with a size of "outer" dimensions (rows of the left matrix and columns of the right).

3.1.2 In a FDTD context

Matrix multiplication when working with FDTD methods usually involves multiplying a square matrix (with equal rows and columns) onto a column vector (see Figure **??**a). Consider a $(N+1) \times (N+1)$ square matrix $\mathbf{A}$ and a $(N+1) \times 1$ column vector $\mathbf{u}$. Multiplying these results in a $(N+1) \times 1$ column vector $\mathbf{w}$:

$$\mathbf{A}\mathbf{u} = \mathbf{w}. \tag{3.3}$$

Expanding this operation results in

$$\underbrace{\begin{bmatrix} a_{00} & a_{01} & \dots & a_{0N} \\ a_{10} & a_{11} & \dots & a_{2N} \\ \vdots & \vdots & & \vdots \\ a_{N0} & a_{N1} & \dots & a_{NN} \end{bmatrix}}_{\mathbf{A}} \underbrace{\begin{bmatrix} u_0 \\ u_1 \\ \vdots \\ u_N \end{bmatrix}}_{\mathbf{u}} = \underbrace{\begin{bmatrix} a_{00}u_0 + a_{01}u_1 + \ldots + a_{0N}u_N \\ a_{10}u_0 + a_{11}u_1 + \ldots + a_{1N}u_N \\ \vdots \\ a_{N0}u_0 + a_{N1}u_1 + \ldots + a_{NN}u_N \end{bmatrix}}_{\mathbf{w}} \tag{3.4}$$

where the indexing of the matrix elements starts at 0 rather than 1 here, as it relates better to a FDTD context.

Operators in Matrix Form

FD operators approximating spatial derivatives and averages introduced in Section **??** can be written in matrix form and applied to a column vector $\mathbf{u}^n$ containing the state of the system at time index n. These matrices are square and their sizes depend on the number of grid points the system is described for and the boundary conditions. Not assuming a specific size for now, the FD operators in (**??**) can be written in matrix form according to

$$\mathbf{D}_{x+} = \frac{1}{h}\begin{bmatrix} \ddots & \ddots & & & \mathbf{0} \\ & -1 & 1 & & \\ & & -1 & 1 & \\ & & & -1 & 1 \\ & & & & -1 \;\; \ddots \\ \mathbf{0} & & & & \ddots \end{bmatrix} \qquad \mathbf{D}_{x-} = \frac{1}{h}\begin{bmatrix} \ddots & & & & \mathbf{0} \\ \ddots & 1 & & & \\ & -1 & 1 & & \\ & & -1 & 1 & \\ & & & -1 & 1 \\ \mathbf{0} & & & \ddots & \ddots \end{bmatrix}$$

$$\mathbf{D}_{x\cdot} = \frac{1}{2h}\begin{bmatrix} \ddots & \ddots & & & \mathbf{0} \\ \ddots & 0 & 1 & & \\ & -1 & 0 & 1 & \\ & & -1 & 0 & 1 \\ & & & -1 & 0 \;\; \ddots \\ \mathbf{0} & & & \ddots & \ddots \end{bmatrix}$$

where the diagonal dots denote that the values on the respective diagonals continue until the top-left and bottom-right corners of the matrix.The **0**s indicate that the rest of the values in the matrix are zeros.

is this how you explain it?

Averaging operators μ_{x+}, μ_{x-} and $\mu_{x\cdot}$ are defined in a similar way:

$$\mathbf{M}_{x+} = \frac{1}{2}\begin{bmatrix} \ddots & \ddots & & & \mathbf{0} \\ & 1 & 1 & & \\ & & 1 & 1 & \\ & & & 1 & 1 & \ddots \\ \mathbf{0} & & & & & \ddots \end{bmatrix} \qquad \mathbf{M}_{x-} = \frac{1}{2}\begin{bmatrix} \ddots & & & & \mathbf{0} \\ \ddots & 1 & & & \\ & 1 & 1 & & \\ & & 1 & 1 & \\ & & & 1 & 1 & \ddots \\ \mathbf{0} & & & & \ddots & \ddots \end{bmatrix}$$

$$\mathbf{M}_{x\cdot} = \frac{1}{2}\begin{bmatrix} \ddots & \ddots & & & \mathbf{0} \\ \ddots & 0 & 1 & & \\ & 1 & 0 & 1 & \\ & & 1 & 0 & 1 & \ddots \\ \mathbf{0} & & & \ddots & \ddots \end{bmatrix}$$

It is important to notice that only spatial operators are written in this matrix form and then applied to state vectors at different time steps ($\mathbf{u}^{n+1}$, $\mathbf{u}^n$ and $\mathbf{u}^{n-1}$).

Finally, the identity matrix is a matrix with only 1s on the diagonal and 0s elsewhere as

$$\mathbf{I} = \begin{bmatrix} \ddots & & & & \mathbf{0} \\ & 1 & & & \\ & & 1 & & \\ & & & 1 & \\ & & & & 1 & \\ \mathbf{0} & & & & & \ddots \end{bmatrix}$$

Schemes and Update Equations in Matrix Form

With the spatial operators in matrix form presented above, the FD scheme of the 1D wave equation in Eq. (**??**) can be written in matrix form.

If the Dirichlet boundary conditions in (**??**) are used, the end points of the system do not have to be included in the calculation. The values of the grid function u_l^n for $l \in \{1, \ldots, N-1\}$ can then be stored in a column vector according to $\mathbf{u}^n = [u_1^n, \ldots, u_{N-1}^n]^T$. Furthermore, $(N-1) \times (N-1)$ matrix

$\mathbf{D}_{xx}$ is defined as

$$\mathbf{D}_{xx} = \frac{1}{h^2}\begin{bmatrix} -2 & 1 & & & \mathbf{0} \\ 1 & -2 & 1 & & \\ & \ddots & \ddots & \ddots & \\ & & 1 & -2 & 1 \\ \mathbf{0} & & & 1 & -2 \end{bmatrix}. \tag{3.5}$$

If instead, Neumann boundary conditions in Eq. (**??**) are used, the values of u_l^n for the full range $l \in \{0, \ldots, N\}$ need be stored as $\mathbf{u}^n = [u_0^n, \ldots, u_N^n]^T$ and the $(N+1) \times (N+1)$ matrix $\mathbf{D}_{xx}$ will be

$$\mathbf{D}_{xx} = \frac{1}{h^2}\begin{bmatrix} -2 & 2 & & & \mathbf{0} \\ 1 & -2 & 1 & & \\ & \ddots & \ddots & \ddots & \\ & & 1 & -2 & 1 \\ \mathbf{0} & & & 2 & -2 \end{bmatrix}, \tag{3.6}$$

where the 2s in the top and bottom row correspond to the multiplication by 2 with u_1^n and u_{N-1}^n in update equations (**??**) and (**??**) respectively.

Regardless of the boundary conditions, the FD scheme in (**??**) can be written in matrix form as

$$\frac{1}{k^2}\left(\mathbf{u}^{n+1} - 2\mathbf{u} + \mathbf{u}^{n-1}\right) = c^2\mathbf{D}_{xx}\mathbf{u}^n, \tag{3.7}$$

and rewritten to a matrix form of the update equation analogous to Eq. (**??**)

$$\mathbf{u}^{n+1} = (2\mathbf{I} + c^2k^2\mathbf{D}_{xx})\mathbf{u}^n - \mathbf{u}^{n-1}. \tag{3.8}$$

The identity matrix is necessary here for correct matrix addition.

3.1.3 Matrix Inverse

If a matrix has the same number of rows as columns, it is called a *square matrix*. Square matrices have special properties, one of which is that it (usually) can be *inverted*. A square matrix $\mathbf{A}$ is invertable if there exists a matrix $\mathbf{B}$ such that

$$\mathbf{AB} = \mathbf{BA} = \mathbf{I}. \tag{3.9}$$

This matrix $\mathbf{B}$ is then called the *inverse* of $\mathbf{A}$ and can be written as $\mathbf{A}^{-1}$. Not all square matrices have an inverse, in which case it is called *singular*. Rather than going through manually inverting a matrix, or determining whether it is singular, the following function in `MATLAB` will provide the inverse of a matrix `A`:

```
A_inverted = inv(A);
```

The inverse of a *diagonal matrix* (a matrix with non-zero elements on its main diagonal and the rest zeros) is obtained by replacing the diagonal elements by their reciprocal. So for a diagonal 3×3 matrix, the following holds:

$$\begin{bmatrix} a_{11} & 0 & 0 \\ 0 & a_{12} & 0 \\ 0 & 0 & a_{33} \end{bmatrix}^{-1} = \begin{bmatrix} \frac{1}{a_{11}} & 0 & 0 \\ 0 & \frac{1}{a_{12}} & 0 \\ 0 & 0 & \frac{1}{a_{33}} \end{bmatrix}.$$

3.1.4 Systems of Linear Equations

Matrices can be conveniently used to solve *systems of linear equations*, a set of linear equations containing the same set of variables.

For example, take the system of linear equations

$$\begin{aligned} x + z &= 6, \\ z - 3y &= 7, \\ 2x + y + 3z &= 15, \end{aligned}$$

with independent variables x, y and z. The goal is to find a solution for these variables that satisfy all three equations. This system could be solved by hand using algebraic methods, but alternatively, the system can be written in matrix form:

$$\mathbf{A}\mathbf{u} = \mathbf{w}. \tag{3.10}$$

Here, column vector $\mathbf{u}$ contains the independent variables x, y, and z, matrix $\mathbf{A}$ contains the coefficients multiplied onto these variables and $\mathbf{w}$ contains the right-hand side, i.e., the coefficients not multiplied onto any of the variables:

$$\underbrace{\begin{bmatrix} 1 & 0 & 1 \\ 0 & -3 & 1 \\ 2 & 1 & 3 \end{bmatrix}}_{\mathbf{A}} \underbrace{\begin{bmatrix} x \\ y \\ z \end{bmatrix}}_{\mathbf{u}} = \underbrace{\begin{bmatrix} 6 \\ 7 \\ 15 \end{bmatrix}}_{\mathbf{w}}$$

We can then solve for $\mathbf{u}$ by taking the inverse of $\mathbf{A}$ (see Section **??**) and multiplying this onto $\mathbf{w}$

$$\mathbf{u} = \mathbf{A}^{-1}\mathbf{w}. \tag{3.11}$$

Generally, if X unknowns are described by X equations, the unknowns can be solved for using this method.

Solving a system of linear equations can be implemented in MATLAB by using the code given in Section **??** and multiplying this onto a vector `w`

```
u = inv(A) * w;
```

or more compactly, by using the '\' operator:

```
u = A\w;
```

3.1.5 Eigenvalue Problems

A square matrix $\mathbf{A}$ is characterised by its *eigenvalues* and corresponding *eigenvectors*. In a FDTD context, these are usually associated with the modes of a system, where the eigenvalues relate to the modal frequencies and the eigenvectors to the modal shapes. Section **??** will provide more information on this.

ask stefan

To find these characteristic values for a $p \times p$ matrix $\mathbf{A}$, an equation of the following form must be solved

$$\mathbf{A}\phi = \lambda\phi. \tag{3.12}$$

This is called is an *eigenvalue problem* and has p solutions (corresponding to the dimensions of $\mathbf{A}$). These are the p^{th} eigenvector ϕ_p and the corresponding eigenvalue λ_p which is calculated using

$$\lambda_p = \text{eig}_p(\mathbf{A}), \tag{3.13}$$

where $\text{eig}_p(\cdot)$ denotes the p^{th} eigenvalue of. Instead of delving too deep into eigenvalue problems and the process of how to solve them, an easy way to obtain the solutions using `MATLAB` is provided here:

```
[phi, lambda] = eig(A, 'vector');
```

The p^{th} eigenvector appears in the p^{th} column of $p \times p$ matrix `phi` and the corresponsding eigenvalues are given in a $p \times 1$ column vector `lambda`. Note that the outcome is not necessarily sorted! To do this, do

check whether this is necessary

```
[lambda, order] = sort(lambda);
phi = phi(:, order);
```

3.2 Mathematical Tools and Product Identities

Some useful mathematical tools used for the energy analysis techniques presented in Section **??** will be shown here. The tools shown here can be applied to 1D systems. These will be extended to 2D systems in Chapter **??**.

3.2.1 Inner product

For two functions $f(x,t)$ and $g(x,t)$ defined for $x \in \mathcal{D}$ where $\mathcal{D} = [0, L]$, their l_2 inner product and l_2 norm are defined as

$$\langle f, g\rangle_{\mathcal{D}} = \int_{\mathcal{D}} fg dx \quad \text{and} \quad \|f\|_{\mathcal{D}} = \sqrt{\langle f, f\rangle_{\mathcal{D}}}. \tag{3.14}$$

These functions do not have to be time-dependent (i.e., they can also simply be $f(x)$ and $g(x)$), but as all functions used in this work are in fact time-dependent, this is left for coherence. It is also important to note that these functions do not have to be 'isolated' state variables per se (such as $u(x,t)$ used in the previous chapter), but could also be a state variable with a derivative applied to it (such as $\partial_t u(x,t)$).

The discrete inner product of any two (1D) functions f_l^n and g_l^n defined for $l \in d$, with discrete domain $d = \{0, \ldots, N\}$, is

$$\langle f_l^n, g_l^n \rangle_d = \sum_{l=0}^{N} h f_l^n g_l^n, \tag{3.15}$$

where the multiplication by h is the discrete counterpart of dx in the continuous definition in (**??**). Also useful are the primed inner product

$$\langle f_l^n, g_l^n \rangle_d' = \sum_{l=1}^{N-1} h f_l^n g_l^n + \frac{h}{2} f_0^n g_0^n + \frac{h}{2} f_N^n g_N^n, \tag{3.16}$$

and the more general weighted inner product

$$\langle f_l^n, g_l^n \rangle_d^{\epsilon_\mathrm{l}, \epsilon_\mathrm{r}} = \sum_{l=1}^{N-1} h f_l^n g_l^n + \frac{\epsilon_\mathrm{l}}{2} h f_0^n g_0^n + \frac{\epsilon_\mathrm{r}}{2} h f_N^n g_N^n, \tag{3.17}$$

which scale the boundary points of the regular inner product. Naturally, if $\epsilon_\mathrm{l} = \epsilon_\mathrm{r} = 1$, Eq. (**??**) reduces to Eq. (**??**), and if $\epsilon_\mathrm{l} = \epsilon_\mathrm{r} = 2$, (**??**) reduces to (**??**).

3.2.2 Summation by Parts

Extremely useful when performing energy analysis on distributed systems is *summation by parts*, which is the discrete counterpart of integration by parts. Although its application will be only be apparent when actually performing an energy analysis (see fx. Sections **??** and **??**) some definitions will be presented here for future reference.

Here, the same functions as in the previous section, $f(x,t)$ and $g(x,t)$ and domain $\mathcal{D}$, will be used. Applying a spatial derivative to g, and using Eq. (**??**), integration by parts is defined as

$$\langle f, \partial_x g \rangle_\mathcal{D} = -\langle \partial_x f, g \rangle_\mathcal{D} + fg|_0^L \tag{3.18}$$

where $fg|_0^L$ describes the boundary terms that appeared in the process. One can observe that the spatial derivative switched function and is now applied to f rather than g.

In discrete time, we use the same two (1D) functions as before f_l^n and g_l and are defined for $l \in d$ with discrete domain $d = \{0, \ldots, N\}$. Then, using

the discrete inner product in Eq. (**??**), two variants of summation by parts are defined as

$$\langle f_l^n, \delta_{x-} g_l^n \rangle_d = -\langle \delta_{x+} f_l^n, g_l^n \rangle_d + f_{N+1}^n g_N^n - f_0^n g_{-1}^n, \tag{3.19a}$$
$$\langle f_l^n, \delta_{x+} g_l^n \rangle_d = -\langle \delta_{x-} f_l^n, g_l^n \rangle_d + f_N^n g_{N+1}^n - f_{-1}^n g_0^n. \tag{3.19b}$$

A derivation of Eq. (**??**) is given below. As in the case of integration by parts in Eq. (**??**), the process of summation by parts causes the derivative to be applied to the other function and the sign of the resulting inner product changes. Important to note, is that the sign (forward / backward) of the derivative operator has also changed. Lastly, discrete boundary terms have appeared and it can be seen that values outside of the defined domain are needed, i.e., g_{N+1}^n and f_{-1}^n. These can be accounted for by the boundary conditions imposed on the system (see Section **??** as an example).

One could also choose to work with reduced domains after summation by parts. Domains that have one fewer point at the boundaries are defined as $\underline{d} = \{0, \ldots, N-1\}$, $\overline{d} = \{1, \ldots, N\}$ and $\underline{\overline{d}} = \{1, \ldots, N-1\}$. The following identities can be shown to hold

$$\langle f_l^n, \delta_{x-} g_l^n \rangle_d = -\langle \delta_{x+} f_l^n, g_l^n \rangle_{\underline{d}} + f_N^n g_N^n - f_0^n g_{-1}^n, \tag{3.20a}$$
$$\langle f_l^n, \delta_{x+} g_l^n \rangle_d = -\langle \delta_{x-} f_l^n, g_l^n \rangle_{\overline{d}} + f_N^n g_{N+1}^n - f_0^n g_0^n, \tag{3.20b}$$

and, using the primed inner product in Eq. (**??**),

$$\langle f_l^n, \delta_{x-} g_l^n \rangle'_d = -\langle \delta_{x+} f_l^n, g_l^n \rangle_{\underline{d}} + f_N^n \mu_{x-} g_N^n - f_0^n \mu_{x-} g_0^n, \tag{3.21a}$$
$$\langle f_l^n, \delta_{x+} g_l^n \rangle'_d = -\langle \delta_{x-} f_l^n, g_l^n \rangle_{\overline{d}} + f_N^n \mu_{x+} g_N^n - f_0^n \mu_{x+} g_0^n, \tag{3.21b}$$

all of which will prove useful in energy analysis techniques later on. A derivation of (**??**) is given below.

Finally, recalling that $\delta_{xx} = dxp\delta_{x-}$, one can apply summation by parts twice to get the following identities

$$\langle f, \delta_{xx} g \rangle_d = \langle \delta_{xx} f, g \rangle_d + f_N \delta_{x+} g_N - g_N \delta_{x+} f_N - f_0 \delta_{x-} g_0 + g_0 \delta_{x-} f_0, \tag{3.22a}$$
$$\langle f, \delta_{xx} g \rangle_d = \langle \delta_{xx} f, g \rangle_{\underline{\overline{d}}} + f_N \delta_{x+} g_N - g_N \delta_{x-} f_N - f_0 \delta_{x-} g_0 + g_0 \delta_{x+} f_0, \tag{3.22b}$$
$$\langle f, \delta_{xx} g \rangle'_d = \langle \delta_{xx} f, g \rangle'_d + f_N \delta_{x\cdot} g_N - g_N \delta_{x\cdot} f_N - f_0 \delta_{x\cdot} g_0 + g_0 \delta_{x\cdot} f_0 \tag{3.22c}$$

Derivations

To see why the above identities hold true, it is useful to briefly go through a derivation. As an example, we go through Eqs. (**??**) and (**??**) as they have the same inner product as a starting point, but yield different results. In the following, $d = \{0, \ldots, N\}$ and $N = 2$ are used.

Starting with Eq. (**??**), suppressing the n superscript for brevity, and using the definition for the discrete inner product in Eq. (**??**), we get

$$\begin{aligned}
\langle f_l, \delta_{x-} g_l \rangle_d &= \sum_{l=0}^{2} h f_l \frac{1}{h} \left(g_l - g_{l-1} \right), \\
&= f_0 g_0 - f_0 g_{-1} + f_1 g_1 - f_1 g_0 + f_2 g_2 - f_2 g_1, \\
&= g_0(f_0 - f_1) - f_0 g_{-1} + g_1(f_1 - f_2) + g_2(f_2 - f_3) + f_3 g_2, \\
&= -g_0(f_1 - f_0) - g_1(f_2 - f_1) - g_2(f_3 - f_2) + f_3 g_2 - f_0 g_{-1}, \\
&= -\sum_{l=0}^{2} h g_l \frac{1}{h} \left(f_{l+1} - f_l \right) + f_3 g_2 - f_0 g_{-1}, \\
&= -\langle \delta_{x+} f_l, g_l \rangle_d + f_3 g_2 - f_0 g_{-1}.
\end{aligned}$$

As $N = 2$, the result is identical to Eq. (**??**).

Similarly, identity (**??**) can be proven to hold:

$$\begin{aligned}
\langle f_l, \delta_{x-} g_l \rangle_d &= \sum_{l=0}^{2} h f_l \frac{1}{h} \left(g_l - g_{l-1} \right), \\
&= f_0 g_0 - f_0 g_{-1} + f_1 g_1 - f_1 g_0 + f_2 g_2 - f_2 g_1, \\
&= -f_0 g_{-1} + g_0(f_0 - f_1) + g_1(f_1 - f_2) + f_2 g_2, \\
&= -g_0(f_1 - f_0) - g_1(f_2 - f_1) + f_2 g_2 - f_0 g_{-1}, \\
&= \sum_{l=0}^{1} h g_l \frac{1}{h} (f_{l+1} - f_l) + f_2 g_2 - f_0 g_{-1}, \\
&= -\langle \delta_{x+} f_l, g_l \rangle_{\underline{d}} + f_2 g_2 - f_0 g_{-1},
\end{aligned}$$

where the resulting inner product has a reduced domain of $\underline{d} = \{0, \ldots, N-1\}$. Similar processes can be used to prove the other identities presented in this section.

3.2.3 Product identities

Some useful identities used in this work are

$$(\delta_{t\cdot} u_l^n)(\delta_{tt} u_l^n) = \delta_{t+}\left(\frac{1}{2}(\delta_{t-} u_l^n)^2\right), \tag{3.23a}$$

$$(\delta_{t\cdot} u_l^n) u_l^n = \delta_{t+}\left(\frac{1}{2} u_l^n e_{t-} u_l^n\right), \tag{3.23b}$$

$$(\delta_{t+} u_l^n)(\mu_{t+} u_l^n) = \delta_{t+}\left(\frac{1}{2}(u_l^n)^2\right), \tag{3.23c}$$

$$(\delta_{t\cdot} u_l^n)(\mu_{t\cdot} u_l^n) = \delta_{t\cdot}\left(\frac{1}{2}(u_l^n)^2\right), \tag{3.23d}$$

$$u_l^n e_{t-} u_l^n = (\mu_{t-} u_l^n)^2 - \frac{k^2}{4}(\delta_{t-} u_l^n)^2 \tag{3.23e}$$

These identities can be used for spatial derivatives as well by substituting the 't' subscripts for 'x'.

When an operator is applied to a product of two grid functions, the discrete counterpart of the product rule needs to be used according to

$$\delta_{t+}(u_l^n w_l^n) = (\delta_{t+} u_l^n)(\mu_{t+} w_l^n) + (\mu_{t+} u_l^n)(\delta_{t+} w_l^n). \tag{3.24}$$

3.3 Frequency Domain Analysis

Frequency domain analysis, also called Fourier analysis, is a way to determine various properties of a FD scheme, including conditions for stability. The process is similar to finding stability for digital filters. In essence, a FD scheme can be seen as a complex filter of which its coefficients are defined by physical parameters. This section will explain how to obtain a frequency-domain representation of a scheme and will mainly follow [**?**], albeit in a slightly more practical manner.

Frequency-domain representation and Ansatz

Frequency-domain analysis of FD schemes starts by performing a *z-transform* on the scheme. The z-transform converts a discrete signal into a frequency-domain representation, and is extensively used in the field of digital signal processing (DSP) to analyse the behaviour and especially stability of digital filters. To not go too much into detail here, the interested reader is referred to the very comprehensive explanation on the z-transform given in [**?**, Ch. 5].

If a system is distributed in space, one can perform a spatial Fourier transform on a grid function. Frequency-domain analysis in the distributed case is called von Neumann analysis which first appeared in [**?**] and is heavily used

in [?]. The discrete-time z-transform and discrete spatial Fourier transform performed on a 1D grid function are defined as [?]

$$\hat{u} = \sum_{n=-\infty}^{\infty} u_l^n z^{-n} \quad \text{and} \quad \tilde{u} = \sum_{l=-\infty}^{\infty} u_l^n e^{-jl\beta h} \tag{3.25}$$

with complex number $z = e^{sk}$, complex frequency $s = j\omega + \sigma$ (more elaborated on in **??**) and real wavenumber β. Frequency-domain analysis in 2D will be elaborated on in Section **??**.

check if I should not refer to a subsection

A shortcut to performing a full frequency-domain analysis is to use a test solution, or *ansatz*, and replace the grid functions by their transforms. The grid function for a 1D system can be replaced by an ansatz of the form (1D) [?]

check reference

$$u_l^n \overset{\mathcal{A}}{\Longrightarrow} z^n e^{jl\beta h} \tag{3.26}$$

where "$\overset{\mathcal{A}}{\Longrightarrow}$" indicates to replace the grid function with the ansatz (the shortcut to taking the full z-transform and spatial Fourier transform).

Like in the DSP realm, the power of z indicates a temporal shift, i.e., z^{-1} is a one-sample delay. In a FDTD context, this corresponds to a time shift as seen in Section **??**. For spatially distributed systems, a shift in l can be interpreted as a phase shift of a frequency with wavenumber β. See Table **??** for the frequency-domain representation of of grid functions with their temporal and spatial indices shifted in different ways.

check

Grid function	Ansatz	Result
u_l^n	$z^0 e^{j0\beta h}$	1
u_l^{n+1}	$z^1 e^{j0\beta h}$	z
u_l^{n-1}	$z^{-1} e^{j0\beta h}$	z^{-1}
u_{l+1}^n	$z^0 e^{j1\beta h}$	$e^{j\beta h}$
u_{l-1}^n	$z^0 e^{j(-1)\beta h}$	$e^{-j\beta h}$
u_{l+2}^n	$z^0 e^{j2\beta h}$	$e^{j2\beta h}$
u_{l-2}^n	$z^0 e^{j(-2)\beta h}$	$e^{-j2\beta h}$
u_{l+1}^{n-1}	$z^{-1} e^{j1\beta h}$	$z^{-1} e^{j\beta h}$
u_{l-1}^{n-1}	$z^{-1} e^{j(-1)\beta h}$	$z^{-1} e^{-j\beta h}$

Table 3.1: Frequency-domain representation of a grid function using ansatz (**??**) with frequently appearing temporal and spatial shifts.

Using these definitions, the effect of various operators on a grid function can be written in their frequency-domain representation. For systems distributed in space, the following trigonometric identities are extremely useful when

performing the analyses [**?**, p. 71]:

$$\sin(x) = \frac{e^{jx} - e^{-jx}}{2j} \quad \Rightarrow \quad \sin^2(x) = \frac{e^{j2x} + e^{-j2x}}{-4} + \frac{1}{2}, \tag{3.27a}$$

$$\cos(x) = \frac{e^{jx} + e^{-jx}}{2} \quad \Rightarrow \quad \cos^2(x) = \frac{e^{j2x} + e^{-j2x}}{4} + \frac{1}{2}. \tag{3.27b}$$

Take for example

$$\delta_{xx} u_l^n = \frac{1}{h^2}\left(u_{l+1}^n - 2u_l^n + u_{l-1}^n\right) \overset{\mathcal{A}}{\Longrightarrow} \frac{1}{h^2}\left(e^{j\beta h} - 2 + e^{-j\beta h}\right).$$

Then, using $x = \beta h/2$, identity (**??**) can be rewritten to

$$e^{j\beta h} - 2 + e^{-j\beta h} = -4\sin^2(\beta h/2),$$

and substituted into the above to get

$$\delta_{xx} u_l^n \overset{\mathcal{A}}{\Longrightarrow} -\frac{4}{h^2}\sin^2(\beta h/2).$$

Examples of various temporal FD operators applied to grid functions in their frequency-domain representation are

$$\begin{aligned} \delta_{t+} u_l^n &\overset{\mathcal{A}}{\Longrightarrow} \frac{1}{k}\left(z - 1\right), & \delta_{t-} u_l^n &\overset{\mathcal{A}}{\Longrightarrow} \frac{1}{k}\left(1 - z^{-1}\right), \\ \delta_{t\cdot} u_l^n &\overset{\mathcal{A}}{\Longrightarrow} \frac{1}{2k}\left(z - z^{-1}\right), & \delta_{tt} u_l^n &\overset{\mathcal{A}}{\Longrightarrow} \frac{1}{k^2}\left(z - 2 + z^{-1}\right) \end{aligned} \tag{3.28}$$

and for spatial operators identity (**??**) can be used to obtain

$$\delta_{xx} u_l^n \overset{\mathcal{A}}{\Longrightarrow} -\frac{4}{h^2}\sin^2(\beta h/2), \tag{3.29a}$$

$$\delta_{xxxx} u_l^n \overset{\mathcal{A}}{\Longrightarrow} \frac{16}{h^4}\sin^4(\beta h/2). \tag{3.29b}$$

Frequency-domain analysis only works on linear and time-invariant (LTI) systems and assumes systems with infinite domains. Energy analysis allows for nonlinear systems to be analysed (see Section **??**) as well as handling boundary conditions.

FULL DOC SWEEP: nonlinear, nonlinear or non linear

Proving stability

not talking about nonlinear systems though

Similar to digital filters, the system is stable when the roots of the characteristic polynomial in z are bounded by 1 (unity)

$$|z| \leq 1. \tag{3.30}$$

only the denominator of the transfer function

In the FDTD context, the frequency-domain representation of a FD scheme results in a *characteristic equation* – which is usually a second-order polynomial

– in z and needs to satisfy condition (**??**) for all wave numbers β. It can be shown that for a polynomial of the form

$$z^2 + a^{(1)}z + a^{(2)} \tag{3.31}$$

its roots satisfy condition (**??**) when it abides the following condition [**?**]

$$|a^{(1)}| - 1 \leq a^{(2)} \leq 1. \tag{3.32}$$

If $a^{(2)} = 1$, the simpler condition

$$|a^{(1)}| \leq 2, \tag{3.33}$$

suffices.

3.3.1 Mass-Spring System

Recalling the FD scheme of the mass-spring system in Eq. (**??**)

$$M\delta_{tt}u_l^n = -Ku_l^n$$

a frequency-domain representation can be obtained using the ansatz in (**??**) with $l = 0$. Using Table **??** and Eqs. (**??**) as a reference and substituting the definitions yields

$$\frac{M}{k^2}\left(z - 2 + z^{-1}\right) = -K.$$

Gathering the terms and moving all to the left-hand side, the characteristic equation for the mass-spring system can be obtained:

$$z - \left(2 - \frac{Kk^2}{M}\right) + z^{-1} = 0. \tag{3.34}$$

To begin to prove stability, this equation needs to be written in the form found in (**??**). Multiplying all the terms by z, and noticing that $a^{(2)} = 1$, we could continue with condition (**??**). However, the scheme used here is a special case where the roots of the characteristic equation can not be identical [**?**]. When this happens, the output of the system will grow linearly and is called "marginally unstable". This means that $|a^{(1)}| \neq 1$ and the condition in (**??**) becomes $|a^{(1)}| < 2$. Continuing with this conditions yields

$$\begin{aligned} \left|-2 + \frac{Kk^2}{M}\right| &< 2, \\ -2 < -2 + \frac{Kk^2}{M} &< 2, \\ 0 < \frac{Kk^2}{M} &< 4. \end{aligned}$$

If only non-zero values are chosen for K, k and M they are positive and the first condition is always satisfied. The second condition is then easily solved for k by

$$k < 2\sqrt{\frac{M}{K}}. \tag{3.35}$$

Recalling that $\omega_0 = \sqrt{K/M}$, Eq (**??**) can be more compactly written as

$$k < \frac{2}{\omega_0}. \tag{3.36}$$

3.3.2 1D Wave Equation

This section will derive the stability condition for the 1D wave equation presented in Section **??** using von Neumann analysis.

Recalling the FD scheme in (**??**):

$$\delta_{tt} u_l^n = c^2 \delta_{xx} u_l^n,$$

its frequency-domain representation can be obtained using the definitions in Eqs. (**??**) and (**??**):

$$\frac{1}{k^2}\left(z - 2 + z^{-1}\right) = -\frac{4c^2}{h^2}\sin^2\left(\beta h/2\right). \tag{3.37}$$

Also recalling that

$$\lambda = \frac{ck}{h},$$

the characteristic equation of the 1D wave equation is

$$z + \left(4\lambda^2 \sin^2(\beta h/2) - 2\right) + z^{-1} = 0. \tag{3.38}$$

The scheme is then stable if the roots satisfy condition (**??**). As the characteristic equation is of the form in (**??**) (after multiplication with z) with $a^{(2)} = 1$, stability is shown by abiding condition (**??**) for all β and when applied to the characteristic equation (**??**), it can be seen that

$$\begin{aligned}
|4\lambda^2 \sin^2(\beta h/2) - 2| &\leq 2, \\
|2\lambda^2 \sin^2(\beta h/2) - 1| &\leq 1, \\
-1 \leq 2\lambda^2 \sin^2(\beta h/2) - 1 &\leq 1, \\
0 \leq 2\lambda^2 \sin^2(\beta h/2) &\leq 2, \\
0 \leq \lambda^2 \sin^2(\beta h/2) &\leq 1.
\end{aligned}$$

Observing that all terms in $\lambda^2 \sin^2(\beta h/2)$ are squared, this term will always be non-negative and therefore always satisfy the first condition. Continuing with

the second condition, and knowing that the $\sin^2(\beta h/2)$-term is bounded by 1 for all β, we arrive at the following stability condition:

$$\lambda \leq 1.$$

This is the CFL condition given in Eq. (**??**). To obtain the stability condition in terms of the grid spacing, the definition for λ is substituted and written in terms of the grid spacing

$$h \geq ck, \tag{3.39}$$

which is the stability condition given in Eq. (**??**).

3.4 Energy Analysis

Of all analysis techniques described in this chapter, energy analysis is without a doubt the most important when working with FDTD methods. First of all, from a practical point of view, it is essential for debugging implementations of FD schemes. Especially when trying to model more complex systems, programming errors are unavoidable, and energy analysis can be extremely helpful in pinpointing where the error lies. Secondly, energy analysis techniques can be used to obtain stability conditions in a much more general sense than the frequency-domain analysis techniques presented in Section **??**. Where frequency-domain analysis is restricted to LTI systems with infinite domains (for distributed systems), energy analysis can be applied to nonlinear systems and boundary conditions [**?**].

Energy analysis techniques first appeared in (the first edition of) [**?**]and was back then referred to the energy method. In [**?**] they have been extensively used to show stability of the FD schemes used.

shouldn't I just cite the first edition then?

One of the main goals when performing energy analysis is to find an expression for the total energy present in the system. This is referred to as the *Hamiltonian* and denoted by $\mathfrak{H}$ in continuous time and $\mathfrak{h}$ in discrete time. In this work, the focus of the energy analysis will be in discrete time.

In this section, four steps are presented and can be followed to perform a full energy analysis of a FD scheme and implement it afterwards. Then, the analysis will be performed on the mass-spring system and the 1D wave equation presented in Chapter **??**. Finally, it will be shown how to obtain stability conditions through the techniques presented in this section.

3.4.1 Energy Analysis: A 4-Step Tutorial

Step 1: Obtain the rate of change of the total energy $\delta_{t+}\mathfrak{h}$

The first step to energy analysis is to take the appropriate *norm* of the scheme (see Eq. (**??**)), which yields and expression for the rate of change of the energy

of the system: $\delta_{t+}\mathfrak{h}$. Usually, this means to take the inner product of the scheme with $(\delta_{t\cdot}u_l^n)$. See Section **??** for more details on the inner product. Note that the forward time difference δ_{t+} is used (and not the backwards or centred) because of convention and preference [Bilbao, verbally].

For the units of the resulting energy balance to add up (also see Step 3), it is useful to perform the analysis on a scheme with all physical parameters written out (so the discretised version of Eq. (**??**) rather than Eq. (**??**)).

Step 2: Identify different types of energy and obtain the total energy $\mathfrak{h}$ by isolating δ_{t+}

The energy of a FD scheme can generally be divided into three different types: the total energy contained within the system, or Hamiltonian $\mathfrak{h}$, energy losses through damping $\mathfrak{q}$ and energy input through external forces or excitations $\mathfrak{p}$. For distributed systems, an additional boundary term $\mathfrak{b}$ appears, but vanishes under 'regular' (lossless and not energy-storing) boundary conditions. Nearly any energy balance is thus of the form

$$\delta_{t+}\mathfrak{h} = \mathfrak{b} - \mathfrak{q} - \mathfrak{p}. \tag{3.40}$$

This equation essentially says that the total energy present in the system changes due to losses and inputs. For a lossless system without externally supplied energy over the course of the simulation (so initial conditions excluded), the energy should remain unchanged over the course of the simulation,

$$\delta_{t+}\mathfrak{h} = 0 \quad \Longrightarrow \quad \mathfrak{h}^n = \mathfrak{h}^0. \tag{3.41}$$

As the eventual interest lies in the total energy of the system $\mathfrak{h}$ and not its rate of change, δ_{t+} must be isolated in the definition of $\delta_{t+}\mathfrak{h}$. In this step, the identities in Section **??** will come in handy, as well as summation by parts described in Section **??** for distributed systems.

The Hamiltonian itself can usually be further subdivided into kinetic energy and potential energy, denoted by the symbols $\mathfrak{t}$ and $\mathfrak{v}$ respectively:

$$\mathfrak{h} = \mathfrak{t} + \mathfrak{v} \tag{3.42}$$

As a rule of thumb, the definition for kinetic energy contains 'velocity squared' (as in the classical-mechanics definition $E_{\text{kin}} = \frac{1}{2}M\dot{u}$) and the potential energy includes the restoring forces of the system.

Step 3: Check units

To know that the previous steps have been carried out correctly, it is good to check whether the units of the resulting expression for $\mathfrak{h}$ is indeed in Joules, or $\text{kg} \cdot \text{m}^2 \cdot \text{s}^{-2}$. The other quantities such as energy losses $\mathfrak{q}$ and inputs $\mathfrak{p}$, should

be in Joules per second or in SI units: kg $\cdot$ m$^2\cdot$ s^{-3}. Some information about operators and grid functions and how they 'add' units to the equation will be given below.

An (1D) inner product (or norm) will 'add' one 'm' unit due to the h in its definition in (**??**). A first-order temporal difference operator will 'add' one 's^{-1}'-unit (because of the $1/k$) and a first-order spatial difference operator will 'add' one 'm^{-1}'-unit ($1/h$). Along these lines, a second-order time or difference operator will 'add' a 's^{-2}' ($1/k^2$) or 'm^{-2}'-unit ($1/h^2$) respectively. It is important to note that the time shift operator (e_{t-}) does not influence the units. Finally, the appearance of a grid function u_l^n 'adds' whatever it describes. Usually, as u_l^n describes a displacement in m, it will 'add' this to the equation. If it describes anything else, it will 'add' that.

Step 4: Implement the definitions for energy and debug the FD scheme

In the end, the definition for the energy can be implemented and used as a check for whether the FD scheme has been implemented correctly. Usually, the energy of the system is calculated for every iteration in the for loop and plotted after the simulation. For a system without losses or energy inputs, the energy should be unchanged according to Eq. (**??**) and can be plotted according

$$\mathfrak{h}_{\mathrm{e}}^n = \frac{\mathfrak{h}^n - \mathfrak{h}^0}{\mathfrak{h}^0}, \quad \text{if } \mathfrak{h}^0 \neq 0, \tag{3.43}$$

where $\mathfrak{h}_{\mathrm{e}}^n$ can be seen as the normalised energy and shows the error variation. Although this equation should always return 0 (as $\mathfrak{h}^n = \mathfrak{h}^0$), in a finite precision simulation, ultra slight fluctuations of the energy should be visible due to rounding errors. Plotting the Hamiltonian should show fluctuations within *machine precision*, which is usually in the range of 10^{-15}. Over time, the fluctuations can add up, and possibly end up out of this range, but generally, any fluctuations less than in the 10^{-10} range indicate that there is no programming error. See fx. Figures **??** and **??**.

For a system with losses or energy inputs, a discrete integration, or summed form can be used (as done in fx. [**?**]):

$$\mathfrak{h}_{\mathrm{e}}^n = \frac{\mathfrak{h}^n - \mathfrak{h}^0 + k\sum_{m=0}^{n-1}(\mathfrak{q}^m + \mathfrak{p}^m)}{\mathfrak{h}^0}, \quad \text{if } \mathfrak{h}^0 \neq 0. \tag{3.44}$$

check if the sum should indeed go until $n-1$ and why

3.4.2 Mass-spring system

Recalling the FD scheme for the simple mass-spring system in Eq. (**??**)

$$M\delta_{tt}u^n = -Ku^n$$

we can start to perform an energy analysis using the five steps described above.

Step 1: Obtain $\delta_{t+}\mathfrak{h}$

The energy balance of the simple mass-spring system presented in Section **??** can be obtained by first taking the product of scheme (**??**) with $(\delta_{t\cdot}u^n)$:

$$\delta_{t+}\mathfrak{h} = M(\delta_{t\cdot}u^n)(\delta_{tt}u^n) + K(\delta_{t\cdot}u^n)(u^n) = 0. \tag{3.45}$$

Note that the inner product is not necessary as the system is not distributed.

Step 2: Identify energy types and isolate δ_{t+}

As there are no losses or externally supplied energy present in the system, all terms are part of the Hamiltonian $\mathfrak{h}$. To isolate δ_{t+} from (**??**), one can use identities (**??**) and (**??**) to get the following:

$$\delta_{t+}\mathfrak{h} = \delta_{t+}\left(\frac{M}{2}(\delta_{t-}u^n)^2 + \frac{K}{2}u^n e_{t-}u^n\right) = 0, \tag{3.46}$$

and the following definition for $\mathfrak{h}$ can be obtained

$$\mathfrak{h} = \frac{M}{2}(\delta_{t-}u^n)^2 + \frac{K}{2}u^n e_{t-}u^n = 0. \tag{3.47}$$

This can be rewritten in terms of the kinetic energy $\mathfrak{t}$ and potential energy $\mathfrak{v}$ according to

$$\mathfrak{h} = \mathfrak{t} + \mathfrak{v}, \quad \text{with} \quad \mathfrak{t} = \frac{M}{2}(\delta_{t-}u^n)^2, \quad \text{and} \quad \mathfrak{v} = \frac{K}{2}u^n e_{t-}u^n. \tag{3.48}$$

Step 3: Check units

As mentioned above, the energy $\mathfrak{h}$ needs to be in Joules, or $\mathrm{kg}\cdot\mathrm{m}^2\cdot\mathrm{s}^{-2}$. Taking the terms in Eq. (**??**) one-by-one and writing them in their units results in

$$\begin{aligned}
\mathfrak{t} = \frac{M}{2}(\delta_{t-}u^n)^2 &\xrightarrow{\text{in units}} \quad \mathrm{kg}\cdot(\mathrm{s}^{-1}\cdot\mathrm{m})^2 = \mathrm{kg}\cdot\mathrm{m}^2\cdot\mathrm{s}^{-2},\\
\mathfrak{v} = \frac{K}{2}u^n e_{t-}u^n &\xrightarrow{\text{in units}} \quad \mathrm{N}\cdot\mathrm{m}^{-1}\cdot\mathrm{m}\cdot\mathrm{m} = \mathrm{kg}\cdot\mathrm{m}^2\cdot\mathrm{s}^{-2},
\end{aligned}$$

and indeed have the correct units.

Step 4: Implementation

Equation (**??**) can then be implemented in same for-loop recursion where the update is calculated.

```
%% Calculate the energy using Eq. (??)

% Kinetic energy
kinEnergy(n) = M / 2 * (1/k * (u - uPrev))^2;

% Potential energy
potEnergy(n) = K / 2 * u * uPrev;

% Total energy (Hamiltonian)
totEnergy(n) = kinEnergy(n) + potEnergy(n);
```

Figure **??** shows the normalised energy (according to Eq. (**??**)) of the mass-spring system and shows that the deviation is indeed within machine precision.

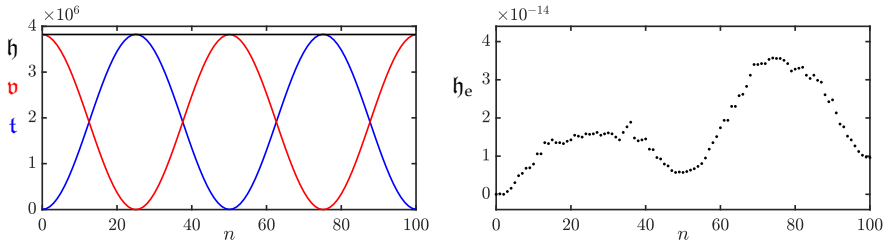

Fig. 3.3: The kinetic (blue), potential (red), and total (black) energy of an implementation of the mass-spring system are plotted in the left panel. The right panel shows the normalised energy (according to Eq. (**??**)). Notice that the scaling of the y-axis is 10^{-14} and the energy is thus within machine precision.

3.4.3 1D Wave Equation

Energy analysis could be directly performed on the FD scheme in (**??**). However, in order for the units of the scheme to add up to energy in Joules, it is useful to write out all physical parameters. Taking the definition for the wave speed for the ideal string $c = \sqrt{T/\rho A}$ and multiplying both sides of Eq. (**??**) by ρA yields

$$\rho A \delta_{tt} u_l^n = T \delta_{xx} u_l^n, \tag{3.49}$$

where $l \in d$ with discrete domain $d \in \{0, \ldots, N\}$ and number of grid points $N + 1$. Furthermore, Dirichlet boundary conditions as given in Eq. (**??**) are used. A note on using Neumann boundary conditions is given at the end of this section.

Step 1: Obtain $\delta_{t+}\mathfrak{h}$

Taking an inner product using Eq. (**??**) with $(\delta_{t\cdot}u_l^n)$ and moving all terms to the left-hand side yields the definition for the rate of change of the Hamiltonian:

$$\delta_{t+}\mathfrak{h} = \rho A\langle\delta_{t\cdot}u_l^n, \delta_{tt}u_l^n\rangle_d - T\langle\delta_{t\cdot}u_l^n, \delta_{xx}u_l^n\rangle_d = 0. \tag{3.50}$$

Step 2: Identify energy types and isolate δ_{t+}

As in the case of the mass-spring system in the previous section, there are no losses or externally supplied energy present in the system, and all terms are part of the Hamiltonian $\mathfrak{h}$.

To isolate δ_{t+} in Eq. (**??**), the terms have to be rewritten in a way that fits the product identities in Section **??**. Summation by parts as described in Section **??** can be used. Using identity (**??**) with $f_l^n \triangleq \delta_{t\cdot}u_l^n$ and $g_l^n \triangleq \delta_{x+}u_l^n$, the second term can be rewritten to

$$-T\langle\delta_{t\cdot}u_l^n, \delta_{xx}u_l^n\rangle_d = T\langle\delta_{x+}(\delta_{t\cdot}u_l^n), \delta_{x+}u_l^n\rangle_{\underline{d}} - \mathfrak{b},$$

where the boundary term

$$\mathfrak{b} = T(\delta_{t\cdot}u_N^n)(\delta_{x+}u_N^n) - T(\delta_{t\cdot}u_0^n)(\delta_{x+}u_{-1}^n),$$

and reduced domain $\underline{d} = \{0, \ldots, N-1\}$. As Dirichlet boundary conditions are used, the boundary term vanishes as

$$u_0^n = u_N^n = 0 \quad \Longrightarrow \quad \delta_{t\cdot}u_0^n = \delta_{t\cdot}u_N^n = 0.$$

In other words, if the states of the system at the boundaries are zero, their velocity will also be zero. Then, using the discrete inner product in Eq. (**??**), Eq. (**??**) can be expanded to

$$\delta_{t+}\mathfrak{h} = \rho A\sum_{l=0}^{N} h(\delta_{t\cdot}u_l^n)(\delta_{tt}u_l^n) + T\sum_{l=0}^{N} h(\delta_{t\cdot}\delta_{x+}u_l^n)(\delta_{x+}u_l^n) \tag{3.51}$$

Then, using identities (**??**) and (**??**), δ_{t+} can be isolated

$$\delta_{t+}\mathfrak{h} = \delta_{t+}\left(\frac{\rho A}{2}\|\delta_{t-}u_l^n\|_d^2 + \frac{T}{2}\langle\delta_{x+}u_l^n, e_{t-}\delta_{x+}u_l^n\rangle_{\underline{d}}\right), \tag{3.52}$$

and the definition for the Hamiltonian and the kinetic and potential energy can be found:

$$\begin{gathered}\mathfrak{h} = \mathfrak{t} + \mathfrak{v}, \\ \text{with} \quad \mathfrak{t} = \frac{\rho A}{2}\|\delta_{t-}u_l^n\|_d^2, \quad \text{and} \quad \mathfrak{v} = \frac{T}{2}\langle\delta_{x+}u_l^n, e_{t-}\delta_{x+}u_l^n\rangle_{\underline{d}}.\end{gathered} \tag{3.53}$$

Step 3: Check units

Writing out the definitions for kinetic and potential energy in Eq. (**??**) respectively, yields

$$\begin{aligned}\mathfrak{t} = \frac{\rho A}{2}\|\delta_{t-}u_l^n\|_d^2 &\xrightarrow{\text{in units}} \mathrm{kg}\cdot\mathrm{m}^{-3}\cdot\mathrm{m}^2\cdot\mathrm{m}\cdot(\mathrm{s}^{-1}\cdot\mathrm{m})^2 \\ &= \mathrm{kg}\cdot\mathrm{m}^2\cdot\mathrm{s}^{-2}, \\ \mathfrak{v} = \frac{T}{2}\langle\delta_{x+}u_l^n, e_{t-}\delta_{x+}u_l^n\rangle_{\underline{d}} &\xrightarrow{\text{in units}} \mathrm{N}\cdot\mathrm{m}\cdot(\mathrm{m}^{-1}\cdot\mathrm{m}\cdot\mathrm{m}^{-1}\cdot\mathrm{m}^{-1}\mathrm{m}) \\ &= \mathrm{kg}\cdot\mathrm{m}^2\cdot\mathrm{s}^{-2},\end{aligned}$$

and are indeed in Joules. Notice that an extra 'm' unit appears due to the norm and inner product.

Step 4: Implementation

The energy balance in Eq. (**??**) can be implemented with the following code in the for-loop recursion:

```
%% Calculate the energy using Eq. (??)

% Kinetic energy
kinEnergy(n) = rho * A / 2 * h * sum((1/k * (u-uPrev)).^2);

% Potential energy
potEnergy(n) = T/(2*h) * sum(([u; 0] - [0; u]) ...
             .* ([uPrev; 0] - [0; uPrev]));

% Total energy (Hamiltonian)
totEnergy(n) = kinEnergy(n) + potEnergy(n);
```

Here, `u` is the vector $\mathbf{u} = [u_1^n, \ldots, u_{N-1}^n]^T$ (as Dirichlet boundary conditions are used) and need to be concatenated with 0 in the calculation of the potential energy as the boundaries need to be included in the calculation (despite them being 0!). Figure **??** shows the plot of the normalised energy according to Eq. (**??**) and shows that the deviation of $\mathfrak{h}^n$ is within machine precision. left off here!

Neumann boundary conditions

If Neumann boundary conditions – as per Eq. (**??**) – are used instead, the primed inner product in Eq. (**??**) needs to be used in Step 1. Using the identity in (**??**), summation by parts of the second term results in

$$-T\langle\delta_{t\cdot}u_l^n, \delta_{xx}u_l^n\rangle_d' = T\langle\delta_{x+}(\delta_{t\cdot}u_l^n), \delta_{x+}u_l^n\rangle_{\underline{d}} - \mathfrak{b},$$

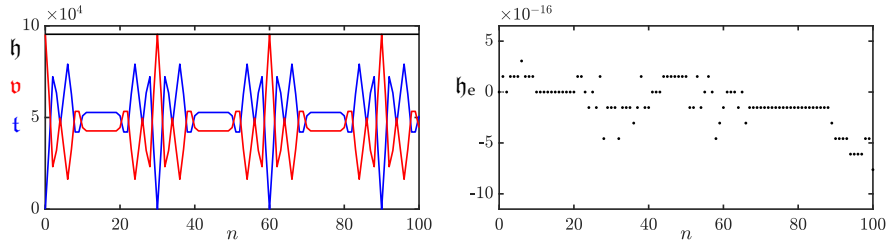

Fig. 3.4: The kinetic (blue), potential (red), and total (black) energy of an implementation of the 1D wave equation are plotted in the left panel. The right panel shows the normalised energy (according to Eq. (**??**)) and shows that the deviation of the energy is within machine precision.

where the boundary term

$$\begin{aligned} \mathfrak{b} &= T(\delta_{t.}u_N^n)(\mu_{x-}\delta_{x+}u_N^n) - T(\delta_{t.}u_0^n)(\mu_{x-}\delta_{x+}u_0^n), \\ \overset{\text{Eq. (??)}}{\Longleftrightarrow} \quad &= T(\delta_{t.}u_N^n)(\delta_{x.}u_N^n) - T(\delta_{t.}u_0^n)(\delta_{x.}u_0^n). \end{aligned}$$

As the Neumann boundary condition states that

$$\delta_{x.}u_0^n = \delta_{x.}u_N^n = 0$$

the boundary term vanishes and the energy balance results in

$$\begin{gathered} \mathfrak{h} = \mathfrak{t} + \mathfrak{v}, \\ \text{with} \quad \mathfrak{t} = \frac{\rho A}{2}\left(\|\delta_{t-}u_l^n\|_d'\right)^2, \quad \text{and} \quad \frac{T}{2}\langle\delta_{x+}u_l^n, e_{t-}\delta_{x+}u_l^n\rangle_{\underline{d}}. \end{gathered} \tag{3.54}$$

Using u for the vector $\mathbf{u} = [u_0^n, \ldots, u_N^n]^T$, this is then implemented as

```
%% Calculate the energy using Eq. (??)

% Scaling of the boundaries through weighted inner product
scaling = [0.5; ones(N-1, 1); 0.5];

% Kinetic energy
kinEnergy(n) = rho * A / 2 * h * sum(scaling .* (1/k * (u-uPrev)).^2);

% Potential energy
potEnergy(n) = T/(2*h) * sum(u(2:end) - u(1:end-1) ...
            .* (uPrev(2:end) - uPrev(1:end-1)));

% Total energy (Hamiltonian)
totEnergy(n) = kinEnergy(n) + potEnergy(n);
```

3.4.4 Stability Analysis using Energy Analysis Techniques

Section **??** showed how to obtain a stability condition of a FD scheme using a frequency-domain representation. Although not operating in the frequency domain, the energy analysis techniques presented here may also be used to obtain stability conditions of FD schemes. Stability analysis using the energy method might even be considered more powerful than the frequency domain approach, as it can also be used to analyse nonlinear systems!

check

To arrive at a stability condition, the energy must be *non-negative* ($\mathfrak{h} \geq 0$) or, in some cases *positive definite* ($\mathfrak{h} > 0$). Below, the mass-spring system and the 1D wave equation will be used as a test case.

Mass-spring system

Section **??** mentions that the mass-spring system is a special case in that the roots of its characteristic equation can not be identical. When proving stability using energy analysis, this means that the energy of the system needs to be positive definite. It can be shown that an equation of the form

$$x^2 + y^2 + 2axy \tag{3.55}$$

is positive definite if $|a| < 1$.

Equation (**??**) can be used to prove stability for the mass spring system using the energy balance in Eq. (**??**). One can easily conclude that $\mathfrak{t}$ is non-negative due to the fact that $M > 0$ and $(\delta_{t-} u^n)$ is squared. The potential energy $\mathfrak{v}$, however, is of indefinite sign. Expanding the operators in Eq. (**??**) yields

$$\begin{aligned}\mathfrak{h} &= \frac{M}{2k^2}\left((u^n)^2 - 2u^n u^{n-1} + (u^{n-1})^2\right) + \frac{K}{2}u^n u^{n-1},\\ &= \frac{M}{2k^2}\left((u^n)^2 + (u^{n-1})^2\right) + \left(\frac{K}{2} - \frac{M}{k^2}\right)u^n u^{n-1}.\end{aligned}$$

Dividing all terms by $M/2k^2$ this equation is of the form in Eq. (**??**):

$$\mathfrak{h} = (u^n)^2 + (u^{n-1})^2 + \left(\frac{Kk^2}{M} - 2\right)u^n u^{n-1}.$$

For $\mathfrak{h}$ to be positive definite, the following condition must hold

$$\left|\frac{Kk^2}{2M} - 1\right| < 1.$$

This can then be written as

$$\begin{aligned}-1 < \frac{Kk^2}{2M} - 1 < 1\\ 0 < \frac{Kk^2}{2M} < 2\end{aligned}$$

where, as long as K and k are non-zero, the first inequality is always satisfied. Then the condition solved for k can easily be shown to be

$$k < 2\sqrt{\frac{M}{K}} \tag{3.56}$$

which is identical to the definition in Eq. (**??**).

1D wave equation

For the 1D wave equation, the energy must be proven to be non-negative. One can take the energy balance in Eq. (**??**) and conclude that $\mathfrak{t}$ is non-negative due to the non-negativity of the parameters and $(\delta_{t-}u_l^n)$ being squared. The potential energy, however, is of indefinite sign. One can rewrite $\mathfrak{v}$ using identity (**??**) as

$$\begin{aligned}
\mathfrak{v} &= \frac{T}{2}\langle \delta_{x+}u_l^n, e_{t-}\delta_{x+}u_l^n\rangle_{\underline{d}}, \\
&= \frac{T}{2}\sum_{l=0}^{N-1} h(\delta_{x+}u_l^n)(e_{t-}\delta_{x+}u_l^n), \\
&= \frac{T}{2}\sum_{l=0}^{N-1} h\left((\mu_{t-}\delta_{x+}u_l^n)^2 - \frac{k^2}{4}(\delta_{t-}\delta_{x+}u_l^n)^2\right), \\
&= \frac{T}{2}\left(\|\mu_{t-}\delta_{x+}u_l^n\|_{\underline{d}}^2 - \frac{k^2}{4}\|\delta_{t-}\delta_{x+}u_l^n\|_{\underline{d}}^2\right).
\end{aligned}$$

One can then use the following bound for spatial differences [**?**]

$$\|\delta_{x+}u_l^n\|_{\underline{d}} \leq \frac{2}{h}\|u_l^n\|_d' \leq \frac{2}{h}\|u_l^n\|_d, \tag{3.57}$$

to put a condition on $\mathfrak{v}$

$$\begin{aligned}
\mathfrak{v} &\geq \frac{T}{2}\left(\|\mu_{t-}\delta_{x+}u_l^n\|_{\underline{d}}^2 - \frac{k^2}{4}\left(\frac{2}{h}\|\delta_{t-}u_l^n\|_d\right)^2\right), \\
&\geq \frac{T}{2}\left(\|\mu_{t-}\delta_{x+}u_l^n\|_{\underline{d}}^2 - \frac{k^2}{h^2}\|\delta_{t-}u_l^n\|_d^2\right),
\end{aligned}$$

Substituting this condition into the energy balance in Eq. (**??**) yields

$$\begin{aligned}
\mathfrak{h} = \mathfrak{t} + \mathfrak{v} &\geq \frac{\rho A}{2}\|\delta_{t-}u_l^n\|_d^2 + \frac{T}{2}\left(\|\mu_{t-}\delta_{x+}u_l^n\|_{\underline{d}}^2 - \frac{k^2}{h^2}\|\delta_{t-}u_l^n\|_d^2\right), \\
&\geq \left(\frac{\rho A}{2} - \frac{Tk^2}{2h^2}\right)\|\delta_{t-}u_l^n\|_d^2 + \frac{T}{2}\|\mu_{t-}\delta_{x+}u_l^n\|_{\underline{d}}^2.
\end{aligned}$$

Recalling that $c = \sqrt{T/\rho A}$ and $\lambda = ck/h$, all terms can be divided by ρA which yields

$$\mathfrak{h} = \mathfrak{t} + \mathfrak{v} \geq \frac{1}{2}\left(1 - \lambda^2\right) \|\delta_{t-} u_l^n\|_d^2 + \frac{c^2}{2} \|\mu_{t-}\delta_{x+} u_l^n\|_{\underline{d}}^2, \tag{3.58}$$

and is non-negative for

$$\begin{aligned} 1 - \lambda^2 &\geq 0, \\ \lambda &\leq 1. \end{aligned}$$

This is the same (CFL) condition obtained through von Neumann analysis in Section **??**.

3.5 Modal Analysis

Modes are the resonant frequencies of a system. The amount of modes that a discrete system contains depends on the amount of moving points. A mass-spring system thus has one resonating mode, but – as briefly touched upon in Section **??** – a FD scheme of the 1D wave equation with $N = 30$ and Dirichlet boundary conditions will have 29 modes. This section will show how to numerically obtain the modal frequencies of an FD implementation using the 1D wave equation as a test case.

We start by using the matrix form of the 1D wave equation from Eq. (**??**)

$$\frac{1}{k^2}\left(\mathbf{u}^{n+1} - 2\mathbf{u}^n + \mathbf{u}^{n-1}\right) = c^2 \mathbf{D}_{xx}\mathbf{u}^n.$$

Following [**?**] we can assume a test solution of the form $\mathbf{u} = z^n \boldsymbol{\phi}$. Substituting this into the above equation yields the characteristic equation

more explanation, perhaps refer to von neumann analysis in **??**

$$(z - 2 + z^{-1})\boldsymbol{\phi} = c^2 k^2 \mathbf{D}_{xx}\boldsymbol{\phi}. \tag{3.59}$$

This is an eigenvalue problem (see Section **??**) where the p^{th} solution $\boldsymbol{\phi}_p$ may be interpreted as the modal shape of mode p. The corresponding modal frequencies are the solutions to the following equations:

$$\begin{aligned} z_p - 2 + z_p^{-1} &= c^2 k^2 \text{eig}_p(\mathbf{D}_{xx}), \\ z_p + \Big(- 2 - c^2 k^2 \text{eig}_p(\mathbf{D}_{xx})\Big) + z_p^{-1} &= 0. \end{aligned} \tag{3.60}$$

Furthermore, we can substitute a test solution $z_p = e^{s_p k}$ with complex frequency $s_p = j\omega_p + \sigma_p$ which contains the (angular) frequency ω_p and damping σ_p of the p^{th} mode. As there is no damping present in the system, the test solution reduces to $z_p = e^{j\omega_p k}$ which can be substituted into Eq (**??**) to get

$$\begin{aligned} e^{j\omega_p k} + e^{-j\omega_p k} - 2 - c^2 k^2 \text{eig}_p(\mathbf{D}_{xx}) &= 0, \\ \frac{e^{j\omega_p k} + e^{-j\omega_p k}}{-4} + \frac{1}{2} + \frac{c^2 k^2}{4} \text{eig}_p(\mathbf{D}_{xx}) &= 0. \end{aligned}$$

Finally, using the trigonometric identity in Eq. (**??**) we get

$$\begin{aligned}\sin^2(\omega_p k/2) + \frac{c^2k^2}{4}\text{eig}_p(\mathbf{D}_{xx}) &= 0,\\ \sin(\omega_p k/2) &= \frac{ck}{2}\sqrt{-\text{eig}_p(\mathbf{D}_{xx})},\\ \omega_p &= \frac{2}{k}\sin^{-1}\left(\frac{ck}{2}\sqrt{-\text{eig}_p(\mathbf{D}_{xx})}\right).\end{aligned} \tag{3.61}$$

and can be rewritten to

$$f_p = \frac{1}{\pi k}\sin^{-1}\left(\frac{ck}{2}\sqrt{-\text{eig}_p(\mathbf{D}_{xx})}\right) \tag{3.62}$$

to get the modal frequency of the p^{th} mode in Hz.

3.5.1 One-Step Form

For more complicated systems, specifically those containing damping terms, it is useful to rewrite the update in *one-step form* (also referred to as a state-space representation). The damping terms cause the coefficients of z and z^{-1} in the characteristic equation to not be identical and the trigonometric identities in (**??**) can not be used directly. Although the eigenfrequency calculation needs to be done on a larger matrix, it allows for a more general and direct way to calculate the modal frequencies and damping coefficients per mode.

If matrix $\mathbf{A}$ has an inverse, any scheme of the form

$$\mathbf{A}\mathbf{u}^{n+1} = \mathbf{B}\mathbf{u}^n + \mathbf{C}\mathbf{u}^{n-1}, \tag{3.63}$$

can be rewritten to

$$\underbrace{\begin{bmatrix}\mathbf{u}^{n+1}\\ \mathbf{u}^n\end{bmatrix}}_{\mathbf{w}^{n+1}} = \underbrace{\begin{bmatrix}\mathbf{A}^{-1}\mathbf{B} & \mathbf{A}^{-1}\mathbf{C}\\ \mathbf{I} & \mathbf{0}\end{bmatrix}}_{\mathbf{Q}}\underbrace{\begin{bmatrix}\mathbf{u}^{n}\\ \mathbf{u}^{n-1}\end{bmatrix}}_{\mathbf{w}^{n}} \tag{3.64}$$

which relates the unknown state of the system to the known state through matrix $\mathbf{Q}$ which encompases the scheme. The sizes of the identity matrix $\mathbf{I}$ and zero matrix $\mathbf{0}$ are the same size as $\mathbf{A}, \mathbf{B}$ and $\mathbf{C}$.

Again, solutions of the form $\mathbf{w} = z^n\boldsymbol{\phi}$ can be assumed (where $\boldsymbol{\phi}$ is now less-trivially connected to the modal shapes)

$$z\boldsymbol{\phi} = \mathbf{Q}\boldsymbol{\phi}, \tag{3.65}$$

which can be solved for the pth eigenvalue as

$$z_p = \text{eig}_p(\mathbf{Q}). \tag{3.66}$$

As the scheme could exhibit damping, the test solution $z_p = e^{s_p k}$ is used. Substituting this yields

$$\begin{aligned} e^{s_p k} &= \text{eig}_p(\mathbf{Q}), \\ s_p &= \frac{1}{k} \ln\left(\text{eig}_p(\mathbf{Q})\right). \end{aligned} \tag{3.67}$$

Solutions for the frequency and damping for the pth eigenvalue can then be obtained through

$$\omega_p = \Im(s_p) \quad \text{and} \quad \sigma_p = \Re(s_p), \tag{3.68}$$

where $\Im(\cdot)$ and $\Re(\cdot)$ denote the "imaginary part of" and "real part of" respectively.

As the elements of $\mathbf{Q}$ are real-valued, the solutions s_p in Eq. (**??**) come in complex conjugates (pairs of numbers of which the imaginary part has an opposite sign). For analysis, only the $\Im(s_p) \geq 0$ should be considered as these correspond to non-negative frequencies.

3.6 Dispersion analysis

not sure whether to include..

Part II

Resonators

Resonators

Although the physical models described in the previous part – the simple mass-spring system and the 1D wave equation – are also considered resonators, they are *ideal* cases. In other words, you would not be able to find these "in the wild" as they do not includes effects such as losses or frequency dispersion.

This part presents the different resonators used over the course of the project and is structured as follows: Chapter **??** introduces the stiff string, a model which has been used a lot over the course of this project, Chapter **??** talks about brass instruments, or more generally, 1D systems of varying geometry along their spatial dimension. Finally, Chapter **??** will introduces 2D systems which, in this project, have been used to simulate (simplified) instrument bodies. The analysis techniques introduced in the previous section will be applied to all models and explained in detail.

Chapter 4

Stiff string

In earlier chapters, the case of the ideal string was presented modelled using the 1D wave equation. As shown, if the CFL condition is satisfied with equality, the model generates an output with harmonic partials which are integer multiples of the fundamental frequency. In the real world, however, strings exhibit a phenomenon called *inharmonicity* due to stiffness in the material.

The restoring force of the 1D wave equation is only due to tension. In the real world, however, this force is also due to stiffness, dependent on the material and geometry of the string. This stiffness causes frequency dispersion and inharmonicity: the "harmonic" partials get exponentially further apart the higher their frequency is.

The stiff string played a prominent part in the following published works [**??**], [**??**], [**??**], [**??**] and [**??**].

This chapter present the PDE of the stiff string, and go through the discretisation process afterwards. The analysis techniques presented in the previous chapter will then be applied to the stiff string.

not done

4.1 Continuous time

should I even include the lossless one? It's just so that we can slowly build up to the damped model...

Consider a lossless stiff string of length L and a circular cross-section. Its transverse displacement is described by $u = u(x,t)$ defined for $x \in \mathcal{D}$ with domain $\mathcal{D} = [0, L]$ and time $t \geq 0$. The PDE describing its motion is

$$\rho A \partial_t^2 u = T \partial_x^2 u - EI \partial_x^4 u \tag{4.1}$$

parameterised by material density ρ (in kg/m^3), cross-sectional area $A = \pi r^2$ (in m^2), radius r (in m), tension T (in N), Young's modulus E (in Pa) and area moment of inertia $I = \pi r^4/4$ (in m^4). If either E or I is 0, Eq (**??**) reduces to the 1D wave equation in Eq. (**??**) where $c = \sqrt{T/\rho A}$. If instead $T = 0$, Eq. (**??**) reduces to the *ideal bar* equation.

Dispersion Analysis or: Frequency Dispersion

The 4th-order spatial derivative models *frequency dispersion*, a phenomenon that causes different frequencies to travel at different speeds. As opposed to the undesired numerical dispersion

not done

4.1.1 Adding Losses

Before moving on to the discretisation of the PDE in Eq. (**??**), losses can be added to the system. In the physical world, strings lose energy through fx. air viscosity and thermoelastic effects. All frequencies lose energy and die out (damp) over time, but higher frequencies do so at a much faster rate. This phenomenon is called *frequency-dependent damping* and can be modelled using a mixed derivative $\partial_t \partial_x^2$. This way of frequency-dependent damping first appeared in [**?**] and has been used extensively in the literature since. A damped stiff string can be modelled as

citations here?

$$\rho A \partial_t^2 u = T \partial_x^2 u - EI \partial_x^4 u - 2\sigma_0 \rho A \partial_t u + 2\sigma_1 \rho A \partial_t \partial_x^2 u, \tag{4.2}$$

where the non-negative loss coefficients σ_0 (in s^{-1}) and σ_1 (in m^2/s) determine the frequency-independent and frequency-dependent losses respectively.

A more compact way to write Eq. (**??**), and as is also found often in the literature [**?**], is to divide both sides by ρA to get

etc.

$$\partial_t^2 u = c^2 \partial_x^2 u - \kappa^2 \partial_x^4 u - 2\sigma_0 \partial_t u + 2\sigma_1 \partial_t \partial_x^2 u \tag{4.3}$$

where $c = \sqrt{T/\rho A}$ is the wave speed (in $\mathrm{m/s}$) as in the 1D wave equation in (**??**) and $\kappa = \sqrt{EI/\rho A}$ is referred to as the stiffness coefficient (in m^2/s).

check wavespeed or wave speed (entire document)

Intuition

Although Eq. (**??**) might look daunting at first, the principle of Newton's second law remains the same.

Something about the 4th spatial derivative and the loss terms here...

Boundary Conditions

Section **??** presents two types of boundary conditions for the 1D wave equation in Eq. (**??**). In the case of the stiff string, these can be extended to

$$u = \partial_x u = 0 \quad \text{(clamped)} \tag{4.4a}$$

$$u = \partial_x^2 u = 0 \quad \text{(simply supported)} \tag{4.4b}$$

$$\partial_x^2 u = \partial_x^3 u = 0 \quad \text{(free)} \tag{4.4c}$$

at $x = 0, L$. See Figure **??** for plots of the first modal shape for each respective boundary condition.

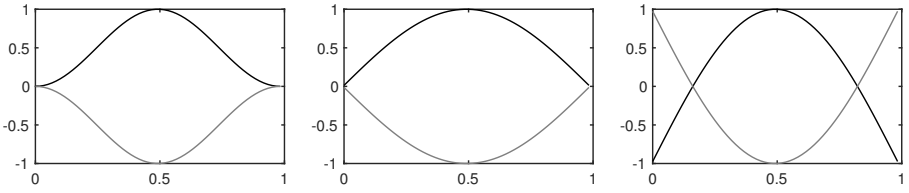

(a) Clamped. **(b)** Simply supported. **(c)** Free.

Fig. 4.1: Plots of the first (normalised) modal shape for the three boundary conditions in Eqs. (**??**). The extremes are indicated with black and grey lines respectively.

4.2 Discrete Time

For the sake of brevity we continue with Eq. (**??**), rather than Eq. (**??**). Naturally, same process can be followed for the latter, the only difference being a multiplication by ρA of all terms.

Equation (**??**) can be discretised as

$$\delta_{tt} u_l^n = c^2 \delta_{xx} u_l^n - \kappa^2 \delta_{xxxx} u_l^n - 2\sigma_0 \delta_{t\cdot} u_l^n + 2\sigma_1 \delta_{t-} \delta_{xx} u_l^n, \tag{4.5}$$

and is defined for domain $l \in \{0, \ldots, N\}$ and number of grid points $N + 1$. The δ_{xxxx} operator is defined as the second-order spatial difference in Eq. (**??**) applied to itself:

$$\delta_{xxxx} = \delta_{xx} \delta_{xx} = \frac{1}{h^4} \left(e_{x+}^2 - 4e_{x+} + 6 - 4e_{x-} + e_{x-}^2 \right). \tag{4.6}$$

A multiplication of two shift operators applied to a grid function simply means to apply each shift individually. The δ_{xxxx} operator applied to u_l^n thus becomes

$$\delta_{xxxx} u_l^n = \frac{1}{h^4} \left(u_{l+2}^n - 4u_{l+1}^n + 6u_l^n - 4u_{l-1}^n + u_{l-2}^n \right). \tag{4.7}$$

A definition for the mixed-derivative operator can similarly be found. Recalling the definitions for δ_{t-} in Eq. (**??**) and δ_{xx} Eq. (**??**), their combination results in

$$\begin{aligned} \delta_{t-} \delta_{xx} &= \frac{1}{k} \left(1 - e_{t-}\right) \frac{1}{h^2} \left(e_{x+} - 2 + e_{x-}\right), \\ &= \frac{1}{kh^2} \left(e_{x+} - 2 + e_{x-} - e_{t-}(e_{x+} - 2 + e_{x-})\right). \end{aligned} \tag{4.8}$$

Two different shift operators multiplied together still simply means to apply them to the grid function individually. The $\delta_{t-} \delta_{xx}$ operator applied to u_l^n thus yields

$$\delta_{t-} \delta_{xx} u_l^n = \frac{1}{hk^2} \left(u_{l+1}^n - 2u_l^n + u_{l-1}^n - u_{l+1}^{n-1} + 2u_l^{n-1} - u_{l-1}^{n-1} \right). \tag{4.9}$$

The reason a backwards difference is used here is to keep the system explicit. An example of an implicit scheme using the centred operator instead can be found in Section **??**.

With these definitions, the operators in scheme (**??**) can be expanded to get

$$\begin{aligned}\frac{1}{k^2}\left(u_l^{n+1} - 2u_l^n + u_l^{n-1}\right) = \frac{c^2}{h^2}\left(u_{l+1}^n - 2u_l^n + u_{l-1}^n\right) \\ - \frac{\kappa^2}{h^4}\left(u_{l+2}^n - 4u_{l+1}^n + 6u_l^n - 4u_{l-1}^n + u_{l-2}^n\right) \\ - \frac{\sigma_0}{k}\left(u_l^{n+1} - u_l^{n-1}\right) \\ + \frac{2\sigma_1}{kh^2}\left(u_{l+1}^n - 2u_l^n + u_{l-1}^n - u_{l+1}^{n-1} + 2u_l^{n-1} + u_{l-1}^{n-1}\right),\end{aligned} \tag{4.10}$$

and after multiplication by k^2 and collecting the terms yields

$$\begin{aligned}(1+\sigma_0 k)u_l^{n+1} = \left(2 - 2\lambda^2 - 6\mu^2 - \frac{4\sigma_1 k}{h^2}\right)u_l^n \\ + \left(\lambda^2 + 4\mu^2 + \frac{2\sigma_1 k}{h^2}\right)(u_{l+1}^n + u_{l-1}^n) \\ - \mu^2(u_{l+2}^n + u_{l-2}^n) + \left(-1 + \sigma_0 k + \frac{4\sigma_1 k}{h^2}\right)u_l^{n-1} \\ - \frac{2\sigma_1 k}{h^2}(u_{l+1}^{n-1} + u_{l-1}^{n-1}),\end{aligned} \tag{4.11}$$

with

$$\lambda = \frac{ck}{h} \quad \text{and} \quad \mu = \frac{\kappa k}{h^2}. \tag{4.12}$$

The update equation follows by dividing both sides by $(1+\sigma_0 k)$.

The stability condition for the FD scheme in (**??**) is defined as

$$h \geq \sqrt{\frac{c^2k^2 + 4\sigma_1 k + \sqrt{(c^2k^2 + 4\sigma_1 k)^2 + 16\kappa^2 k^2}}{2}}, \tag{4.13}$$

and will be derived in Section **??** using von Neumann analysis. This condition can then be used to calculate the number of intervals N in a similar fashion as for the 1D wave equation shown in Eq. (**??**). First, Eq. (**??**) should be satisfied with equality, after which

$$N := \left\lfloor \frac{L}{h} \right\rfloor, \quad \text{and} \quad h := \frac{L}{N}$$

which can then be used to calculate λ and μ in (**??**).

Stencil

As done in Section **??**, a stencil for the FD scheme implementing the damped stiff string can be created. This is shown in Figure **??**. In order to calculate u_l^{n+1}, 5 points at the current time step are needed due to the 4$^{\text{th}}$-order spatial derivative. Due to the mixed derivative in the frequency-dependent damping term neighbouring points at the previous time step are also required.

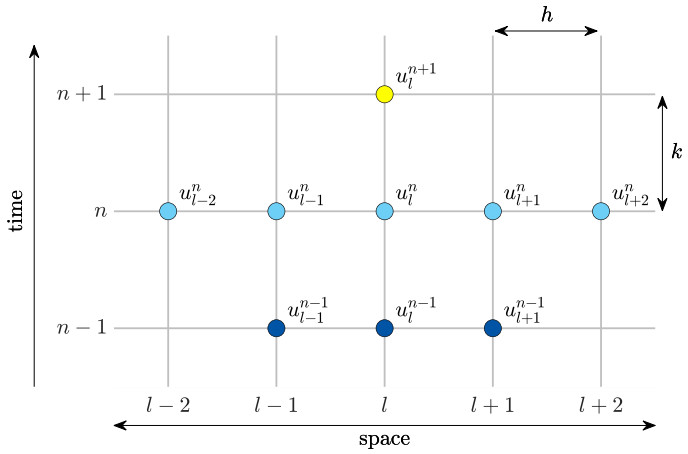

Fig. 4.2: The stencil for the damped stiff string scheme in Eq. (**??**).

4.2.1 Boundary conditions

Due to the 4$^{\text{th}}$-order spatial derivative, two virtual grid points need to be accounted for at the boundaries of the system. Discretising the boundary conditions in (**??**) yields

$$u_l^n = \delta_{x\pm} u_l^n = 0 \quad \text{(clamped)} \tag{4.14a}$$

$$u_l^n = \delta_{xx} u_l^n = 0 \quad \text{(simply supported)} \tag{4.14b}$$

$$\delta_{xx} u_l^n = \delta_{x.} \delta_{xx} u_l^n = 0 \quad \text{(free)} \tag{4.14c}$$

at $l = 0, N$. The operator in the clamped condition uses the δ_{x+} operator at the left boundary ($l = 0$) and δ_{x-} at the right ($l = N$). Note that for the free boundary condition in Eq. (**??**), to discretise ∂_x^3 the more accurate $\delta_{x.}\delta_{xx}$ operator has been chosen over the less accurate $\delta_{t-}\delta_{xx}$ and $\delta_{t+}\delta_{xx}$ operators for the left and right boundary respectively.

Below, the boundary conditions are expanded to get definitions for the virtual grid points.

insert figure showing virtual grid points somewhere in this section

Clamped

Expanding the operators for the clamped condition yields

$$u_0^n = u_1^n = 0 \quad \text{and} \quad u_{N-1}^n = u_N^n = 0. \tag{4.15}$$

This can be simplified by reducing the range of calculation to $l \in \{2, \ldots, N-2\}$.

Simply supported

As the states of the end points of a system with simply supported boundary conditions are 0 at all times, the range of calculation can be reduced to $l \in \{1, \ldots, N-1\}$. At $l = 1$ and $l = N-1$, definitions for the virtual grid points u_{-1}^n and u_{N+1}^n are needed. A definition for u_{-1}^n can be found by expanding Eq. (**??**) at $l = 0$:

$$\begin{aligned} & \frac{1}{h^2}\left(u_1^n - 2u_0^n + u_{-1}^n\right) = 0, \\ \overset{u_0^n=0}{\Longleftrightarrow} \quad & u_1^n + u_{-1}^n = 0, \\ & u_{-1}^n = -u_1^n, \end{aligned} \tag{4.16}$$

and similarly for u_{N+1}^n by expanding the condition at $l = N$:

$$u_{N+1}^n = -u_{N-1}^n.$$

Filling the first definition into the expanded scheme at $l = 1$ in (**??**) and collecting the terms yields

$$\begin{aligned} (1+\sigma_0 k)u_1^{n+1} = & \left(2 - 2\lambda^2 - 5\mu^2 - \frac{4\sigma_1 k}{h^2}\right) u_1^n + \left(\lambda^2 + 4\mu^2 + \frac{2\sigma_1 k}{h^2}\right) u_2^n \\ & - \mu^2 u_3^n + \left(-1 + \sigma_0 k + \frac{4\sigma_0 k}{h^2}\right) u_1^{n-1} - \frac{2\sigma_1 k}{h^2} u_2^{n-1}. \end{aligned} \tag{4.17}$$

Doing the same for $l = N-1$, we get

$$\begin{aligned} (1+\sigma_0 k)u_{N-1}^{n+1} = & \left(2 - 2\lambda^2 - 5\mu^2 - \frac{4\sigma_1 k}{h^2}\right) u_{N-1}^n + \left(\lambda^2 + 4\mu^2 + \frac{2\sigma_1 k}{h^2}\right) u_{N-2}^n \\ & - \mu^2 u_{N-3}^n + \left(-1 + \sigma_0 k + \frac{4\sigma_0 k}{h^2}\right) u_{N-1}^{n-1} - \frac{2\sigma_1 k}{h^2} u_{N-2}^{n-1}. \end{aligned} \tag{4.18}$$

Free

Finally, the free boundary condition requires all points to be calculated and the range of calculation is $l \in \{0, \ldots, N\}$. At each respective boundary, two virtual grid points are needed: u_{-1}^n and u_{-2}^n at the left and u_{N+1}^n and u_{N+2}^n at

the right boundary respectively. The combined operator in Eq. (**??**) is defined as:

$$\begin{aligned}\delta_x.\delta_{xx} &= \frac{1}{2h^3}\left(e_{x+} - e_{x-}\right)\left(e_{x+} - 2 + e_{x-}\right), \\ &= \frac{1}{2h^3}\left(e_{x+}^2 - 2e_{x+} + 1 - \left(1 - 2e_{x-} + e_{x-}^2\right)\right., \\ &= \frac{1}{2h^3}\left(e_{x+}^2 - 2e_{x+} + 2e_{x-} - e_{x-}^2\right), \end{aligned} \tag{4.19}$$

and can be used to solve for u_{-2}^n at $l = 0$:

$$\begin{aligned}\frac{1}{2h^3}\left(u_2^n - 2u_1^n + 2u_{-1}^n - u_{-2}^n\right) &= 0, \\ u_{-2}^n &= u_2^n - 2u_1^n + 2u_{-1}^n.\end{aligned}$$

As u_0^n is not necessarily 0 at all times, solving the first part of the boundary condition yields a different result than in the simply supported case:

$$\begin{aligned}\frac{1}{h^2}\left(u_1^n - 2u_0^n + u_{-1}^n\right) &= 0, \\ u_{-1}^n &= 2u_0^n - u_1^n.\end{aligned}$$

The same can be done at $l = N$ to get the following definitions for the virtual grid points

$$u_{N+2}^n = u_{N-2}^n - 2u_{N-1}^n + 2u_{N+1}^n \quad \text{and} \quad u_{N+1}^n = 2u_N^n - u_{N-1}^n.$$

The update equations for the boundary points will not be given here. Instead the matrix form of the FD scheme with free boundaries will be provided below.

In practice, the simply supported boundary condition is mostly chosen as this reflects reality the most. The clamped condition could be chosen for simplicity as this does not require an alternative update at the boundaries. The free boundary condition is more often used to model a (damped) ideal bar, (Eq. (**??**) with $T = 0$).

4.2.2 Implementation and Matrix Form

When using `MATLAB`, for a more compact implementation, it is useful to write the scheme in matrix form. The FD scheme of the stiff string in (**??**) can be written as

$$A\mathbf{u}^{n+1} = \mathbf{B}\mathbf{u}^n + \mathbf{C}\mathbf{u}^{n-1} \tag{4.20}$$

where

$$A = (1 + \sigma_0 k), \quad \mathbf{B} = c^2k^2\mathbf{D}_{xx} - \kappa^2k^2\mathbf{D}_{xxxx} + 2\sigma_1 k\mathbf{D}_{xx}$$
$$\text{and} \quad \mathbf{C} = -(1 - \sigma_0 k)\mathbf{I} - 2\sigma_1 k\mathbf{D}_{xx}.$$

Notice that A is a scalar rather than a matrix.

The size of the state vectors and the matrix-form operators depend on the boundary conditions. For clamped conditions, the state vectors ($\mathbf{u}^{n+1}$, $\mathbf{u}^n$ and $\mathbf{u}^{n-1}$) and matrices will be of size $(N-3)\times 1$ and $(N-3)\times(N-3)$ respectively. The $\mathbf{D}_{xx}$ matrix will be of the form given in (**??**) and the matrix form of the δ_{xxxx} operator is

$$\mathbf{D}_{xxxx} = \frac{1}{h^4}\begin{bmatrix} 6 & -4 & 1 & & \mathbf{0} \\ -4 & 6 & \ddots & \ddots & \\ 1 & \ddots & \ddots & \ddots & 1 \\ & \ddots & \ddots & 6 & -4 \\ \mathbf{0} & & 1 & -4 & 6 \end{bmatrix}. \tag{4.21}$$

For simply supported conditions, the state vectors and matrices will be of size $(N-1)\times 1$ and $(N-1)\times(N-1)$ respectively. Again, $\mathbf{D}_{xx}$ is as defined in (**??**) and $\mathbf{D}_{xxxx}$ can be obtained by multiplying two $\mathbf{D}_{xx}$ matrices according to

$$\mathbf{D}_{xxxx} = \mathbf{D}_{xx}\mathbf{D}_{xx} = \frac{1}{h^4}\begin{bmatrix} 5 & -4 & 1 & & & \mathbf{0} & \\ -4 & 6 & \ddots & \ddots & & & \\ 1 & \ddots & \ddots & -4 & 1 & & \\ & \ddots & -4 & 6 & -4 & \ddots & \\ & & 1 & -4 & \ddots & \ddots & 1 \\ & & & \ddots & \ddots & 6 & -4 \\ & \mathbf{0} & & & 1 & -4 & 5 \end{bmatrix}. \tag{4.22}$$

Finally for free boundary conditions as given in (**??**), the state vectors and matrices are $(N+1)\times 1$ and $(N+1)\times(N+1)$ respectively. Now, the $\mathbf{D}_{xx}$ matrix is of the form in (**??**) instead, and

$$\mathbf{D}_{xxxx} = \frac{1}{h^4}\begin{bmatrix} 2 & -4 & 2 & & & \mathbf{0} & \\ -2 & 5 & -4 & 1 & & & \\ 1 & -4 & 6 & -4 & 1 & & \\ & \ddots & \ddots & \ddots & \ddots & \ddots & \\ & & 1 & -4 & 6 & -4 & 1 \\ & & & 1 & -4 & 5 & -2 \\ & \mathbf{0} & & & 2 & -4 & 2 \end{bmatrix}. \tag{4.23}$$

4.2.3 Parameters and output

There exists a formula to calculate the loss coefficients σ_0 and σ_1 from T_{60} values at different frequencies (see [**?**, Eq (7.29)]). During this project, however, these values have been tuned by ear and are usually set to be in the range of $\sigma_0 = 1$ $\sigma_1 = 0.005$. See Table **??** for parameters most commonly used in this project.

Name	Symbol (unit)	Value
Length	L (m)	1
Material density	ρ (kg/m^3)	7850
Radius	r (m)	$5 \cdot 10^{-3}$
Tension	T (N)	$100 \leq T \leq 15^4$
Young's modulus	E (Pa)	$2 \cdot 10^{11}$
Freq.-independent damping	σ_1 (s^{-1})	1
Freq.-dependent damping	σ_0 (m^2/s)	0.005

Table 4.1: Parameters and the values most commonly used over the course of this project.

Output

Apart from the obvious material properties such as density, stiffness and geometry, the sound surprisingly much determined by σ_1, and for lower values the output can become extremely metallic.

time-domain and ff

4.3 von Neumann Analysis and Stability Condition

In order to obtain the stability condition for the damped stiff string, one can perform von Neumann analysis as presented in Section **??** on the FD scheme in (**??**).

Using the definitions found in Eq. (**??**) for the temporal operators and Eqs. (**??**) and (**??**) for the spatial operators, the frequency-domain representation of Eq. (**??**) can be obtained:

$$\frac{1}{k^2}\left(z - 2 + z^{-1}\right) = -\frac{4c^2}{h^2}\sin^2(\beta h/2) - \frac{16\kappa^2}{h^4}\sin^4(\beta h/2) - \frac{\sigma_0}{k}z + \frac{\sigma_0}{k}z^{-1} - \frac{8\sigma_1}{kh^2}\sin^2(\beta h/2) + \frac{8\sigma_1}{kh^2}\sin^2(\beta h/2)z^{-1},$$

and after collecting the terms, the characteristic equation follows:

$$(1+\sigma_0 k)z + \left(16\mu^2 \sin^4(\beta h/2) + \left(4\lambda^2 + \frac{8\sigma_1 k}{h^2}\right)\sin^2(\beta h/2) - 2\right) + \left(1 - \sigma_0 k - \frac{8\sigma_1 k}{h^2}\sin^2(\beta h/2)\right) z^{-1} = 0. \tag{4.24}$$

Rewriting this to the form in Eq. (**??**), and using $\mathcal{S} = \sin^2(\beta h/2)$ for brevity, yields

$$z^2 + \left(\frac{16\mu^2\mathcal{S}^2 + \left(4\lambda^2 + \frac{8\sigma_1 k}{h^2}\right)\mathcal{S} - 2}{1+\sigma_0 k}\right) z + \frac{1 - \sigma_0 k - \frac{8\sigma_1 k}{h^2}\mathcal{S}}{1+\sigma_0 k} = 0.$$

Stability of the system can then be proven using condition (**??**) and substituting the coefficients into this condition yields

$$\left|\frac{16\mu^2\mathcal{S}^2 + \left(4\lambda^2 + \frac{8\sigma_1 k}{h^2}\right)\mathcal{S} - 2}{1+\sigma_0 k}\right| - 1 \leq \frac{1 - \sigma_0 k - \frac{8\sigma_1 k}{h^2}\mathcal{S}}{1+\sigma_0 k} \leq 1,$$

$$\left|16\mu^2\mathcal{S}^2 + \left(4\lambda^2 + \frac{8\sigma_1 k}{h^2}\right)\mathcal{S} - 2\right| - (1+\sigma_0 k) \leq 1 - \sigma_0 k - \frac{8\sigma_1 k}{h^2}\mathcal{S} \leq 1 + \sigma_0 k,$$

$$\left|16\mu^2\mathcal{S}^2 + \left(4\lambda^2 + \frac{8\sigma_1 k}{h^2}\right)\mathcal{S} - 2\right| \leq 2 - \frac{8\sigma_1 k}{h^2}\mathcal{S} \leq 2 + 2\sigma_0 k.$$

The second condition is always true due to the fact that $\sigma_0, \sigma_1 \geq 0$. Continuing with the first condition:

$$-2 + \frac{8\sigma_1 k}{h^2}\mathcal{S} \leq 16\mu^2\mathcal{S}^2 + \left(4\lambda^2 + \frac{8\sigma_1 k}{h^2}\right)\mathcal{S} - 2 \leq 2 - \frac{8\sigma_1 k}{h^2}\mathcal{S},$$

$$0 \leq 16\mu^2\mathcal{S}^2 + 4\lambda^2\mathcal{S} \leq 4 - \frac{16\sigma_1 k}{h^2}\mathcal{S}.$$

As $16\mu^2\mathcal{S}^2 + 4\lambda^2\mathcal{S}$ is non-negative, the first condition is always satisfied. Continuing with the second condition:

$$16\mu^2\mathcal{S}^2 + \left(4\lambda^2 + \frac{16\sigma_1 k}{h^2}\right)\mathcal{S} \leq 4,$$

$$4\mu^2\mathcal{S}^2 + \left(\lambda^2 + \frac{4\sigma_1 k}{h^2}\right)\mathcal{S} \leq 1.$$

different wording

As $\mathcal{S}$ is bounded by 1, this can be substituted as it challenges the condition the most. Continuing with the substituted definitions for λ and μ from Eq. (**??**) yields

$$\frac{4\kappa^2 k^2}{h^4} + \frac{c^2 k^2 + 4\sigma_1 k}{h^2} \leq 1,$$

$$4\kappa^2 k^2 + (c^2 k^2 + 4\sigma_1 k)h^2 \leq h^4,$$

$$h^4 - (c^2 k^2 + 4\sigma_1 k)h^2 - 4\kappa^2 k^2 \geq 0,$$

which is a quadratic equation in h^2. The grid spacing h is then bounded by

$$h \geq \sqrt{\frac{c^2k^2 + 4\sigma_1 k + \sqrt{(c^2k^2 + 4\sigma_1 k)^2 + 16\kappa^2 k^2}}{2}}, \tag{4.25}$$

which is the stability condition for the damped stiff string also shown in Eq. (**??**).

4.4 Energy Analysis

As mentioned in Section **??**, it is useful to perform the energy analysis on the scheme with all physical parameters written out. Discretising the PDE in (**??**) yields

$$\rho A \delta_{tt} u_l^n = T \delta_{xx} u_l^n - EI \delta_{xxxx} u_l^n - 2\sigma_0 \rho A \delta_{t\cdot} u_l^n + 2\sigma_1 \rho A \delta_{t-} \delta_{xx} u_l^n, \tag{4.26}$$

defined for $l \in d$ with discrete domain $d = \{0, \ldots, N\}$. This section will follow the 4 steps described in Section **??**.

Step 1: Obtain $\delta_{t+}\mathfrak{h}$

The first step is to take the inner product (see Eq. (**??**)) of the scheme with $(\delta_{t\cdot} u_l^n)$ over discrete domain d:

$$\begin{aligned}\delta_{t+}\mathfrak{h} = \rho A \langle \delta_{t\cdot} u_l^n, \delta_{tt} u_l^n \rangle_d - T \langle \delta_{t\cdot} u_l^n, \delta_{xx} u_l^n \rangle_d + EI \langle \delta_{t\cdot} u_l^n, \delta_{xxxx} u_l^n \rangle_d \\ + 2\sigma_0 \rho A \langle \delta_{t\cdot} u_l^n, \delta_{t\cdot} u_l^n \rangle_d - 2\sigma_1 \rho A \langle \delta_{t\cdot} u_l^n, \delta_{t-} \delta_{xx} u_l^n \rangle_d = 0.\end{aligned} \tag{4.27}$$

Step 2: Identify energy types and isolate δ_{t+}

As there is damping present in the system, and the system is distributed, the damping term $\mathfrak{q}$ and boundary term $\mathfrak{b}$ appear and the energy balance will be of the form

$$\delta_{t+}\mathfrak{h} = \mathfrak{b} - \mathfrak{q}. \tag{4.28}$$

The damping term is defined as

$$\mathfrak{q} = 2\sigma_0 \rho A \| \delta_{t\cdot} u_l^n \|_d^2 - 2\sigma_1 \rho A \langle \delta_{t\cdot} u_l^n, \delta_{t-} \delta_{xx} u_l^n \rangle_d, \tag{4.29}$$

and the boundary term $\mathfrak{b}$ appears after rewriting Equation (**??**) using summation by parts (see Section **??**). Specifically, using Eq. (**??**) for the second term and Eq. (**??**) for the third, we get

$$\begin{aligned}\delta_{t+}\mathfrak{h} &= \rho A \langle \delta_{t\cdot} u_l^n, \delta_{tt} u_l^n \rangle_d + T \langle \delta_{t\cdot} \delta_{x+} u_l^n, \delta_{x+} u_l^n \rangle_{\underline{d}} + EI \langle \delta_{t\cdot} \delta_{xx} u_l^n, \delta_{xx} u_l^n \rangle_{\overline{\underline{d}}} \\ &= \mathfrak{b} - \mathfrak{q}\end{aligned}$$

where the boundary term becomes

$$\begin{aligned}\mathfrak{b} = T\Big((\delta_{t\cdot}u_N^n)(\delta_{x+}u_N^n) - (\delta_{t\cdot}u_0^n)(\delta_{x+}u_{-1}^n)\Big)\\ + EI\Big((\delta_{t\cdot}u_N^n)(\delta_{x+}\delta_{xx}u_N^n) - (\delta_{xx}u_N^n)(\delta_{x-}\delta_{t\cdot}u_N^n)\Big)\\ + EI\Big(-(\delta_{t\cdot}u_0^n)(\delta_{x-}\delta_{xx}u_0^n) + (\delta_{xx}u_0^n)(\delta_{x+}\delta_{t\cdot}u_0^n)\Big).\end{aligned}$$

For the clamped and simply supported boundary conditions in (**??**) and (**??**) it can easily be shown that $\mathfrak{b} = 0$. If free conditions as in Eq. (**??**) are used, the boundary conditions will vanish when the primed inner product in Eq. (**??**) is used in Step 1 and identity (**??**) when performing summation by parts. Here, we continue with the clamped / simply supported case.

Isolating δ_{t+} to obtain the total energy $\mathfrak{h}$ in the definition for $\delta_{t+}\mathfrak{h}$ above, requires identities (**??**) and (**??**) and yields

$$\begin{aligned}\delta_{t+}\mathfrak{h} &= \delta_{t+}\left(\frac{\rho A}{2}\|\delta_{t-}u_l^n\|_d^2 + \frac{T}{2}\langle\delta_{x+}u_l^n, e_{t-}\delta_{x+}u_l^n\rangle_{\underline{d}} + \frac{EI}{2}\langle\delta_{xx}u_l^n, e_{t-}\delta_{xx}u_l^n\rangle_{\underline{\overline{d}}}\right)\\ &= -\mathfrak{q}.\end{aligned}$$

From this, the definition for the Hamiltonian $\mathfrak{h}$, the kinetic energy $\mathfrak{t}$ and potential energy $\mathfrak{v}$ can be found:

$$\begin{aligned}\mathfrak{h} = \mathfrak{t} + \mathfrak{v}, \quad \text{with} \quad \mathfrak{t} = \frac{\rho A}{2}\|\delta_{t-}u_l^n\|_d^2, \text{and}\\ \mathfrak{v} = \frac{T}{2}\langle\delta_{x+}u_l^n, e_{t-}\delta_{x+}u_l^n\rangle_{\underline{d}} + \frac{EI}{2}\langle\delta_{xx}u_l^n, e_{t-}\delta_{xx}u_l^n\rangle_{\underline{\overline{d}}}.\end{aligned} \tag{4.30}$$

Step 3: Check units

Comparing the acquired energy balance in Eq. (**??**) to the energy balance for the 1D wave equation in Eq. (**??**), one can observe that the balances are nearly identical, the only difference being the second term in the definition for $\mathfrak{v}$ in Eq. (**??**). Writing this term out in units, and recalling that Pa (the unit for E) in SI units is $\text{kg}\cdot\text{m}^{-1}\cdot\text{s}^{-2}$, yields

$$\begin{aligned}\frac{EI}{2}\langle\delta_{xx}u_l^n, e_{t-}\delta_{xx}u_l^n\rangle_{\underline{\overline{d}}} &\xrightarrow{\text{in units}} \text{Pa}\cdot\text{m}^4\cdot\text{m}\cdot(\text{m}^{-2}\cdot\text{m}\cdot\text{m}^{-2}\cdot\text{m})\\ &= \text{kg}\cdot\text{m}^2\cdot\text{s}^{-2},\end{aligned}$$

and indeed has the correct units.

The damping terms in $\mathfrak{q}$ need to be in Joules per second, or $\text{kg}\cdot\text{m}^2\cdot\text{s}^{-3}$.

Writing the terms in Eq. (**??**) out in their units yields

$$\begin{aligned} 2\sigma_0\rho A\|\delta_{t\cdot}u_l^n\|_d^2 &\xrightarrow{\text{in units}} \mathrm{s}^{-1}\cdot\mathrm{kg}\cdot\mathrm{m}^{-3}\cdot\mathrm{m}^2\cdot\mathrm{m}\cdot(\mathrm{s}^{-1}\cdot\mathrm{m})^2 \\ &= \mathrm{kg}\cdot\mathrm{m}^2\cdot\mathrm{s}^{-3}, \\ -2\sigma_1\rho A\langle\delta_{t\cdot}u_l^n, \delta_{t-}\delta_{xx}u_l^n\rangle_d &\xrightarrow{\text{in units}} \mathrm{m}^2\cdot\mathrm{s}^{-1}\cdot\mathrm{kg}\cdot\mathrm{m}^{-3}\cdot\mathrm{m}^2 \\ &\quad\cdot\mathrm{m}\cdot(\mathrm{s}^{-1}\cdot\mathrm{m})(\mathrm{s}^{-1}\cdot\mathrm{m}^{-2}\cdot\mathrm{m}), \\ &= \mathrm{kg}\cdot\mathrm{m}^2\cdot\mathrm{s}^{-3}, \end{aligned}$$

and also have the correct units.

Step 4: Implementation

Matrix form...

4.5 Modal Analysis

To be able to perform a modal analysis on the FD scheme in (**??**), it must be written in one-step form – introduced in Section **??** – due to the damping present in the system. Using with the matrix form of the damped stiff string in Eq. (**??**), it can be written as

$$\underbrace{\begin{bmatrix}\mathbf{u}^{n+1}\\ \mathbf{u}^{n}\end{bmatrix}}_{\mathbf{w}^{n+1}} = \underbrace{\begin{bmatrix}\mathbf{B}/A & \mathbf{C}/A\\ \mathbf{I} & \mathbf{0}\end{bmatrix}}_{\mathbf{Q}}\underbrace{\begin{bmatrix}\mathbf{u}^{n}\\ \mathbf{u}^{n-1}\end{bmatrix}}_{\mathbf{w}^{n}} \tag{4.31}$$

where the definitions for $\mathbf{B}$, $\mathbf{C}$ and A can be found in Section **??**. The definitions for $\mathbf{D}_{xx}$ and $\mathbf{D}_{xxxx}$ those for simply supported boundary conditions as these are used most often in the case of strings.

Assuming test solutions of the form $\mathbf{w} = z^n\boldsymbol{\phi}$, and recalling that $z = e^{sk}$ and complex frequency $s = j\omega + \sigma$, we get the following eigenvalue problem (see Section **??**)

$$z\boldsymbol{\phi} = \mathbf{Q}\boldsymbol{\phi}, \tag{4.32}$$

which has the following solutions

$$s_p = \frac{1}{k}\ln\left(\mathrm{eig}_p(\mathbf{Q})\right). \tag{4.33}$$

The (angular) frequency of the p^{th} mode can then be obtained using $\Im(s_p)$ and the damping per mode as $\Re(s_p)$. Only selecting the non-negative frequencies obtained from $\Im(s_p)$, these can be plotted and are shown in Figure **??**.

make figure

The parameters used are the ones found in Table **??** with $T = 13000$ N, $f_\mathrm{s} = 44100$.

not done...

4.6 Implicit Scheme

Although not used in the published work of this project, it is useful to touch upon an example of an implicit scheme. Consider a discretisation of Eq. (**??**) where the (more accurate) centred operator is used for the frequency-dependent damping term:

$$\delta_{tt} u_l^n = c^2 \delta_{xx} u_l^n - \kappa^2 \delta_{xxxx} u_l^n - 2\sigma_0 \delta_{t.} u_l^n + 2\sigma_1 \delta_{t.} \delta_{xx} u_l^n. \tag{4.34}$$

Using the centred operator in the mixed-spatial-temporal operator renders the system *implicit*, meaning that a definition for u_l^{n+1} can not explicitly be found from known values. The stencil in Figure **??** also shows this: in order to calculate u_l^{n+1}, neighbouring points at the next time step u_{l+1}^{n+1} and u_{l-1}^{n+1} are needed. The issue is that these values are unknown at the time of calculation.

Luckily, as the scheme is linear, it can be treated as a system of linear equations and solved following the technique described in Section **??**. The drawback is that this requires one matrix inversion per iteration which can be extremely costly (see Section **??**). However, both von Neumann and modal analysis (below) show that using the centred instead of the backwards operator has a positive effect on the stability and the modal behaviour of the scheme.

Left off here!! taking simply supported boundary conditions such that $l \in \{1, \ldots, N-1\}$ are $N-1$ unknowns that can be calculated using $N-1$ equations. The column vector $\mathbf{u}^n = [u_1^n, u_2^n, \ldots, u_{N-1}^n]$

$$\mathbf{A}\mathbf{u}^{n+1} = \mathbf{B}\mathbf{u}^n + \mathbf{C}\mathbf{u}^{n-1} \tag{4.35}$$

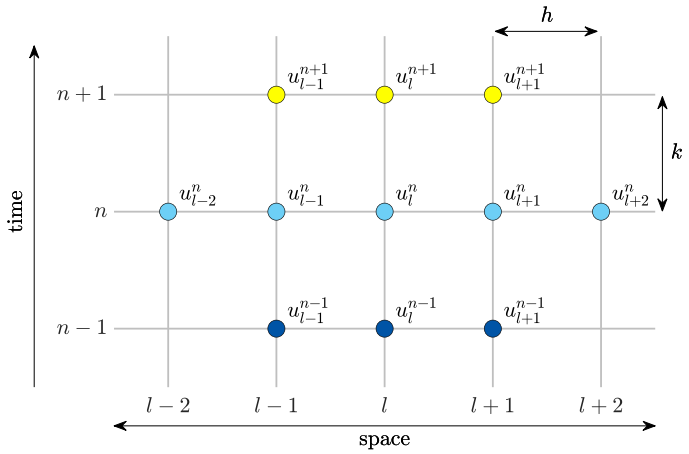

Fig. 4.3: The stencil for the damped stiff string scheme in (**??**).

4.6.1 von Neumann analysis

Following Section **??**..

below is the exact same wording as above

$$\frac{1}{k^2}\left(z-2+z^{-1}\right) = -\frac{4c^2}{h^2}\sin^2(\beta h/2) - \frac{16\kappa^2}{h^4}\sin^4(\beta h/2) - \frac{\sigma_0}{k}z + \frac{\sigma_0}{k}z^{-1} - \frac{4\sigma_1}{kh^2}\sin^2(\beta h/2)z + \frac{4\sigma_1}{kh^2}\sin^2(\beta h/2)z^{-1} \tag{4.36}$$

and after collecting the terms, the characteristic equation follows

$$\left(1+\sigma_0 k + \frac{4\sigma_1 k}{h^2}\sin^2(\beta h/2)\right)z + \left(16\mu^2\sin^4(\beta h/2) + 4\lambda^2\sin^2(\beta h/2) - 2\right) + \left(1-\sigma_0 k - \frac{4\sigma_1 k}{h^2}\sin^2(\beta h/2)\right)z^{-1} = 0. \tag{4.37}$$

Rewriting this to the form (**??**) and, again, using $\mathcal{S} = \sin^2(\beta h/2)$ yields:

$$z^2 + \frac{16\mu^2\mathcal{S}^2 + 4\lambda^2\mathcal{S} - 2}{1+\sigma_0 k + \frac{4\sigma_1 k}{h^2}\mathcal{S}}z + \frac{1-\sigma_0 k - \frac{4\sigma_1 k}{h^2}\mathcal{S}}{1+\sigma_0 k + \frac{4\sigma_1 k}{h^2}\mathcal{S}} = 0.$$

stability of the system can be proven using condition (**??**). Continuing with $\mathcal{S} = \sin^2(\beta h/2)$ and substituting the coefficients into this condition yields

$$\left|\frac{16\mu^2\mathcal{S}^2 + 4\lambda^2\mathcal{S} - 2}{1+\sigma_0 k + \frac{4\sigma_1 k}{h^2}\mathcal{S}}\right| - 1 \leq \frac{1-\sigma_0 k - \frac{4\sigma_1 k}{h^2}\mathcal{S}}{1+\sigma_0 k + \frac{4\sigma_1 k}{h^2}\mathcal{S}} \leq 1,$$

$$\left|16\mu^2\mathcal{S}^2 + 4\lambda^2\mathcal{S} - 2\right| - \left(1+\sigma_0 k + \frac{4\sigma_1 k}{h^2}\mathcal{S}\right) \leq 1-\sigma_0 k - \frac{4\sigma_1 k}{h^2}\mathcal{S} \leq 1+\sigma_0 k + \frac{4\sigma_1 k}{h^2}\mathcal{S},$$

$$\left|16\mu^2\mathcal{S}^2 + 4\lambda^2\mathcal{S} - 2\right| \leq 2 \leq 2+2\sigma_0 k + \frac{8\sigma_1 k}{h^2}\mathcal{S}$$

Because $\sigma_0, \sigma_1, k, \mathcal{S}$ and h are all non-negative, the last condition is always satisfied. Continuing with the first condition:

4.6.2 Modal analysis

As Eq. (**??**) matches the form in Eq. (**??**), one can perform a modal analysis by writing the scheme in one-step form as explained in Section **??**

Chapter 5

Brass

Bore

5.1 Second-order system

The first main difference between the 1D brass PDE and the 1D wave equation is the possibility of having a variable cross-section. Following Section 19.3 from [**?**], the PDE for a 1D (axially symmetric) acoustic tube with variable cross-section is (also known as *Webster*'s equation)

$$S\partial_t^2\Psi = c^2\partial_x(S\partial_x\Psi), \tag{5.1}$$

with *acoustic potential* $\Psi = \Psi(x,t)$ (m^2/s), $S = S(x)$ is the cross sectional area (m^2) and wave speed c ($\mathrm{m/s}$).

5.1.1 Discretisation

Introducing interleaved gridpoints at $n - 1/2$ and $n + 1/2$ for S, a we can discretise Eq. (**??**) (following [**?**]) to

$$\bar{S}\delta_{tt}\Psi_l^n = c^2\delta_{x+}(S_{l-1}(\delta_{x-}\Psi_l^n)), \tag{5.2}$$

where

$$\bar{S} = \mu_{t+}S_{l-1} = \frac{S_{l+1} + S_{l-1}}{2}. \tag{5.3}$$

The right side of the equation in (**??**) contains an operator applied to two grid functions (S and Ψ) multiplied onto each other. In order to expand this, we need to use the product rule (Eq. (2.23) in [**?**]) which is

$$\delta_{x+}(u_l w_l) = (\delta_{x+}u_l)(\mu_{x+}w_l) + (\mu_{x+}u_l)(\delta_{x+}w_l). \tag{5.4}$$

In the case of (**??**), $u_l \triangleq S_{l-1}$ and $w_l \triangleq \delta_{x-}\Psi_l^n$. Expanding (retaining the notation for $\bar{S}$) and solving for Ψ_l^{n+1} yields (Appendix **??**)

$$\Psi_l^{n+1} = 2(1-\lambda^2)\Psi_l^n - \Psi_l^{n-1} + \frac{\lambda^2 S_{l+1}}{\bar{S}}\Psi_{l+1}^n + \frac{\lambda^2 S_{l-1}}{\bar{S}}\Psi_{l-1}^n, \tag{5.5}$$

which is identical to Eq. (19.51) in [**?**].

5.1.2 Boundary Conditions

The choices for boundary conditions in an acoustic tube are open and closed, defined as [**?**]

$$\begin{aligned} \partial_t \Psi &= 0 \text{ (open, Dirichlet)} \\ \partial_x \Psi &= 0 \text{ (closed, Neumann),} \end{aligned} \tag{5.6}$$

at the ends of the tube. This might be slightly counter-intuitive as in the case of a string "closed" might imply the "clamped" or Dirichlet boundary condition. The opposite can be intuitively shown imagining a wave front with a positive acoustic potential moving through a tube and hitting a closed end. What comes back is also a wave front with a positive acoustic potential, i.e., the sign of the potential does not flip, which also happens using the free or Neumann condition for the string.

In this case we follow [**?**, Chapter 9] and use the following

$$\partial_x \Psi(0,t) = 0 \quad \text{and} \quad \partial_t \Psi(L,t) = 0 \tag{5.7}$$

i.e. closed at the left end and open at the right end. In discrete time we have two choices for the closed condition

$$\begin{aligned} \delta_{x\cdot}\Psi_0^n = 0 \;\Rightarrow\; \Psi_{-1}^n = \Psi_1^n \quad \text{(centered)} \\ \delta_{x-}\Psi_0^n = 0 \;\Rightarrow\; \Psi_{-1}^n = \Psi_0^n \quad \text{(non-centered)} \end{aligned} \tag{5.8}$$

At the left boundary we can now solve Eq. (**??**) for the centered case:

$$\begin{aligned} \Psi_0^{n+1} &= 2(1-\lambda^2)\Psi_0^n - \Psi_0^{n-1} + \frac{\lambda^2 S_{1/2}}{\bar{S}_0}\Psi_1^n + \frac{\lambda^2 S_{-1/2}}{\bar{S}_0}\Psi_{-1}^n \\ \Psi_0^{n+1} &= 2(1-\lambda^2)\Psi_0^n - \Psi_0^{n-1} + \frac{\lambda^2 (S_{1/2} + S_{-1/2})}{\bar{S}_0}\Psi_1^n \\ \Psi_0^{n+1} &= 2(1-\lambda^2)\Psi_0^n - \Psi_0^{n-1} + 2\lambda^2\Psi_1^n, \end{aligned}$$

and the non-centered case

$$\Psi_0^{n+1} = 2(1-\lambda^2)\Psi_0^n - \Psi_0^{n-1} + \frac{\lambda^2 S_{1/2}}{\bar{S}_0}\Psi_1^n + \frac{\lambda^2 S_{-1/2}}{\bar{S}_0}\Psi_0^n. \tag{5.9}$$

As can be seen from the equations above, we need undefined points $\bar{S}_0$ and $S_{-1/2}$. At the left boundary, we set $\bar{S}_0 = S_0$ from which, we can calculate $S_{-1/2}$:

$$S_0 = \frac{1}{2}(S_{1/2} + S_{-1/2}) \;\Rightarrow\; S_{-1/2} = 2S_0 - S_{1/2} \tag{5.10}$$

The same can be done for the right boundary ($\bar{S}_N = S_N$) if this is chosen to be anything else but open (e.g., closed or radiating – see Section **??**):

$$S_N = \frac{1}{2}(S_{N+1/2} + S_{N-1/2}) \;\Rightarrow\; S_{N+1/2} = 2S_N - S_{N-1/2}. \tag{5.11}$$

For now though, we follow the conditions given in (**??**) and we can simply set the right boundary to its initial state

$$\Psi_N^n = \Psi_N^0 \tag{5.12}$$

which is normally 0. A more realistic open end is a radiating one, which can be found below.

Radiating end

We can change the condition presented in Eq. (**??**) to a radiating end,

$$\partial_x \Psi(L,t) = -a_1 \partial_t \Psi(L,t) - a_2 \Psi(L,t) \tag{5.13}$$

where [**?**]

$$a_1 = \frac{1}{2(0.8216)^2 c} \quad \text{and} \quad a_2 = \frac{L}{0.8216\sqrt{S_0 S(1)/\pi}}. \tag{5.14}$$

taken from [**?**] and are valid for a tube terminating on an infinite plane. The terms in Eq. (**??**) are a damping and an inertia term where a_1 is a loss coefficient (in s/m) and a_2 is the **inertia coefficient** (in m^{-1}). The centered and non-centered case are defined as

$$\begin{aligned} \delta_{x\cdot}\Psi_N^n = 0 \;&\Rightarrow\; \Psi_{N+1}^n = \Psi_{N-1}^n \quad \text{(centered)} \\ \delta_{x+}\Psi_N^n = 0 \;&\Rightarrow\; \Psi_{N+1}^n = \Psi_N^n \quad \text{(non-centered)} \end{aligned} \tag{5.15}$$

First, we solve Eq. (**??**) for the centered (Eq. (9.16) in [**?**])

$$\delta_{x\cdot}\Psi_N^n = -a_1 \delta_{t\cdot}\Psi_N^n - a_2 \mu_{t\cdot}\Psi_N^n \tag{5.16}$$

which can be expanded and solved for Ψ_{N+1}^n according to

$$\begin{aligned} \frac{1}{2h}(\Psi_{N+1}^n - \Psi_{N-1}^n) &= -\frac{a_1}{2k}(\Psi_N^{n+1} - \Psi_N^{n-1}) - \frac{a_2}{2}(\Psi_N^{n+1} + \Psi_N^{n-1}) \\ \Psi_{N+1}^n &= h\left(-\frac{a_1}{k}(\Psi_N^{n+1} - \Psi_N^{n-1}) - a_2(\Psi_N^{n+1} + \Psi_N^{n-1})\right) + \Psi_{N-1}^n, \end{aligned} \tag{5.17}$$

which can be substituted into Eq. (**??**) (Appendix **??**)

$$\Psi_N^{n+1} = \frac{2(1-\lambda^2)\Psi_N^n - \Psi_N^{n-1} + \frac{h\lambda^2 S_{N+1/2}}{\bar{S}_N}\left(\frac{a_1}{k} - a_2\right)\Psi_N^{n-1} + 2\lambda^2\Psi_{N-1}^n}{\left(1 + \left(\frac{a_1}{k} + a_2\right)\frac{h\lambda^2 S_{N+1/2}}{\bar{S}_N}\right)}. \tag{5.18}$$

The same can be done for the non-centered case (Eq. (9.15) in [**?**])

$$\delta_{x+}\Psi_N^n = -a_1\delta_{t\cdot}\Psi_N^n - a_2\mu_{t\cdot}\Psi_N^n \tag{5.19}$$

which when solved for Ψ_{N+1}^n yields

$$\begin{aligned}\frac{1}{h}(\Psi_{N+1}^n - \Psi_N^n) &= -\frac{a_1}{2k}(\Psi_N^{n+1} - \Psi_N^{n-1}) - \frac{a_2}{2}(\Psi_N^{n+1} + \Psi_N^{n-1}) \\ \Psi_{N+1}^n &= h\left(-\frac{a_1}{2k}(\Psi_N^{n+1} - \Psi_N^{n-1}) - \frac{a_2}{2}(\Psi_N^{n+1} + \Psi_N^{n-1})\right) + \Psi_N^n.\end{aligned} \tag{5.20}$$

Substituted into Eq. (**??**) yields (Appendix **??**)

$$\Psi_N^{n+1} = \frac{2(1-\lambda^2)\Psi_N^n - \Psi_N^{n-1} + \frac{h\lambda^2 S_{N+1/2}}{\bar{S}_N}\left(\frac{a_1}{2k} - \frac{a_2}{2}\right)\Psi_N^{n-1} + \frac{\lambda^2 S_{N+1/2}}{\bar{S}_N}\Psi_N^n + \frac{\lambda^2 S_{N-1/2}}{\bar{S}_N}\Psi_{N-1}^n}{\left(1 + \left(\frac{a_1}{2k} + \frac{a_2}{2}\right)\frac{h\lambda^2 S_{N+1/2}}{\bar{S}_N}\right)}. \tag{5.21}$$

5.2 First-order system

This will be the first appearance of a first-order system.

Chapter 6

2D Systems

In this work, it is mainly used to model a simplified body in papers...

State variable $u = u(x, y, t)$ where $t \geq 0$ and $(x, y) \in \mathcal{D}$ where $\mathcal{D}$ is 2-dimensional. The state variable can then be discretised according to $u(x, y, t) \approx u^n_{l,m}$ with space $x = lh$ and $y = mh$ and time $t = nk$ and $k = 1/f_\mathrm{s}$. For simplicity the grid spacing in both the x and y directions are set to be the same but could be different.

In continuous time the operators:

$$\Delta = \partial_x^2 + \partial_y^2 \tag{6.1}$$

The same shift operators as defined in Chapter **??** can be applied to grid function $u^n_{l,m}$. Additional ones are

$$e_{y+}u^n_{l,m} = u^n_{l,m+1}, \quad \text{and} \quad e_{y-}u^n_{l,m} = u^n_{l,m-1}. \tag{6.2}$$

6.1 Analysis Techniques in 2D

Here, some of the differences between the analysis techniques presented in Chapter **??** and those in 2D will be elaborated on. Although, modal analysis remains the same

6.1.1 Frequency Domain Analysis

$p_x + p_y$

ansatz:

$$u^n_{l,m} = z^n e^{jh(l\beta_x + m\beta_y)} \tag{6.3}$$

6.1.2 Energy Analysis

Squared domain $d \in \{0, \ldots, N_x\} \times \{0, \ldots, N_y\}$

$$\langle f^n, g^n \rangle_d = \sum_{l=0}^{N_x} \sum_{m=0}^{N_y} h^2 f^n_{l,m} g^n_{l,m} \tag{6.4}$$

6.1.3 Modal Analysis

Stacked matrix form

6.2 2D Wave Equation

The 2D wave equation be used to model an ideal membrane such as done in

It has identical behaviour to the 2D waveguide mesh presented by van Duyne and Smith [**?**].

Consider a square ideal membrane with side lengths L_x and L_y (both in m) and its transverse displacement described by $u = u(x, y, t)$. The membrane is defined over $(x, y) \in \mathcal{D}$ with domain $\mathcal{D} = [0, L_x] \times [0, L_y]$ and its motion is described by the following PDE

$$\partial_t^2 u = c^2 \Delta u \tag{6.5}$$

with wave speed $c = \sqrt{T/\rho H}$ (in m/s), tension per unit length (applied to the boundary)T (in N/m), material density ρ (in kg/m^3) and thickness H.

check whether this is right..

6.3 Thin plate

Used in [**??**], [**??**], [**??**] and [**??**] biharmonic operator, Laplacian in (**??**) applied to itself.

$$\rho H \partial_t^2 u = -D \Delta \Delta u \tag{6.6}$$

where $D = EH^3/12(1 - \nu^2)$

6.4 Stiff membrane

Combination between Eqs. (**??**) and (**??**)

$$\rho H \partial_t^2 u = T \Delta u - D \Delta \Delta u \tag{6.7}$$

[**??**]

check whether all references are used

Part III

Appendix

Appendix A

List of Symbols

The list of symbols found below contains often-used symbols in the thesis in the context that they are normally used. Depending on the context they might carry a different meaning (y being displacement of the lip-reed in Chapter **??** but the vertical spatial coordinate for 2D systems in fx. Chapter **??**). Some might also be accompanied by a subscript in the main document

Symbol	Description	Unit
α	Fractional part of	
A	Cross-sectional area of string	m^2
c	Wave speed	$\mathrm{m/s}$
$\frac{d^n}{dt^n}$	n^{th} order derivative with respect to t	-
∂_t^n	n^{th} order partial derivative with respect to t	-
δ_{t+}, δ_{t-}, $\delta_{t\cdot}$	Forward, backward and centred difference in time operator	-
δ_{x+}, δ_{x-}, $\delta_{x\cdot}$	Forward, backward and centred difference in space operator	-
δ_{tt}	Second order difference in time operator	-
δ_{xx}	Second order difference in space operator	-
δ_{xxxx}	Fourth order difference in space operator	-
μ_{t+}, μ_{t-}, $\mu_{t\cdot}$	Forward, backward and centred average in time operator	-
μ_{x+}, μ_{x-}, $\mu_{x\cdot}$	Forward, backward and centred average in space operator	-
μ_{tt}	Second order average in time operator	-
μ_{xx}	Second order average in space operator	-

Symbol	Description	Unit
E	Young's Modulus	Pa ($\mathrm{kg{\cdot}m^{-1}{\cdot}s^{-2}}$)
f	Force	N
f	Frequency	Hz
f_s	Sample rate	Hz
F	Scaled force	depends on system
h	Grid spacing	m
H	Membrane / Plate thickness	m
I	Area moment of inertia	m^4
l	Spatial index to grid function	-
L	Length	m
k	Time step ($= 1/f_\mathrm{s}$)	s
K	Spring coefficient	$\mathrm{N/m}$
κ	Stiffness coefficient	$\mathrm{m^2/s}$ (1D) $\mathrm{m^4{\cdot}s^{-2}}$ (2D)
n	Sample index to grid function	-
N	Number of points string	-
$\mathbb{N}^0$	Set of non-negative integers	-
p	Pressure	Pa
r	Radius	m
S	Cross-sectional area (brass)	m^2
t	Time	s
T	Tension	N (1D) $\mathrm{N/m}$ (2D)
u	State variable	m
v	Particle velocity	$\mathrm{m/s}$
x	Spatial dimension (horizontal for 2D systems)	m
y	Vertical spatial dimension	m
γ	Scaled wave speed	s^{-1}
λ	Courant number for 1D wave eq. ($= ck/h$)	-
μ	Stiffness free parameter	-
ν	Poisson's ratio	-
η	Relative displacement spring	m
ρ	Material density	$\mathrm{kg{\cdot}m^{-3}}$

Operations

Symbol	Description	Unit
$\mathfrak{I}(\cdot)$	Imaginary part of	
$\mathfrak{R}(\cdot)$	Real part of	
$\lfloor \cdot \rfloor$	Flooring operation	
$\lceil \cdot \rceil$	Ceiling operation	
Subscripts		
c	Connection	
p	Plate	
s	String	

Appendix A. List of Symbols

Appendix B

List of Abbreviations

Abbreviation	Definition
1D	one-dimensional
2D	two-dimensional
3D	three-dimensional
DoF	Degrees of freedom
DSP	Digital signal processing
Eq.	Equation
Eqs.	Equations
FD	Finite-difference
FDTD	Finite-difference time-domain
LTI	Linear time-invariant
ODE	Ordinary differential equation
PDE	Partial differential equation

Appendix C

Code Snippets

C.1 Mass-Spring System (Section ??)

```
%% Initialise variables
fs = 44100;              % sample rate [Hz]
k = 1 / fs;              % time step [s]
lengthSound = fs;        % length of the simulation (1 second) [samples]

f0 = 440;                % fundamental frequency [Hz]
omega0 = 2 * pi * f0;    % angular (fundamental) frequency [Hz]
M = 1;                   % mass [kg]
K = omega0^2 * M;        % spring constant [N/m]

%% initial conditions (u0 = 1, d/dt u0 = 0)
u = 1;
uPrev = 1;

% initialise output vector
out = zeros(lengthSound, 1);

%% Simulation loop
for n = 1:lengthSound

    % Update equation Eq. (??)
    uNext = (2 - K * k^2 / M) * u - uPrev;

    out(n) = u;

    % Update system states
    uPrev = u;
    u = uNext;
end
```

C.2 1D Wave Equation (Section ??)

```
%% Initialise variables
fs = 44100;          % Sample rate [Hz]
k = 1 / fs;          % Time step [s]
lengthSound = fs;    % Length of the simulation (1 second) [samples]

c = 300;             % Wave speed [m/s]
L = 1;               % Length [m]
h = c * k;           % Grid spacing [m] (from CFL condition)
N = floor(L/h);      % Number of intervals between grid points
h = L / N;           % Recalculation of grid spacing based on integer N

lambdaSq = c^2 * k^2 / h^2; % Courant number squared

% Boundary conditions ([D]irichlet or [N]eumann)
bcLeft = "D";
bcRight = "D";

%% Initialise state vectors (one more grid point than the number of
    intervals)
uNext = zeros(N+1, 1);
u = zeros(N+1, 1);

%% Initial conditions (raised cosine)
loc = round(0.8 * N);        % Center location
halfWidth = round(N/10);     % Half-width of raised cosine
width = 2 * halfWidth;       % Full width
rcX = 0:width;               % x-locations for raised cosine

rc = 0.5 - 0.5 * cos(2 * pi * rcX / width); % raised cosine
u(loc-halfWidth : loc+halfWidth) = rc; % initialise current state

% Set initial velocity to zero
uPrev = u;

% Range of calculation
range = 2:N;

% Output location
outLoc = round(0.3 * N);

%% Simulation loop
for n = 1:lengthSound

    % Update equation Eq. (??)
    uNext(range) = (2 - 2 * lambdaSq) * u(range) ...
        + lambdaSq * (u(range+1) + u(range-1)) - uPrev(range);

    % boundary updates Eq. (??)
    if bcLeft == "N"
        uNext(1) = (2 - 2 * lambdaSq) * u(1) - uPrev(1) ...
        + 2 * lambdaSq * u(2);
```

```
    end

    % Eq. (??)
    if bcRight == "N"
        uNext(N+1) = (2 - 2 * lambdaSq) * u(N+1) - uPrev(N+1) ...
        + 2 * lambdaSq * u(N);
    end

    out(n) = u(outLoc);

    % Update system states
    uPrev = u;
    u = uNext;
end
```

Part IV

Papers

Paper Errata

Here, some errors in the published papers will be listed:

Real-Time Tromba [??]

- The minus sign in Eq. (28) (and thus Eqs. (31) and (35)) should be a plus sign.
- $\sigma_{1,\mathrm{s}}$ in Eq. (21) should obviously be $\sigma_{1,\mathrm{p}}$
- the unit of the spatial Dirac delta function δ should be m^{-1}

DigiDrum [??]

- σ_0 and σ_1 should be multiplied by ρH in order for the stability condition to hold.
- stability condition is wrong. Should be:

$$h \geq \sqrt{c^2k^2 + 4\sigma_1 k + \sqrt{(c^2k^2 + 4\sigma_1 k)^2 + 16\kappa^2 k^2}} \tag{1}$$

- Unit for membrane tension is $\mathrm{N/m}$.

Dynamic grids [??]

- Reference in intro for 'recently gained popularity' should go to **[?]**
  Note: not really an error, but should be changed before resubmission

Paper A

Real-Time Control of Large-Scale Modular Physical Models using the Sensel Morph

Silvin Willemsen, Nikolaj Andersson, Stefania Serafin and Stefan Bilbao

The paper has been published in the
Proceedings of the 16th Sound and Music Computing (SMC) Conference, pp. 275–280, 2019.

changed the template here, should check if it's ok like this

Abstract

Here is an abstract.

A.1 Introduction

Here is an introduction.

A.2 Conclusion

Here is the conclusion.

Paper B

Physical Models and Real-Time Control with the Sensel Morph

Paper C

Real-Time Implementation of an Elasto-Plastic Friction Model applied to Stiff Strings using Finite Difference Schemes

Paper D

Real-time Implementation of a Physical Model of the Tromba Marina

Paper E

Resurrecting the Tromba Marina: A Bowed Virtual Reality Instrument using Haptic Feedback and Accurate Physical Modelling

Paper F

DigiDrum: A Haptic-based Virtual Reality Musical Instrument and a Case Study

Paper G

Dynamic Grids for Finite-Difference Schemes in Musical Instrument Simulations

Paper H

A Physical Model of the Trombone using Dynamic Grids for Finite-Difference Schemes

format the blurb

Digital versions of musical instruments have been created for several decades, and for good reason! They are more compact, more easy to maintain, and less difficult to play than their real-life counterparts. One way to digitise an instrument is to record it and play back the samples, but this does not capture the entire range of expression of the real instrument. Simulating an instrument based on its physics, including its geometry and material properties, is much more flexible to player control. Although it requires more computational power to generate the sound in real time, the simulation could possibly go beyond what is physically possible. A violin growing into a cello, bowing your trumpet, your imagination is the limit...